KTH ROYAL INSTITUTE
OF TECHNOLOGY

Degree Project in Energy Technology

Second cycle 30 credits

Techno-economic feasibility of a hybrid CSP(sCO2) – PV plant for hydrogen production

PATRICIA PEREZ DE LA CALLE

KTH Industrial Engineering and Management

Master of Science Thesis

Department of Energy Technology

KTH 2023

Techno-economic feasibility of a hybrid CSP(sCO2) – PV plant for hydrogen production

TRITA: TRITA-ITM-EX 2023:475 Patricia Perez De La Calle

Patricia Perez de la Calle

Approved	Examiner	Supervisor
Date	Björn Laumert	Salvatore Guccione
	Industrial Supervisor	Contact person

Abstract

The global need to eliminate CO2 emissions and its consequent reduction in the use of fossil fuels drives the ongoing energy transition that highly involves the research achievements of the scientific community to reach the goals of this purpose. Renewable sources like photovoltaic and wind energy, are central to this endeavor, however, the intermittency of natural resources makes it non-dispatchable and energy storage is fundamental. According to the *European Roadmap* [1] just a 60% of the CO2 emissions reduction goal can be achieved with available technologies and existing energy. However, the production, use and specially storage opportunities that hydrogen offers can drive non-dispatchable renewable sources to achieve its full potential by clearing up the intermittency problem as well as covering the remained 40% gap.

This master's thesis aims to investigate the techno-economic feasibility of integrating a Solid Oxide Electrolyzer Cell (SOEC) into a hybrid PV-CSP(sCO2) plant. The study focuses on assessing various indicators related to electricity, energy, and hydrogen production prices. To achieve this, three different integration strategies within the hybrid PV-CSP(sCO2) plant were selected for analysis: Soec using heat from the particles coming from the receiver, soec using heat coming from the particles available in the thermal energy storage (TES) and soec recovering heat from the sCO2 power block.

A sensitivity analysis was conducted on different PV sizes (MWp), battery capacities (MWh), and SOEC installed capacities (MWh) to investigate the technology's potential in the plant and determine optimal sizing of subsystems. However, the individual optimization of economic indicators presented technical and economic challenges. Scenarios allowing individual optimization of hydrogen production prices (€/kg H2) resulted in 10.9, 11.7, and 14.6 €/kg h2 for receiver, TES, and sCO2 integration strategy, respectively. These scenarios, however, require high SOEC installed capacities, leading to elevated electricity and energy production prices. On the other hand, the individual optimization of electricity and energy production prices led to better and lower results when no hydrogen production presence within the plant. However, this analysis also showed that soec capacities below **5MWh** together with no installation of batteries and a new definition for calculating hydrogen production prices (LCOH) allows feasible integration of hydrogen production within the plant. LCOH(€/kg h2) results were 10.2€/kg h2, 7.6€/kg h2, and 9.4€/kg h2 for receiver, TES, and sCO2, respectively, for a soec installed capacity of 0.5MWh (119m2 size) along with energy production values not exceeding 101€/MWh.

While the results present a favorable outlook for SOEC installations based on literature review data [2] [3] [4] they still face challenges when competing with the cost-efficient PEM technology, which offers 4.5-5.5€/kg H2 [5] without storage. Nonetheless, this research contributes valuable insights into the integration of SOEC technology within hybrid renewable energy systems and provides a comprehensive analysis of the techno-economic aspects related to hydrogen production following different integration strategies. The findings may inform decision-making processes and promote further advancements in sustainable energy solutions.

Sammandrag

Det globala behovet av att eliminera CO2-utsläpp och därmed minska användningen av fossila bränslen driver pågående energiomställning, som starkt involverar forskningsresultaten från vetenskapssamhället för att nå syftet med detta mål. Förnybara källor som solceller och vindkraft är centrala i detta arbete, men intermittensen hos naturliga resurser gör dem icke-disponibla och energilagring är grundläggande. Enligt den europeiska vägkartan [1] kan endast 60% av målet att minska CO2-utsläppen uppnås med tillgängliga teknologier och befintlig energi. Produktionen, användningen och särskilt lagringsmöjligheterna som väte erbjuder kan emellertid driva icke-disponibla förnybara källor att nå sin fulla potential genom att lösa intermittensproblemet och täcka den återstående 40% klyftan.

Detta examensarbete syftar till att undersöka den teknisk-ekonomiska genomförbarheten av att integrera en fastoxid-elektrolysör (SOEC) i en hybrid PV-CSP(sCO2)-anläggning. Studien fokuserar på att utvärdera olika indikatorer relaterade till el-, energi- och vätgasproduktionspriser. För att uppnå detta har tre olika integrationsstrategier inom hybrid PV-CSP(sCO2)-anläggningen valts för analys: SOEC med hjälp av värme från partiklar som kommer från mottagaren, SOEC med hjälp av värme från partiklar som finns i termisk energilagring (TES) och SOEC som återvinner värme från sCO2-kraftblocket.

En känslighetsanalys har genomförts för olika PV-storlekar (MWp), batterikapaciteter (MWh) och SOEC installerade kapaciteter (MWh) för att undersöka teknologins potential i anläggningen och bestämma optimal dimensionering av delsystem. Resultaten från individuell optimering av ekonomiska indikatorer ledde dock till flera tekniska och ekonomiska utmaningar. Scenarier som tillåter individuell optimering av vätgasproduktionspriser (€/kg H2) resulterade i 10,9, 11,7 respektive 14,6 €/kg H2 för mottagare, TES och sCO2 integrationsstrategi. Dessa scenarier kräver dock höga SOEC installerade kapaciteter, vilket leder till höga el- och energipriser. Å andra sidan ledde individuell optimering av el- och energiproduktionspriser till bättre och lägre resultat när ingen vätgasproduktion fanns i anläggningen. Denna analys visade också att SOEC-kapaciteter under 5MWh tillsammans med ingen installation av batterier och en ny definition för beräkning av vätgasproduktionspriser (LCOH) möjliggör genomförbar integration av vätgasproduktion i anläggningen. LCOH (€/kg H2) resultaten var 10,2 €/kg h2, 7,6 €/kg h2 respektive 9,4 €/kg h2 för mottagare, TES och sCO2, för en SOEC installerad kapacitet på 0,5 MWh (storlek 119m2) tillsammans med energiproduktionsvärden som inte överstiger 101 €/MWh.

Medan resultaten visar en gynnsam utsikt för SOEC-installationer baserat på data från litteraturöversikter [2] [3] [4], står de ändå inför utmaningar när de konkurrerar med den kostnadseffektiva PEM-teknologin, som erbjuder 4,5-5,5 €/kg H2 [5] utan lagring. Trots detta bidrar forskningen med värdefulla insikter i integrationen av SOEC-teknologi i hybrid förnybara energisystem och ger en omfattande analys av de teknisk-ekonomiska aspekterna relaterade till vätgasproduktion enligt olika integrationsstrategier. Resultaten kan informera beslutsprocesser och främja ytterligare framsteg inom hållbara energilösningar.

Key words

Soec oxide electrolyzer cell (SOEC); Concentrated solar plant (CSP); Super critical cO2 (sCO2); photovoltaic field (PV); Thermal storage (TES); electrolyzer; MoSES; high temperature electrolysis (THE).

Contents

List of Figures

List of Tables

List of Equations

Chapter 1

Introduction

This first chapter presents an introduction of the thesis. Section 1.1 gives a brief overview of the research topic including its importance aligned with the context. Section 1.2 set up the goals followed by the main benefits in section 1.3 and previous related work in section 1.4. Finally, section 1.5 concludes the chapter showing the report outline.

1.1. Context

The increasing need of finding alternative sources to fossil fuels is nowadays one of the major concerns in society and scientific research. Renewable energies play a key role in the ongoing energy transition that seek for achieving cO2 emissions neutrality. In order to achieve such state, renewable energies potential should be brought as main contributor into electricity production and transportation [6] using the energy from the most abundant natural resources: solar in photovoltaic (PV) or concentrated solar plants (CSP), wind in wind turbines and hydropower.

However, solar and wind are non-dispatchable renewable energies, dependent on the available natural resources and it can not be controlled whether or not to produce energy. This is how the energy storage necessity has been raised up placing hydrogen production and its storage as a very promising solution for this matter. Although it is a less mature way of energy storage if compared with thermal energy storage (TES) or batteries, renewable hydrogen, (among other uses) can be used for large-scale and long term energy storage [7]. This not only helps to address the intermittency issues associated with non-dispatch renewable energies but also improves the flexibility of energy systems by effectively balancing supply and demand, in situations of excess or insufficient power generation and therefore optimizing overall energy efficiency [8].

This thesis aims to investigate the potential of integrating both, renewable energy technologies and green hydrogen production from a technical and economic perspective with focus on optimizing the energy (€/MWh) and hydrogen (€/kg h2) production prices. For this study a hybrid PV-CSP plant will be the source to cover the electric and thermal need of the electrolyzer which in this case is a high temperature one; solid oxide electrolyzer (soec). The research will employ mathematical modeling and simulation to assess the performance of 3 different integration strategies. The strategies respond to the different thermal inputs that the electrolyzer receives depending on where in the hybrid plant the soec electrolyzer is installed. In Figure 1 it is represented the 3 different integration strategies which correspond with the 3 different thermal sources that can be used in the system: particles coming from the receiver, particles available in the thermal energy storage (TES) or waste heat coming from the sCO2 in the power block.

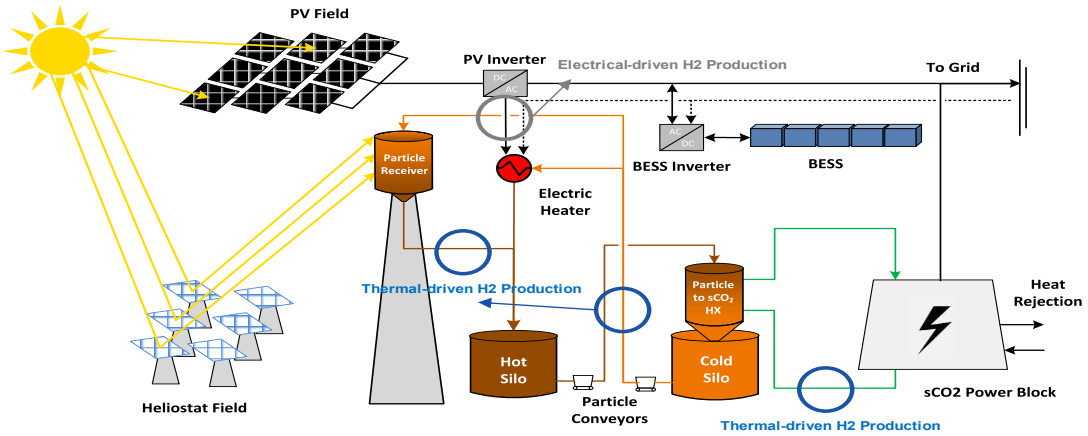

Figure 1. Hybrid pv-csp(sCO2) plant with locations selected to study

The results of this study will be obtained by running a custom-developed Python code (MoSES) that incorporates all the relevant energy system components showed in Figure 1 as well as the necessary components for high temperature hydrogen production, allowing for a comprehensive and systematic analysis. The results of this study will provide valuable insights into the design and implementation of renewable energy systems, and will also inform decision-makers about the feasibility and potential of integrating CSP, PV, battery storage, and hydrogen production.

1.2. Objectives

The aim of this master thesis is to assess the techno-economic feasibility of high temperature hydrogen production in a hybrid PV-CSP(sCO2) integrating a solid oxide electrolyzer (SOEC) through 3 different integration strategies. Through this study it is expected to address whether or not hydrogen production can be implemented as well as the conditions and set of parameters that allows it for each case: PV size (MWp), battery capacity (MWh) and soec installed capacity (MWh).

For each of the 3 integration strategies: receiver, TES and sCO2 based it is aimed to find and understand the patterns that lead to individually optimize hydrogen production prices (€/kg h2) as well as electricity and energy production prices (€/MWh). Also, this study will seek for a feasible hybrid scenario that minimizes hydrogen and energy production prices (€/kg h2 , €/kg/MWh) at the same time and it will asses its technical feasibility depending on the goal as well as its economical feasibility in the market.

In order to do so, some other specific objectives were set up:

- Investigation of different configurations for each of the 3 integration strategies and identification of several technical and ecnomic key performance indicators (KPIs).
- Development of a custom-python code that integrates the 3 different integration strategies for HTE hydrogen production into an already existing PV-CSP modeled code (MoSES).
- Analysis of KPIs after running sensitivity analysis for each case.

1.3. Benefits and Sustainability

The results and conclusions obtained from this research are expected to help the scientific community and the energy transition. High temperature electrolysis is still a technology that needs of much further investigation. However, its higher efficiency (up to 95%) compared with low temperature electrolysis (62-85%) [9] makes it highly interesting specially for systems that produces heat waste.

The first main benefit from this thesis is the deliverable of some of the first conclusions for a hybrid CSP(sCO2)- PV system. This degree of innovation plus the fact of its actual development state on the research frame could make this investigation to be the basis for future research with similar approaches or configurations. Another benefit relies on the method used to obtained the results from the sensitivity analysis. A python coded software was developed which will allow easy future self custom-investigation according to the different researcher interests. For example, by changing its weather file and extrapolate it to different potential locations around the world or by studying fictitious scenarios where the hydrogen technology initial investment is cheaper.

Finally, it is important to mention that if a project like this is eventually brought into practice some other different benefits will be found. Not only helping to achieve goals concerning significant reductions of CO2 emissions but also in form of savings, consequence from a more efficient use of renewable energies and less dependency of fossil fuels.

1.4. Previous Related Work

Hydrogen technology has become an extensively researched area nowadays because of the benefits it offers regarding energy storage at long term and large scale. While low temperature electrolyzers such as: proton membrane exchange (PEM) or alkaline are more consolidated technologies in the industry [10], high temperature electrolyzers are still in the early stages of development and implementation. The reason why is very straighforward, low temperature electrolyzers present a simple operating process where the injection of water and electricity enables hydrogen production. This allows more flexible installations since its temperature of operation remains below 120ºC and can easily operate within a wide range of scenarios.

Contrary, high temperature electrolyzers involve more complex working processes, as they require both: electricity and heat in order to operate at a temperature between 600ºC and 1200ºC. This narrows the potential of installation for green hydrogen production to concentrated solar plants (CSP). In this way, we can found several examples in literature review that have already investigated such configurations.

High temperature electrolyzers coupled with CSP systems have been already investigated using several approaches. Linear fresnel collectors potentital were investigated by Mehrpooya et. al being coupled with a rankine cycle and thermochemical storage to allow hydrogen production during no radiation hours [11]. Also, dish collectors were implemented in the research conducted by Mohammadi et. al where there is not only electricity and hydrogen production but also electricity coming from the grid to be used during off peak hours (mainly during the night) for hydrogen production [10]. Furthermore, some other CSP technologies configurations have been explored such as parabolic through collectors to provide both thermal and electrical energy to the electrolyzer [3] as well as solar tower based like we find in the study developed by AlZahrani et. al. [12]. Here the system includes thermal energy storage (fluoride salts) and it is coupled with a sCO2 power subsystem. Research on hybrid systems has been also conducted but it not so common. In this field we can find the results from S. Koumi Ngoh et. al investigation where a solid oxide steam electrolyzer (SOSE) was coupled to a Photovoltaic array and to a Parabolic Trough Collector.

Not only CSP technologies can be coupled with high temperature electrolyzers but also nuclear reactors like Harvego et. al investigation shows. Here the potential of a high temperature electrolyzer (HTE) was investigated by being coupled with 3 different advanced reactor concepts: a high-temperature helium cooled reactor and two different supercritical CO2 advance reactors [13]. In addition, alternative methods can also be employed to provide the necessary heat to the electrolyzer. This can be achieved by recovering heat if the system allows it through several heat recovery systems and implementing auxiliary heat from electric heaters [14] or using heat waste as a subproduct from other applications.

This master thesis aims to investigate the techno-economic feasibility of high temperature hydrogen production using a combined photovoltaic (PV) and concentrated solar plant (CSP) like the sources to cover the electrical and thermal needs of the soec. This hybrid configuration has never been studied by scientific community under the scenario of high temperature hydrogen production and it will contribute to increase the scope and opportunities for possible implementation of this technology.

1.5. Outline

This section is going to describe the information distribution in the following sections. Section 2 will cover the theoretical background, with special focus on energy storage systems, hydrogen types and its importance under the EU energy transition goals. In section 3 the methodology used will be explained in higher detail while section 4 will cover a description of the system as well as the elements involved in each of the configurations. Then, the results will be presented in section 5 and discussed in section 6 and finally section 7 will include the final conclusions as well as future steps.

Chapter 2

Theoretical Background

2.1. Solar Energy Technologies

Solar radiation is one of the most abundant natural resources with great potential for producing big amounts of clean energy. Some of most common types for producing solar energy are photovoltaic fields (PV) and concentrated solar power plants (CSP). However, the interest about the combination of PV-CSP is growing from the advantages resulting in their hybridization. [15]

2.1.1. Photovoltaic (PV)

Photovoltaic solar energy is a renewable energy source that uses solar radiation to produce electricity. To do so, photovoltaic cells are used and these are normally made of monocrystalline, polycrystalline or an amorphous silicon material. The energy generated can be injected into the grid or use for self-consumption.

Although Photovoltaic energy faces several challenges regarding the intermittency of natural resources, it has achieved very competitive prices (0.048€/MWh) since 2010 where the energy production cost was 0.417€/MWh [16] making it as one the most world widely used renewable energies. The fact of a grown economy of scale during the last years plus the development of more efficient solar panels have allowed to consolidate the economic feasibility of this technology

2.1.2. Concentrated Solar Power (CSP)

Concentrated solar plants (CSP) consist on a set of mirrors that concentrates the light into a receiver to produce heat. There are 4 different types of CSP technology and these are categorized like: parabolic trough, central tower, fresnel and dish CSP.

Heat produced at a CSP can be stored and being used later to produce steam to run a turbine and produce electricity or it can be used directly as a product in the industry [17]. sCO2 Brayton cycles are recommended because of their reduction in costs due to the incompressibility of the fluid allowing compact turbomachinery [15]. There are several types of sCO2 Brayton cycles that can be coupled: sCO2 Brayton cycle with recompression, reheat or intercooling are just some examples. [18]. The higher the complexity, the higher will be the costs but also its the efficiency.

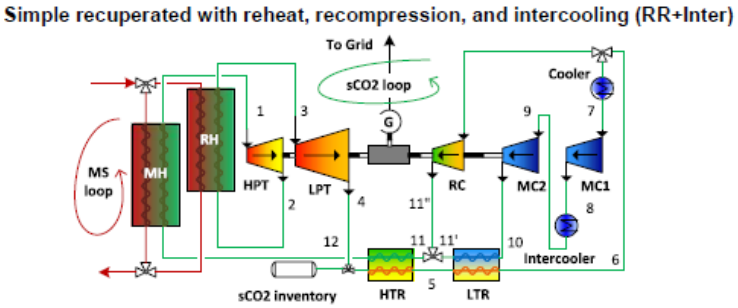

Figure 2. Example of a sCO2 Brayton cycle with reheat, recompression and intercooling

The main advantage of CSP against PV is that this technology commonly includes thermal energy storage (TES) of typically 10 hours . This makes possible to produce energy during the night or time

when the sun radiation is low. Also, makes economically feasible to storage larger quantities of energy compared to batteries (2-4 hours). [17]

Although CSP prices are not as low as PV ones, this technology has suffered a great transition since 2010 where the levelized cost of electricity was 0.358€/MWh, until now 0.114€/MWh [16].

2.2. Energy Storage Systems (ESS)

As renewable energy sources become more prevalent and the need for grid stability increases, energy storage technologies play a key role in supporting the transition to a more sustainable future. Energy storage systems provide flexibility into the system by supplying or capturing energy according to the need. This fact not only allows to improve the behavior of the grid but also helps to consolidate the future of renewable energies solving the intermittency gap due to their reliance on natural resources. Using energy storage system helps to reduce the dependence on fossil fuels which eventually would lead to a reduction in the dependence of fossil fuels. [19] [20]

Several types of energy storage can be used and each type has its advantages and limitations. The choice of storage method depends on factors such as the application, scale, type of energy being stored or cost [21] and it has to be studied what is best for each situation. According to the type of energy stored, energy storage systems can be classified into: electrical, mechanical, thermal and chemical energy.

- Mechanical energy storage (EESS): this type of storage consists into transforming the energy into both mechanical and electrical energy. When the demand is low the electrical energy is converted into mechanical. Then, when the demand is high mechanical energy is converted into electrical and injected into the system or grid [21]. The most common types include: pumped hydro storage (PHS), flywheel energy storage (FES) and compressed air energy storage (CAES) [20].
- Thermal energy storage (TES): TES systems use sensible and latent heat plus chemical reactions to store energy through a certain media contained in an insulated reservoir. [21] [19]. The media can be quite diverse, however molten salts are widely used specially for environmental reasons. Finally, thermal heat is later converted into electricity through a power unit that consist in a steam cycle for power generation. TES is often used in concentrated solar plants (CSP) so there can be electricity production during the night. Depending on how big the installed thermal storage tanks are, there will be more or less hours of production with no sun radiation.
- Electrochemical energy storage (EESS): when talking about electrochemical storage we can find capacitors, supercapacitors, superconducting magnetic energy storage and of course batteries (BESS). Lead-acid batteries are frequently used for storage applications because of their efficiency; 75-80% as well as high life cycle, 1200-1800 cycles. [21]
- Chemical energy storage (CES): under this type hydrogen and biofuel energy storage can be found. Hydrogen is commonly found under 200-250 bar steal tanks or slightly higher pressures (350 bar) if the tank is made of carbon fiber. [21]

When talking about integration of energy storage into renewable energy systems there are some storage options with great potential. For example, superconducting magnetic energy storage, flywheels or supercapacitors must be considered. These methods offer a solution to frequency challenges, supplying an steady voltage stage during the energy generation process. On the other hand, hydrogen storage is also a very promising alternative, specially for long-term storage applications. However, this technology faces some problems of integration because of its elevated costs [21].

2.3. Hydrogen Categories by Production Method

Hydrogen is the most abundant element in the universe. However, in the earth it is needed to be obtained from water or chemical compounds [22]. There are several ways of categorizing hydrogen depending on which process has been employed to be obtained. However, not all of them are sustainable [23] and colors are commonly used to distinguish them. In this section it is going to be defined the main types as well as its production processes.

2.3.1. Green Hydrogen

Green hydrogen stands for production without greenhouse emissions [24]. Green hydrogen is commonly produced in electrolyzers using water and electricity coming from renewable sources like wind or solar energy [23]. However, other less common methods like biogas or biomethane can also be employed resulting in low or zero carbon emissions [22]. Green hydrogen production still represents a small percentage but growing compared with other types such as blue hydrogen [23] because of its production costs 3-7.5$/kg [25]

2.3.2. Grey Hydrogen

Grey hydrogen is the most common type because of its cheap production, 1,50$/kg [23] [24]. Grey hydrogen is produced from fossil fuels and commonly uses a process called steam methane reforming (SMR), where natural gas is reacted with high-temperature steam to produce hydrogen [22]. During the process CO_2 emissions are typically released into the atmosphere, making it one of the least environmentally friendly methods of hydrogen production.

2.3.3. Blue Hydrogen

Blue hydrogen is also obtained from a steam reforming process, similar to grey hydrogen and it commonly uses natural gas and steam react to form hydrogen [24]. However, in this case CO_2 emissions are treated being captured and stored preventing them from entering the atmosphere and reducing the environmental impact [23]. Its production price is found around 2.5$/kg [25].

2.3.4. Black and brown Hydrogen

Black and brown hydrogen stands for the type of bituminous (black) and lignite (brown) coal [22]. It is produced from coal through a process called gasification that converts carbon-rich materials into hydrogen [23]. CO_2 emissions are not captured during the process and that makes it the one with the highest rate of green house gases [24].

2.3.5. Turquoise Hydrogen

Turquoise hydrogen is quite new and it is produced using methane pyrolysis. In this process, methane is split into hydrogen and solid carbon by using heat. No carbon is released and instead is stored [22] [23] [24]. If later stages of development determine that turquoise hydrogen is effective then it will be categorized as low-carbon hydrogen. Also, the carbon stored can potentially be used in different industrial applications, providing an additional economic value.

2.3.6. Pink Hydrogen

Pink hydrogen is generated from the electrolysis of water using electricity coming from a nuclear plant. [24] [23]. It can also be referred like red hydrogen when using high-temperature catalysis to split water or purple when using nuclear power and heat through a combined chemo-thermal electrolysis process [22] .

As shown, hydrogen has a wide range of different production sources. However, hydrogen production approach nowadays consists on reducing dependance on fossil fuels so CO_2 emissions can be

neutralized. For this reason it is expected a growing utilization percentage of hydrogen types with non or low carbon emissions, in particular of **green hydrogen**.

2.4. Importance of Hydrogen for addressing climate change and reducing dependance of fossil fuels

There is an energy transition ongoing which implies a high decarbonization degree of energy systems to fulfill the objectives stablished in the Paris agreement [1]. This implies to limit energy-related CO2 emissions to less than 770 megatons (Mt) per year by 2050 and keep global warming raise below 2 degrees. Additionally, member states seek for greenhouse gas neutrality by 2050. [1] [26].

The energy share from renewable energies in the EU in 2021 was 21.8%, which represented a 0.3% less than in 2020, probably influenced from the worldwide covid situation. From the total energy a 37.5% was employed in electricity consumption (32.5% from wind, 37.5% from hydro, 15.1% from solar, 7.4% from biofuels and 7.9% others), 22.9% in heating and cooling and 9.1% in transport. These data represent an increased use of renewable energies but it is still far to achieve the goals set up for 2030: 32% of energy share from renewable energies and 14% dedicated to transport. [27] . On the other hand, green hydrogen production just represented a 1% in 2021, which stands for a total energy contribution of 0.7GW [28]. In order to achieve the goals stablished for 2050 it has been estimated a large scale contribution of hydrogen (4-5 TW) that will require a huge rate of growth [27] [28].

Even though hydrogen has a long journey ahead, its role is essential for the energy transition as it is expected to lead the large scale integration of renewable energies by converting and storing energy as a renewable gas. [1]. Additionally, hydrogen's importance to the contribution of decarbonization can be divided into three main sections according to the *Hydrogen Roadmap Europe*:

- **Hydrogen is the best or only option for selected segments**: transport, industry and buildings. This is the case of heating for old constructions difficult to bring electrification, heavy duty transport (trucks, buses, ships, trains, large cars) fueled with hydrogen or synthetic fuels making a subsequent considerable difference into their weight and finally industrial processes where hydrogen can be use as feedstock or as a synfuel (ammonia production or steelmaking). [1] [26]
- **Hydrogen has a systemic role in energy transition** that allows flexible transference of energy accordingly with sectors, time and place. Nowadays hydrogen is the only option that could allow the storage of clean energy at large scale with the use of electrolyzers. This fact allows for greater stability, seasonal energy balancing and long term storage in different possible ways such as, manufactured storage tanks, salt caverns, and depleted gas fields. Finally, hydrogen can be also easily transported between long distance regions in pipelines, ships, or trucks in gas, liquid or other forms. [1] [8]
- **Hydrogen is aligned with customer preferences and convenience.** This point is key since the social and technological development need to be aligned to have a successful integration of hydrogen. Nowadays hydrogen can be implemented in a wide range of sectors and in many different areas. However to make a 100% use of this energy vector it will still need of much more resources that allows economic feasibility.

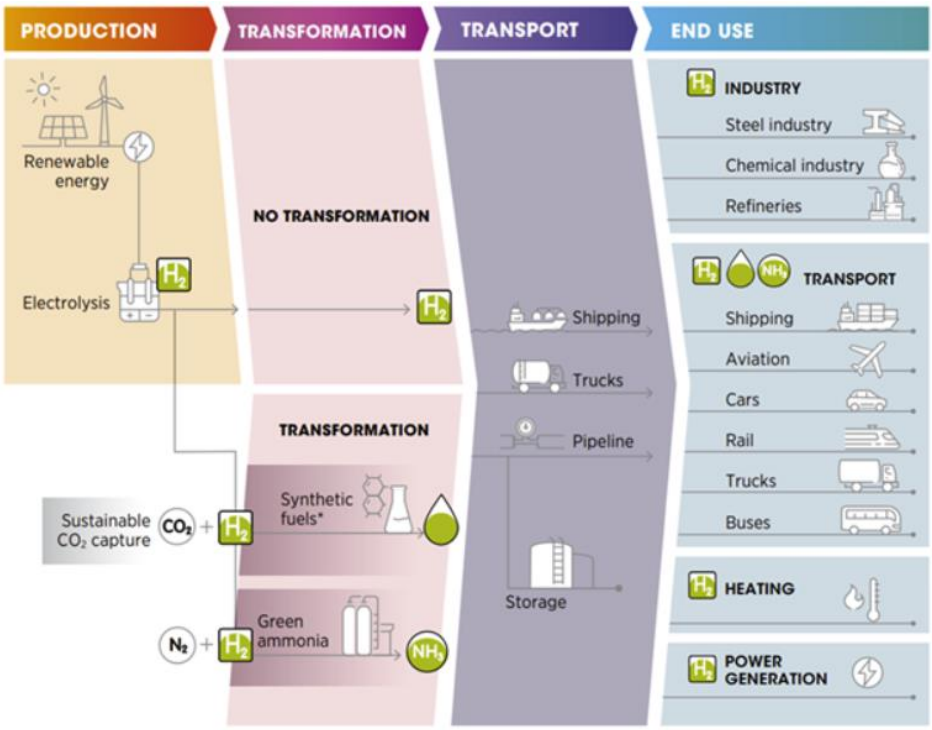

Figure 3. Green hydrogen production, conversion and end uses across the energy system [28]

Chapter 3

Methodology

The third chapter describes the methodology followed along the thesis. Section 3.1 gives an overview of the methodology and steps followed. Section 3.2 is going to cover the development of the configurations where a detailed description of each one is included. Then, section 3.3 will tell about the modeling approach and the dispatch strategy followed for the control of the plant and section 3.4 will include the case analysis where a description of the sensitivity analysis conducted is included. Section 3.5 will talk about the techno-economic analysis performed and about the importance of its outcomes. Section 3.6 will also be described the technical and economical indicators used for analyzing and reaching the conclusions of the research as well as the importance and contribution to the study. Finally section 3.7 will show a preliminary analysis.

3.1. Methodology

Figure 4 shows the methodology followed along the thesis. Firstly, literature review was conducted on previous similar works and hydrogen technologies. The outcome of this first stage helped to have the first ideas for the 3 different integration strategies as well as to identify several technical and economic indicators that could address the final goals of the study. Secondly, in the development phase 3 different configurations were developed through a python-custom code for the 3 different integration strategies identified in the hybrid plant. These are the receiver, TES and sCO2 based configurations receiving their name attending to where in the system the electrolyzer is placed.

Thirdly, in the modeling phase each configuration was integrated in an existing code were the PV-CSP (sCO2) hybrid plant was already modeled (MoSES). Then, in the simulation phase, for the 3 cases it was ran a sensitivity analysis attending to different parameters which outcome was the result for several technical and economic KPIs. Once the sensitivity analysis was conducted and the simulation phase was concluded the study finished with an analysis of the different KPIs, a discussion and comparison between different results and finally the conclusion.

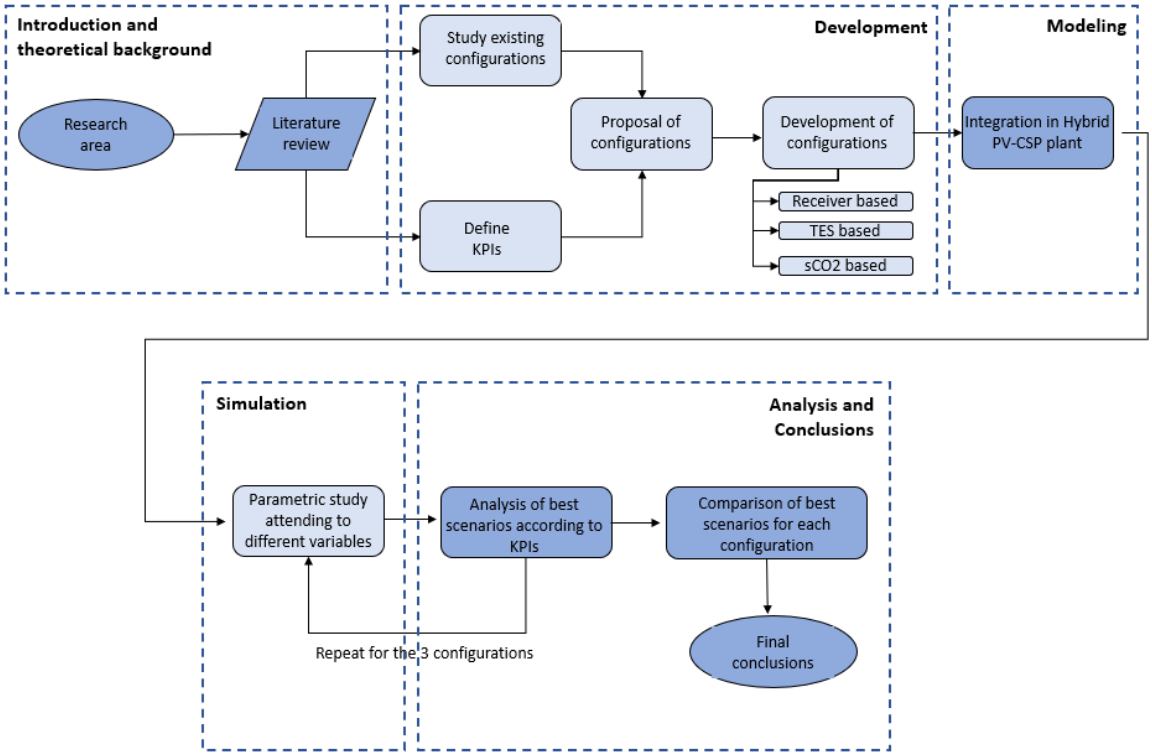

Figure 4. Flowchart describing the methodology framework for the project.

3.2. System Layouts: Development of configurations

In this thesis there were 3 different configurations developed and analyzed. All of them follow the same principle: hydrogen production at high temperature using a soec electrolyzer and a series of heat exchangers for this matter. The integration strategies respond to the different locations to install the electrolyzer that enables to conduct different studies according to the different methods to cover its thermal need (particles and sCO2) . Look at Figure 1.

The way to transform water into steam is similar for the 3 cases. Firstly, in a heat recovery system water at 26ºC interchanges heat with the products coming out from the electrolyzer (h2 and 02) at 750ºC. Secondly, water raises its temperature up to 100ºC in a steam generator and then, the steam gets close to operating temperatures in a super heater. Both heat exchangers use particles or heat waste from sCO2 in the power block. Finally, a heat booster raises up the steam temperature up to temperature working conditions 750ºC.

For the receiver based configuration, hot particles coming from the receiver will be the main source of thermal energy for the soec. These particles come from the receiver at 780ºC and after being used accordingly in each of the heat exchangers, these are later sent to the cold silo. However, for this configuration hydrogen production is totally conditioned to sun hours since the receiver only enables circulation of particles under the condition of receiving a certain radiation.

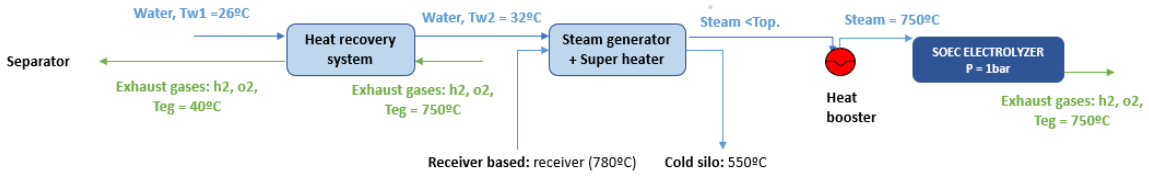

Figure 5. System layout for receiver based configuration

For the TES based configuration, the electrolyzer is installed after the cold silo. In this case particles come from both TES units, using particles from the cold silo (550°C) in the steam generator and particles from the hot silo (780°C) in the superheater. Particles, once used accordingly in each of the heat exchangers, are later sent to the cold silo. This configuration enables hydrogen production when there is not sun radiation since now not only the electrical need can be covered with energy storage (batteries) but also the thermal one (TES).

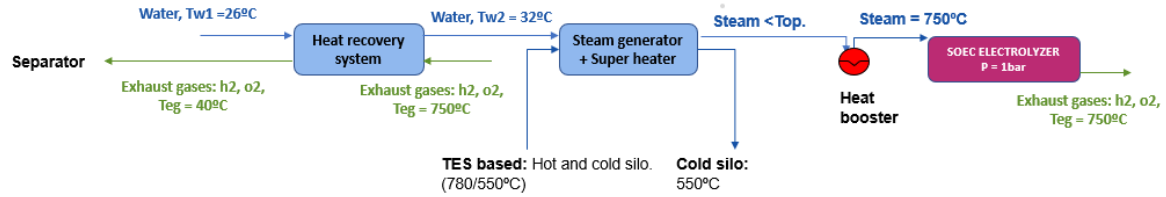

Figure 6. System layout for TES based configuration

Finally, the sCO2 based configuration, uses waste heat from the sCO2 at the outlet of the turbine (590°C) to cover soec thermal requirements. Once sCO2 it is used accordingly in the heat exchangers it is sent back into the cycle where it is injected into the recuperator of the power block.

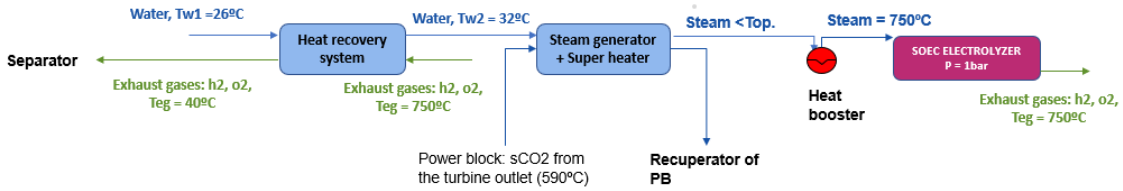

Figure 7. System layout for sCO2 configuration

3.3. Modeling approach

In this master thesis and for the three different configurations developed it has been used the following elements. Firstly, a heat recovery system where heat is recovered from h2 and o2 at high temperature coming from the electrolyzer. Secondly, a steam generator followed by a super heater where depending on the configuration particles or super critical CO2 is injected. Finally, a heat booster which helps to achieve the last degrees of temperature required to be under operating temperature conditions. All elements mentioned have been modeled and integrated into different python files under the names of "soec.py", "heat recovery system.py", "steam generator.py", and "heat booster.py" where all equations required for the design, control and the operation of each element have been written in their respective code. Finally all these equations are called from a main code or file ("main.py") which is mainly divided in the same way as the code of each element does (design, control and operation). Table 1 shows the structure of the code once hydrogen production is implemented. There, the elements in green color show the new components added into the main MoSES code already developed for a hybrid PV-CSP(sCO2) system.

Table 1: Structure of the code

Inputs	Location
Inputs	PV
Inputs	Dispatch
Inputs	Electric Heater
Inputs	Heliostat field
Inputs	Tower and receiver
Inputs	Storage
Inputs	Control
Inputs	sCO2 Power block
Inputs	Cost
Inputs	System optimization
Inputs	Handling of outputs
Inputs	Other
Inputs	Soec electrolyzer
Inputs	Heat booster
Inputs	Battery
Inputs	Heat exchangers
Inputs	Thermodynamic states
Design	Soec electrolyzer
Design	Heat exchangers
Design	Heat booster
Design	PV field calculated parameters
Design	Power block calculated parameters (pb type and sco2 thermodynamic states)
Design	Control of the power block calculated parameters
Design	Storage calculated parameters
Design	Electric heater calculated parameters
Design	Heliostat field and receiver calculated parameters
Costs	
Operation	Sun operation
Definition and initialization of variables	
Control	Hydrogen production
Control	Soec
Control	Mass of particles/sCO2

Control	Replacement of elements
Operation	Hourly heliostat field
Operation	Hourly PV
Control	Hourly receiver output
Control	Hourly electric heater output
Operation	Hourly receiver
Operation	Hourly electric heater
Control	Hourly power block output
Operation	Hourly TES: hot tank
Control	Primary heat exchanger(s) in the power block
Operation	Power block
Operation	Heat exchangers
Operation	Heat booster
Operation	Hourly TES: cold tank
Operation	Soec electrolyzer
Hourly Temperature calculations	
Results	KPIs
Results	Costs
Results	Design
Results	Operation
Results	Summary

The equations for design, control and operation of the soec and heat exchangers are included in appendix A. For the main control part, it was developed a dispatch strategy (Figure 8) that will allow the plant to decide whether the system can operate under hydrogen production mode or not and consequently how the flux of electricity and particles/sCO2 is going to be distributed through the elements. If there is enough energy coming from PV or available at the energy storage systems (TES and batteries) to cover soec and heat booster needs, then the plant will operate under hydrogen production mode. Otherwise the electrolyzer will operate under stand by mode.

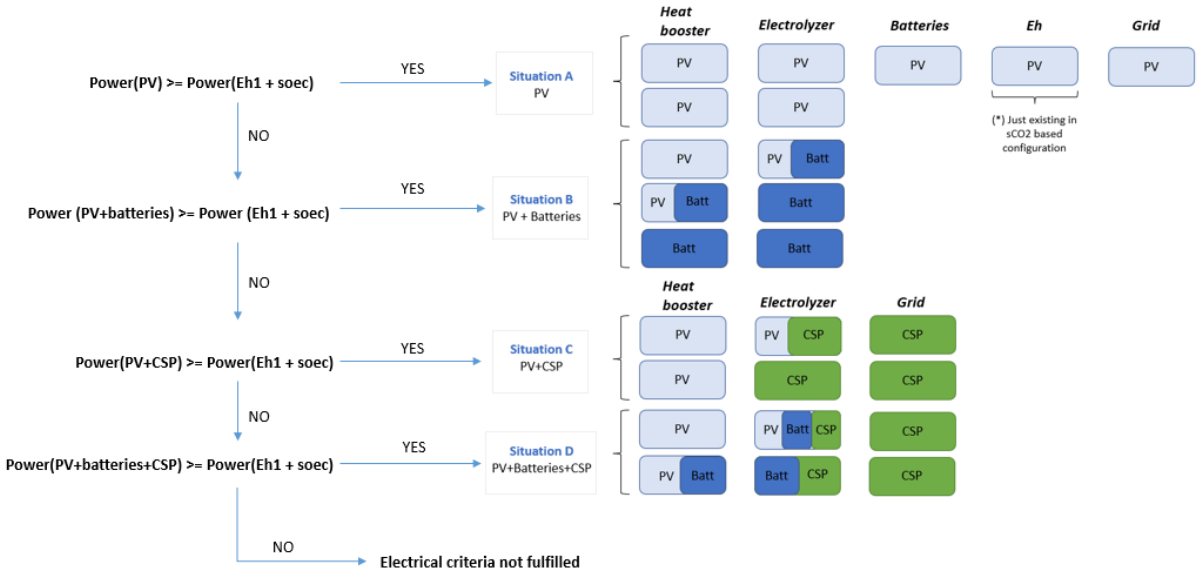

Figure 8. Dispatch Strategy for electricity flow control within the hybrid plant

The control part has been coded separately in other independent python file under the name of "main control.py". This file has all the equations needed to verify the available energy in the hybrid plant and to make it run under the appropriate mode. The plant can operate under three main different modes: hydrogen production mode, hydrogen production and energy injection into the grid simultaneously or just delivering energy into the grid and/or energy storage systems while the electrolyzer is under stand-by mode. Finally, the equations written in these files are called from a main file ("main.py") where these are executed with the rest of existing design, individual control and cost equations as shown in Table 1.

Not only technical aspects were covered but also economical ones. In order to do so, the already existing file "costs.py" was extended. Here, all equations related with the costs of the new integrated elements were written. Finally, the equations related with key performance indicators were introduced into the existing file of "KPIs.py" which was called at the end of the main file since priorly all technical and economical parameters needed to be calculated. The KPIs will be the parameters that will help out to reach the conclusions on whether or not each of the configurations are techno-economic feasible. In section 3.6 KPIs will be explained with more detail.

3.4. Case Analysis Methodology

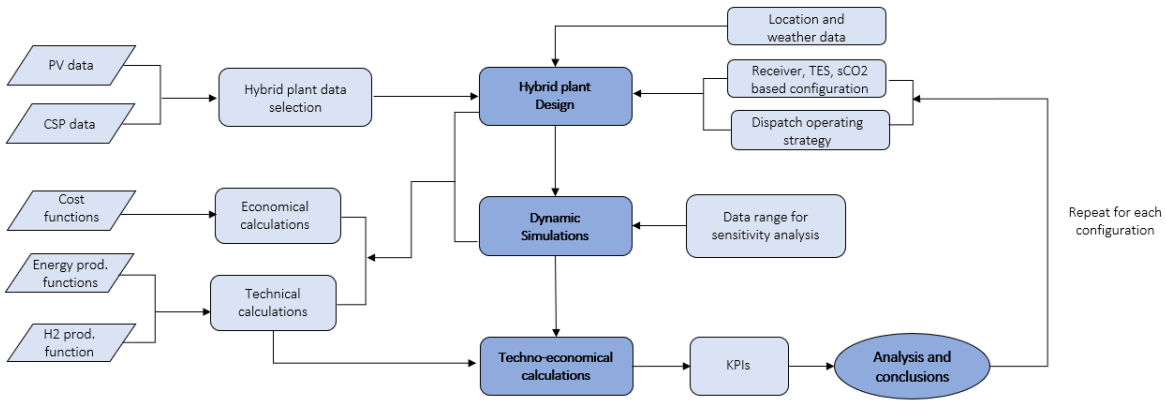

Figure 9. Case analysis flowchart methodology

3.4.1. Sensitivity Analysis

With the aim of finding which configuration could result more feasible to integrate from a technical and economical point of view a sensitivity analysis was conducted. The reason why this method was chosen is to have the outline of many different scenarios attending to 3 different main parameters: size of the photovoltaic plant (MWp), battery capacity (MWh) and soec installed capacity (MWh). Also, by performing a sensitivity analysis it is being covered a wider scope.

The parameters under study in the sensitivity analysis were specified in a separate python code with the name of "permutation.py" were each of the parameters has a range of values assigned. Once the values were specified the simulation went on until all possible permutations were performed. This methodology was applied for the three configurations included in the thesis and the range of values assigned were the following ones:

- PV size: 10-100MWp.
- Battery size: 0-90MW for a capacity of 3 hours.
- Soec installed capacity: 0-100MWh.
- Others: power output in the power block, 50MW and energy injection limit into the grid, 25MW.

3.5. Techno-Economic Analysis

With the aim to prove whether or not is feasible the integration of high temperature electrolysis a techno-economic analysis has been performed for the three configurations presented in section 3.2.

The economical analysis has been based on quantifying and study the price per kilogram of hydrogen, megawatt of electricity and finally megawatt of energy to have a global economic indicator of hydrogen and electricity combined. To be able to calculate these three main indicators it has been previously calculated the capital (CAPEX) and operating (OPEX) expenditure of all components integrated in the system: PV, CSP and hydrogen production unit (soec, heat exchangers and heat booster). Later on, technical indicators such as total annual energy injected into the grid or total annual hydrogen production will be introduced into the economical KPIs equations to quantify the unitary price in each case as mentioned above. On the other hand, technical indicators will also cover a large part of the results, in its majority these will refer to annual energy productions, energy sent to the electrolyzer and to the grid respectively from PV, CSP or batteries and of course size of the elements (MWh, m2).

All equations mentioned before are integrated into the code with a .py file that receives the name of "KPIs.py". The main file has imported all equations in the KPIs.py file and it generates all the economical and technical indicators mentioned before in every new iteration according to the new inputs that it receives as specified in the sensitivity analysis.

3.6. Key Performance Indicators (KPIs)

To be able to assess the techno-economic feasibility of the results obtained different key performance indicators were defined and calculated along the study. Key Performance Indicators (KPIs) are considered as valuable tools for assessing various aspects of a project with the aim of enabling decision-making and driving performance improvements. This section aims to provide a comprehensive overview of technical and economical KPIs, their significance, and their role in evaluating performance.

Key points covered in this section will include:

- Definition and characteristics of KPIs: Clarifying the concept and definition of each of the KPIs as well as defining the limitations that each indicator offers.
- Importance of KPIs: Discussing why each KPI was used and the benefits they provide in terms of performance evaluation, goal alignment, and decision-making.
- Types and categories of KPIs: in this master thesis indicators are mainly divided in 2 different categories; technical and economic ones. However, further discussion is recommended in the future along with other indicators such as environmental ones.

3.6.1. Technical KPIs

- Annual energy production KPIs:

Some of the most relevant technical indicators are the total annual energy generated from hydrogen production AEY_{h2} and the total annual energy injected directly into the grid AEY_{grid}. However, it is also important to determine the annual energy generation from both solar plants; PV and CSP (AEY_{pv} and AEY_{csp}). This way of calculating the flow of the energy will be useful when analyzing results from an economical point of view. Here, a very interesting and main point will be the study and analysis of consequences from sending energy into the electrolyzer instead of directly into the grid.

$$AEY_{grid} = \left(\sum_{t=1}^{t=8760} (energy\ injected\ into\ the\ grid\ _t) \right) * 10^{-9}\ \text{[GWh/year]}$$

$$AEY_{h2} = \left(\sum_{t=1}^{t=8760} (hydrogen\ mass\ produced\ _t) \right) * lhv * 10^{-9}\ [\frac{MWh}{year}]$$

$$AEY_{csp} = \left(\sum_{t=1}^{t=8760} (total\ energy\ produced\ in\ CSP\ _t) \right) * 10^{-9}\ \text{[GWh/year]}$$

$$AEY_{pv} = \left(\sum_{t=1}^{t=8760} (total\ energy\ produced\ in\ PV\ _t) \right) * 10^{-9}\ \text{[GWh/year]}$$

- Energy production distribution KPIs:

In addition, energy distribution parameters concerning a more detail flow distribution of the energy were also included. In this way it is possible to know the energy sent from the PV and power block of the CSP to the grid like $AEY_{pv\ to\ grid}$ and $AEY_{csp\ to\ grid}$ respectively. Parallelly, it is obtained the energy sent from the PV, CSP and set batteries to the electrolyzer like $AEY_{pv\ to\ soec}$, $AEY_{csp\ to\ soec}$ and $AEY_{bess\ to\ soec}$ respectively. These parameters are specially interesting when looking for the most appropriate size of PV and set of batteries. For example, a configuration which outcome of hydrogen is imposed to be high will need a higher input of energy. Consequently, higher PV sizes will fit better with the requirements of these type of configurations, and this eventually will translate into more hours of production. The contrary will happen when a low hydrogen mass flow rate is imposed. Even though the production requirement will be always covered, we can tend to oversize the photovoltaic field or the battery capacity which eventually would translate into higher investment costs than it is needed.

$$AEY_{pv\ to\ grid} = \left(\sum_{t=1}^{t=8760} (total\ energy\ from\ PV\ to\ grid\ _t) \right) * 10^{-9}\ \text{[GWh/year]}$$

$$AEY_{csp\ to\ grid} = \left(\sum_{t=1}^{t=8760} (total\ energy\ from\ CSP\ to\ grid\ _t) \right) * 10^{-9}\ \text{[GWh/year]}$$

$$AEY_{pv\ to\ soec} = \left(\sum_{t=1}^{t=8760} (total\ energy\ from\ PV\ to\ soec\ _t) \right) * 10^{-9}\ \text{[GWh/year]}$$

$$AEY_{bess\ to\ soec} = \left(\sum_{t=1}^{t=8760} (total\ energy\ from\ BESS\ to\ soec\ _t) \right) * 10^{-9}\ \text{[GWh/year]}$$

$$AEY_{csp\ to\ soec} = \left(\sum_{t=1}^{t=8760} (total\ energy\ from\ CSP\ to\ soec\ _t) \right) * 10^{-9}\ \text{[GWh/year]}$$

- Other KPIs:

Some other important KPIs that need to be considered are the energy waste and the "capacity factor" in each case. Waste of energy ($AEY_{PV\ waste}$) is something that wants to be avoided for 2 reasons, efficiency and costs. All the energy that is produced and not used translates into revenues that we are not obtaining with the configuration installed. Also, it can be an indicator of needing to readjust some parameter (size of PV, CSP or energy limit imposed to the grid). On the other hand, "capacity factors" will give an idea about during which percentage of the year there is energy injected into the grid (CF_{grid}) and hydrogen production (CF_{soec}). These 2 will depend mainly on the hydrogen mass flow rate imposed so this should be considered along with the CF in each case. In other words, a configuration with high "capacity factor" for hydrogen production can produce the same amount of hydrogen per year as a low "capacity factor" one. The reason why this happens is that the configuration with low capacity factor runs out of resources (energy storage) faster than the one with high capacity factor one. Eventually, the yearly production gets similar values but the time that production takes changes. This will be an interesting point to have a look depending on the future application. For example, for an application where there is no much space or budget for storage it will be preferable to have a production more distributed during the time while if it is needed immediate large quantities of hydrogen such as in transportation it will be preferable to have a production concentrated in a shorter period of time.

$$AEY_{PV\ used} = \left(\sum_{t=1}^{t=8760} (energy\ PV\ to\ eh1\ _t) + (energy\ PV\ to\ soec\ _t) + (energy\ PV\ to\ bess\ _t) + (energy\ PV\ to\ grid\ _t) \right) * 10^{-9}\ \text{[GWh/year]}$$

$$AEY_{PV\ waste} = \left(AEY_{pv} - AEY_{PV\ used} \right) * 10^{-9}\ \text{[GWh/year]}$$

$$AEY_{pv\ to\ eh1} = \left(\sum_{t=1}^{t=8760} (total\ energy\ from\ PV\ to\ eh1\ _t) \right) * 10^{-9}\ \text{[GWh/year]}$$

$$CF_{grid} = \left(\frac{AEY_{grid}}{(8760 * Max.energy\ injected) * 10^{-9}} \right) * 100\ [\%]$$

$$CF_{soec} = \frac{Total\ hours\ soec\ on}{8760} * 100\ [\%]$$

- Mass distribution:

The mass of particles used can be divided into 2 different categories. Particles sent to the heat exchanger placed in the power block of the CSP for electricity production and particles sent to the heat exchangers in charge of covering soec' thermal need; steam generator and superheater. The reason to make this division is the following. In order to have a levelized cost of the hydrogen (LCOH) that just involves the elements taking part in hydrogen production there should be a division of CAPEX. When talking about CAPEX it involves the capital expenditure of all the elements of the hybrid plant: PV, CSP, set of batteries, electrolyzer and heat exchangers. The division of the CAPEX is done according to the percentage of energy injected into the grid and into the SOEC. When splitting the CAPEX of the photovoltaic field it seems straightforward since the energy is used in form of electricity in both scenarios: grid and h2 production. However, when splitting the CAPEX of the CSP it turns more complicated. Now, particles are not only used for producing electrical energy but also

thermal in the case of hydrogen production. Once the division of particles used in each case is done it can be calculated a more accurate CAPEX for hydrogen production and eventually the LCOH as it is going to be shown in the economical KPIs section.

$$percentage_{pv\ to\ grid} = \left(AEY_{pv\ to\ grid}\ /AEY_{PV\ used}\right) * 100\ [\%]$$

$$percentage_{pv\ to\ soec} = 100 - percentage_{pv\ to\ grid}\ [\%]$$

$$percentage_{csp\_el\ to\ grid} = \left(AEY_{csp\ to\ grid}\ /AEY_{csp}\right) * 100\ [\%]$$

$$percentage_{csp\_el\ to\ soec} = 100 - percentage_{csp\_el\ to\ grid}\ [\%]$$

$$percentage_{csp\ to\ grid} = \frac{percentage_{csp\_el\ to\ grid} * \sum_{t=1}^{t=8760}\left(particles_{sent\ to\ pb\ HX}\right)}{\sum_{t=1}^{t=8760}(particles_{sent\ to\ pb\ HX}) + \sum_{t=1}^{t=8760}(particles_{sent\ to\ h2\ HXs*})}\ [\%]$$

$$percentage_{csp\ to\ soec} = \frac{\sum_{t=1}^{t=8760}(particles_{sent\ to\ h2\ HXs\ *}) + \left(percentage_{csp\_el\ to\ soec} * \sum_{t=1}^{t=8760}\left(particles_{sent\ to\ pb\ HX}\right)\right)}{\sum_{t=1}^{t=8760}(particles_{sent\ to\ pb\ HX}) + \sum_{t=1}^{t=8760}(particles_{sent\ to\ h2\ HXs\ *})}\ [\%]$$

*In sCO2 based configuration there are no particles sent to the heat exchangers involved in hydrogen production as for this configuration is sCO2 used instead. In the equation it will be introduced as 0.

3.6.2. Economical KPIs

The economical KPIs can be divided into three main different categories: CAPEX, OPEX and indicators. CAPEX is defined as the capital expenses for assets involved in a certain operation or project. In this case, the total CAPEX has been calculated as the sum of several "individual" CAPEX since the plant is formed by more than 1 energy generation source. As a result CAPEX is calculated for: PV ($CAPEX_{PV}$), CSP ($CAPEX_{CSP}$), batteries ($CAPEX_{BESS}$) and electrolyzer and heat exchangers ($CAPEX_{H2}$). The calculation of CAPEX was done by calculating total direct and indirect costs. Total capital direct costs already include subsidies and a contingency factor of 0.07 for CSP and 0.03 for PV and batteries. Indirect costs include a factor EPC (engineering, procurement and construction) of 0.13 for CSP and 0.1 for PV and batteries while the decommissioning factor is assumed to be 0.

- CAPEX:

$$CAPEX_{CSP} = Total\ capital\ direct\ costs_{csp} + Capital\ indirect\ costs_{csp}$$
$$= \left(\left(1 + factor\ cont._{csp}\right) * Capital\ direct\ costs\ with\ subsidies_{csp}\right)$$
$$+ \left(\left(factor\ EPC_{csp} + factor\ decom._{csp}\right) * Total\ capital\ direct\ costs_{csp} + Cost\ of\ land_{csp}\right)$$

$$CAPEX_{PV} = Total\ capital\ direct\ costs_{PV} + Capital\ indirect\ costs_{PV}$$
$$= \left(\left(1 + factor\ cont._{PV}\right) * Capital\ direct\ costs\ with\ subsidies_{PV}\right)$$
$$+ \left(\left(factor\ EPC_{PV} + factor\ decom._{PV}\right) * Total\ capital\ direct\ costs_{PV} + Cost\ of\ land_{PV}\right)$$

$$CAPEX_{BESS} = Total\ capital\ direct\ costs_{BESS} + Capital\ indirect\ costs_{BESS}$$
$$= \left(\left(1 + factor\ cont._{BESS}\right) * Capital\ direct\ costs\ with\ subsidies_{BESS}\right)$$
$$+ \left(\left(factor\ EPC_{BESS} + factor\ decom._{BESS}\right) * Total\ capital\ direct\ costs_{BESS}\right.$$
$$\left. + Cost\ of\ land_{BESS}\right)$$

$$CAPEX_{H2} = Total\ capital\ direct\ costs_{H2} + \ Capital\ indirect\ costs_{H2}$$
$$= 1.1(cost\ soec + cost\ hrs + cost\ sg + cost\ sh + cost\ eh)$$

$$CAPEX = CAPEX_{CSP} + CAPEX_{PV} + CAPEX_{BESS} + CAPEX_{H2}$$

Finally, CAPEX was also divided into 2 different categories: CAPEX for elements taking part in hydrogen production and CAPEX for elements taking part into delivering energy into the grid. To do so, it was applied the percentages calculated in the section of mass distribution as well as the CAPEX values previously calculated. In the equations below it is explained in detail how it was calculated for each case.

$$CAPEX_{H2\ PRODUCTION} = (percentage_{csp\ to\ soec} * CAPEX_{CSP}) + (percentage_{pv\ to\ soec} * CAPEX_{PV}) + CAPEX_{BESS} + CAPEX_{H2}$$

$$CAPEX_{EL.PRODUCTION} = (percentage_{csp\ to\ grid} * CAPEX_{CSP}) + (percentage_{pv\ to\ grid} * CAPEX_{PV})$$

- OPEX:

Likewise, OPEX was divided in the same way that CAPEX was. This means calculating OPEX for PV ($OPEX_{PV}$), CSP ($OPEX_{CSP}$), batteries ($OPEX_{BESS}$) and electrolyzer and heat exchangers ($OPEX_{H2}$). To calculate each of the OPEX values it was calculated its operating and maintenance fixed costs plus the rest of operating and maintenance costs times the annual energy yield for each case except for the case of $OPEX_{H2}$ that it was approximated to be a 12% of its CAPEX.

$$OPEX_{CSP} = Fixed\ OM\ costs_{CSP} + OM_{CSP} * AEY_{CSP} * 10^6$$

$$OPEX_{PV} = Fixed\ OM\ costs_{PV} + OM_{PV} * AEY_{PV} * 10^6$$

$$OPEX_{BESS} = Fixed\ OM\ costs_{BESS} + OM_{BESS} * AEY_{BESS} * 10^6$$

$$OPEX_{H2} = 0.12 * CAPEX_{H2}$$

$$OPEX = Fixed\ OM\ costs_{year} + OPEX_{CSP} + OPEX_{PV} + OPEX_{BESS} + OPEX_{h2}$$

Finally, OPEX was also divided into 2 different categories: OPEX for elements taking part in hydrogen production and OPEX for elements taking part into delivering energy into the grid. To do so, it was applied the percentages calculated in the section of mass distribution as well as the OPEX values previously calculated. In the equations below it is explained in detail how it was calculated for each case.

$$OPEX_{H2\ PROD.} = (OPEX_{CSP} * percentage_{csp\ to\ soec}) + (OPEX_{PV} * percentage_{pv\ to\ soec}) + OPEX_{BESS} + OPEX_{H2}$$

$$OPEX_{EL.\ PROD.} = (OPEX_{CSP} * percentage_{csp\ to\ grid}) + (OPEX_{PV} * percentage_{pv\ to\ grid})$$

- Indicators:

After calculating all annual energy yields (AEY), CAPEX and OPEX values for each case, it can be calculated the levelized costs of electricity ($LCOE$) and hydrogen ($LCOH$). However, it is also needed 2 additional indicators that will give us a more real perspective of economic feasibility, especially for the case of $LCOE$.

In this case, $LCOE$ can not be used as a reliable indicator since the definition that describes $LCOE$ will lead to a conclusion where the lowest values to produce electricity are found at the highest hydrogen productions. The reason for this to happen comes from the capex distribution formula. If CAPEX related with hydrogen production becomes larger, then by percentage distribution the CAPEX related with electricity production will become smaller. This conclusion could never take place and continuing with this definition could mislead the results of the thesis. For this reason, the economic KPIs that will be considered in the section of results and discussion will be: the electricity indicator, hydrogen indicator, energy indicator or LCOEn and finally the LCOH.

$$LCOE = \frac{CAPEX_{EL.PRODUCTION} * CRF + OPEX_{EL.PROD.}}{AEY_{grid}}$$

$$LCOH = \frac{CAPEX_{H2.PRODUCTION} * CRF + OPEX_{H2.PROD}}{AEY_{H2}}$$

$$LCOEn = \frac{CAPEX * CRF + OPEX}{AEY_{H2} + AEY_{EL}}$$

$$electricity\ indicator = \frac{CAPEX * CRF + OPEX}{AEY_{EL}}$$

$$hydrogen\ indicator = \frac{CAPEX * CRF + OPEX}{AEY_{H2}}$$

$$energy\ indicator = LCOEn$$

$$electricity\ indicator = \frac{Total\ annual\ costs\ (€)}{Annual\ energy\ injected\ into\ grid\ (MWh)}$$

$$hydrogen\ indicator = \frac{Total\ annual\ costs\ (€)}{Annual\ hydrogen\ production\ (kg)}$$

$$energy\ indicator = \frac{Total\ annual\ costs\ (€)}{Total\ annual\ energy\ production\ (MWh)}$$

$$LCOH = \frac{Total\ annual\ h2\ costs\ related\ (€)}{Annual\ hydrogen\ production\ (kg)}$$

3.7. Preliminary Analysis

A preliminary analysis was performed at the beginning and previous to any simulations in the code for 2 reasons: first to understand the behavior of the electrolyzer and second to choose its design features. To do so, first a hydrogen production mass flow rate of 36kg/h (0.01kg/s) was selected. Then, the overpotential or irreversibilities in the electrolyzer were plotted in function of several possible operating temperatures and current densities. The reason to choose these 3 parameters for the preliminary study is important since these will take place in the code and they will be introduced by the user. Having in mind a general understanding on how they can influence the final results from an energy and economic perspective will save time from non-helpful future simulations.

The overpotential or irreversibilities of an electrolyzer can be divided into three different categories: ohm (η_{ohm}) activation ($\eta_{act,a}$ and $\eta_{act,c}$) and concentrartion losses ($\eta_{conc,a}$ and $\eta_{conc,c}$). [29]. According to the type of irreversibility it will be found more or less sensitivity to temperature and current density changes. Once each of them are calculated it is possible to know the operation voltage of the soec.

$$V_{operation.SOEC} = E_{Nerst} + \eta_{ohm} + \eta_{act.} + \eta_{conc.}$$

Equation 1. SOEC operation voltage [30]

Where E is the equilibrium voltage that can be expressed with Nerst equation.

$$E_{Nerst} = E^0 + \frac{RT}{2F} \ln \left(\frac{P^0_{H_2} P^0_{O_2}{}^{\frac{1}{2}}}{P^0_{H2O}}\right)$$

Equation 2. Nerst Equation [30]

Firstly, ohm losses were studied. This type of irreversibility occurs when there is a voltage drop caused by the resistance offered by the electrodes and electrolyte to the flow of electrons. In this case the conductivity of the materials chosen as well as the thicknesses (specially electrolyte one) will not only influence the voltage need but also the life-span of the soec [31]. Having that into account the materials are chosen accordingly. When talking about the material is important that the materials chosen have the highest possible conductivity so that the electrical resistance is low and the ohm's overpotentital required is minimized. This is shown in the equation below where σ_a, σ_c and σ_e are the conductivities of the anode, cathode and electrolyte respectively.

$$V_{ohm} = jR_{ohm} = j\left(\frac{L_a}{\sigma_a} + \frac{L_c}{\sigma_c} + \frac{L_e}{\sigma_e}\right)$$

Equation 3. Ohmic overpotential [32]

Secondly when talking about thicknesses it is possible to find three different configurations: anode supported, cathode supported or electrolyte supported electrolyzers depending on which one is larger [29] [32] In this case, anode supported was chosen as it shows better electrical performance in terms of voltage irreversibilities [29]. Finally, having looking at Figure 10 it can be concluded that ohm irreversibilities get larger at higher current densities and lower at higher temperatures.

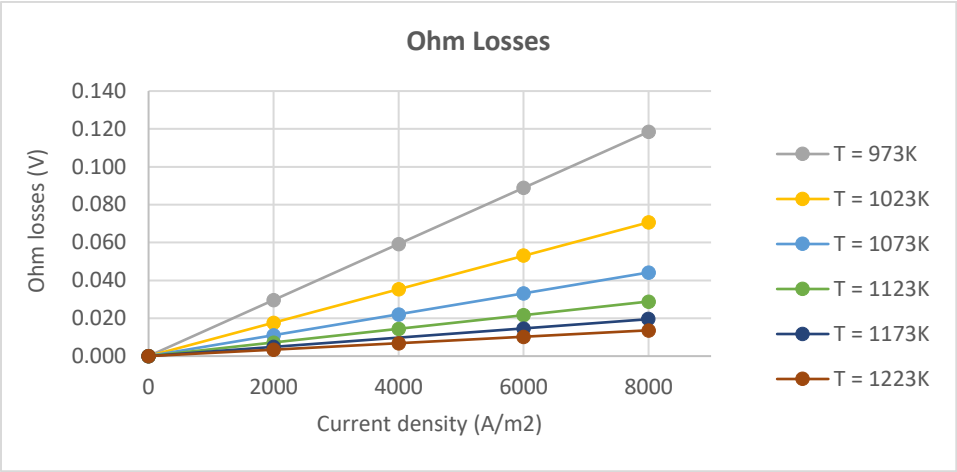

Figure 10. Ohm losses vs current density for different temperatures

Secondly, activation losses were studied. These losses occur as a consequence of the electrochemical reaction that transfers electrons from or to the electrodes. It can also be used as a reference to know about the activity in the electrodes [29]. The higher io,a or io,c gets (exchange current densities of the anode and cathode) the more active will be the electrode. [29]. The relationship between the electrodes and current density can be expressed with Butler-Volmer equation as shown in the following equations:

$$V_{act} = \frac{2RT}{nF} sinh^{-1}\left(\frac{i}{2i_{o,a}}\right) + \frac{2RT}{nF} sinh^{-1}\left(\frac{i}{2i_{o,c}}\right)$$

Equation 4. Butler-Volmer Equation – Activation losses [11]

$$i_o = i_{o,a} + i_{o,c} = \Upsilon_a * \exp\left(\frac{-E_{act,a}}{RT}\right) + \Upsilon_c * \exp\left(\frac{-E_{act,c}}{RT}\right)$$

Equation 5. Exchange current density for anode and cathode. [32]

Similar to the results found for ohm losses and as represented in Figure *11*, this type of irreversibility gets bigger at higher current densities and lower at higher temperatures. This happens because the exchange current density is also dependent on temperature.

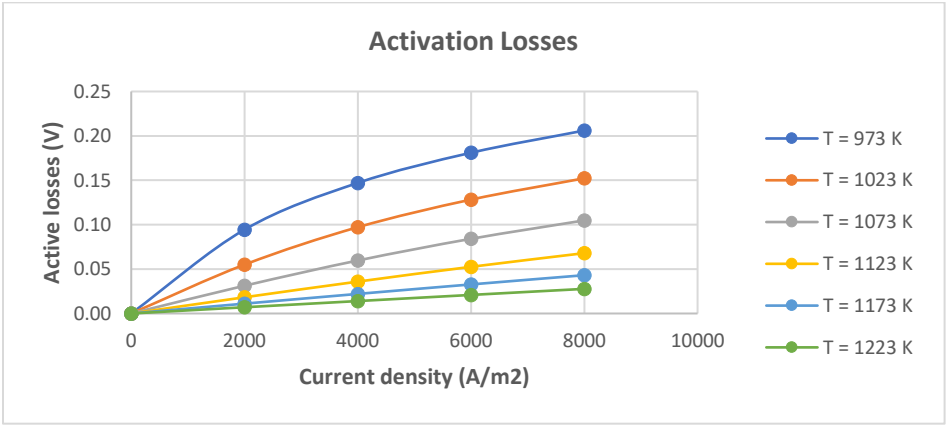

Figure 11. Activation losses vs current density for different temperatures

In third place; concentration or mass transportation losses were studied. This voltage loss occurs as a result of a change in the concentration of the reactant species in the surface of the electrodes as well

as in the concentration of the product leaving the electrodes [29] The concentration losses can be expressed as the difference in gas concentration in the electrode surface and at the electrode-electrolyte interface using the following expression [29]

$$V_{conc} = \frac{RT}{2F}\ln\left(\frac{P^*_{H2O} * P^0_{H2O}}{P^*_{H2} * P^0_{H2}}\right) + \frac{RT}{4F}\ln\left(\frac{P^*_{O2}}{P^0_{O2}}\right)$$

Equation 6. Concentration overpotential [11]

As it is represented in Figure *12* this type of irreversibility is not temperature dependent and as shown in the equation above it is mainly influenced by the different pressures taking place in the process. Pi^* represents the partial pressure of species at the electrode-electrolyte interface (Pa) while Pi^0 stands for partial pressure of species at the electrode surface [11].

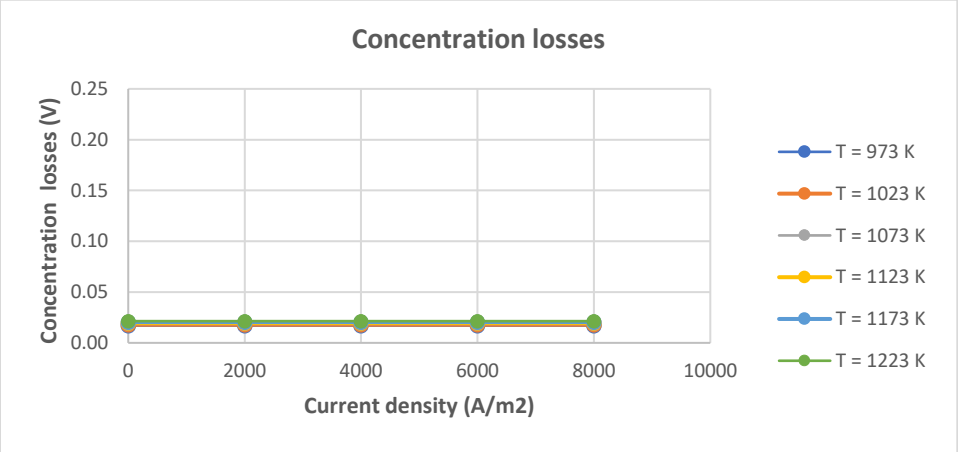

Figure 12. Concentration losses vs current density for different temperatures

Finally, having all irreverstibilites calculated, Figure *13* shows the total cell potential needed (operation voltage) depending on temperature and current density. When looking at it, it can be concluded that irreversibilities are highly sensitive to current density and temperature changes. The best and more stable results (at 101325Pa) in terms of losses are found at high temperatures and low current densities so it is also expected that in the future the code presents more stable results under these conditions. In opposite, scenarios with low temperatures will need of lower current densities in order to be competitive with high temperature ones.

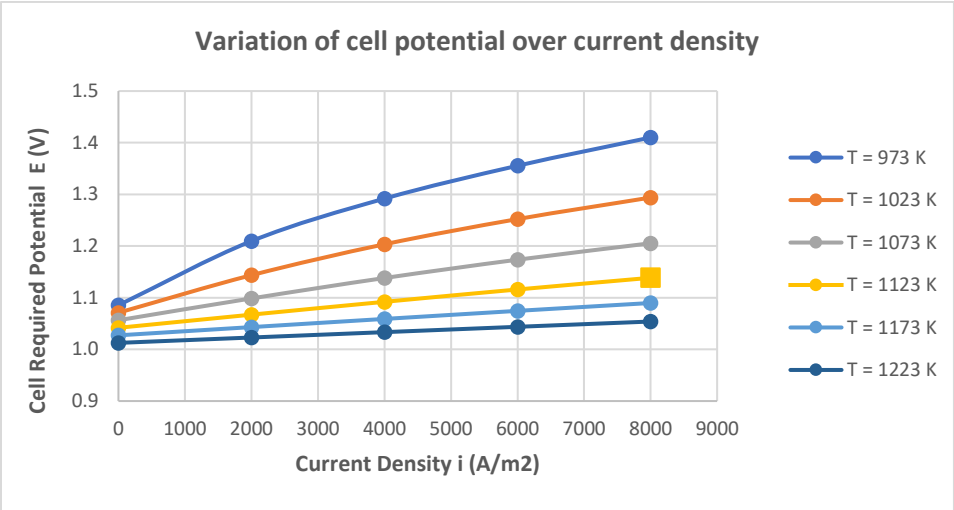

Figure 13. Cell potential vs current density for different temperatures

To conclude this preliminary analysis, a brief summary of electrical and thermal theoretical needs for the soec are presented at figures 14 and 15. Figure 13 shows how the electrical need keeps growing specially at high current densities while figure 14 proves that thermal need keeps stable once the current density values become larger than 4000A/m2 for all temperatures. For this reason, the future approach will be to keep this variable not larger than 5000 A/m2 like literature recommends for a soec electrolyzer runned at 1bar and anode-supported [29]. Otherwise, pressure operating conditions would need to be increased which would lead to a pressurization process that will be translated into more energy costs.

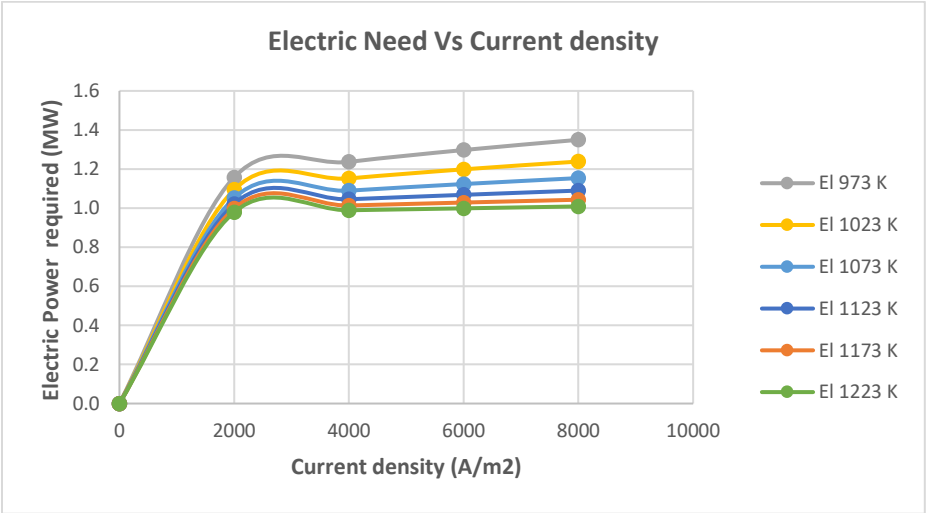

Figure 14. Electric need vs current density for different temperatures

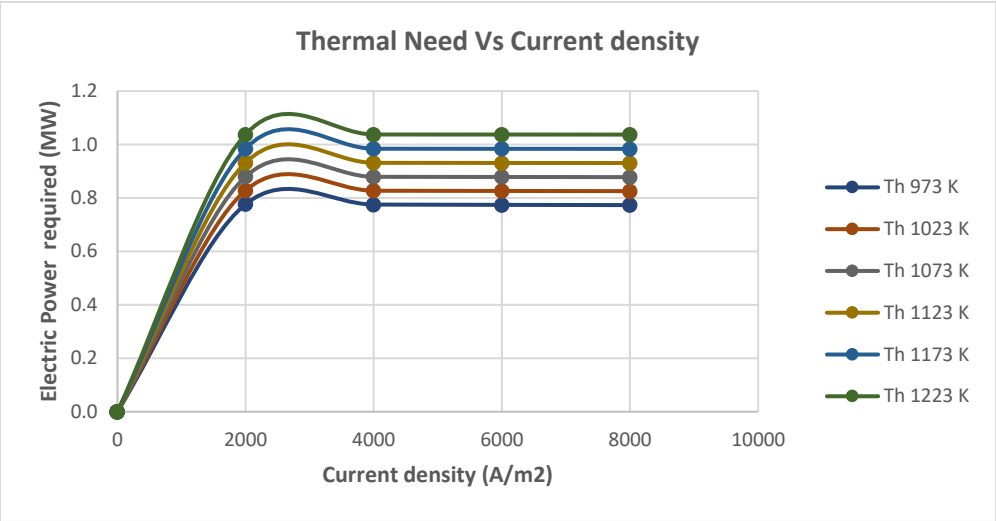

Figure 15. Thermal need vs current density for different temperatures

Summing up, after the preliminary analysis it is expected that future results will turn better at higher temperatures (towards 850°C-900°C in this case). Also, a value of 4000A/m2 will be fixed for all the simulations performed for the 3 configurations. The simulations conducted will later show what are the effects of the size of the electrolyzer or in other words of the hydrogen mass flow rate imposed (kg/h) as well as other elements taking place (PV size, battery capacity and CSP size).

Chapter 4

Model Description

4.1. System description

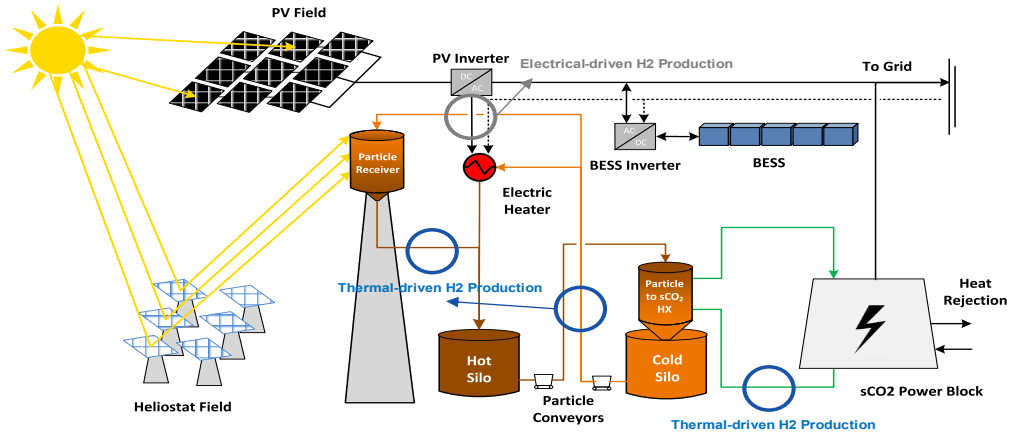

Figure 16. Hybrid plant description with potential integration strategies

The plant can be divided into 3 different systems. First, a photovoltaic plant (PV) with energy storage in form of batteries (BESS). The photovoltaic field supplies energy to the electrolyzer and heat booster and the surplus is sent to the batteries, electric heater and grid (in this order). Then, when there is low or no radiation batteries supply energy to the electrolyzer and/or heat booster.

Second, a concentrated solar plant (CSP) with thermal energy storage (TES = 14.5 hours). Thermal energy storage is installed into the plant through 2 insulated tanks or silos, one contains warm particles (T.hot = 780ºC) and the other one contains cold particles (T.cold = 550ºC). Particles are sent to a coupled power block which consists in a Brayton cycle with sCO2 where a steam turbine is ran to generate electricity. The electricity can be injected into the electrolyzer, heat booster or directly into the grid if the energy coming from the PV and/or batteries is not enough to cover the grid limits and the soec electrical requirements.

Third, a hydrogen production unit that consists on a high temperature electrolyzer (soec) and a system of heat exchangers that transforms water into steam and covers the soec thermal need. These are 1 heat recovery system, 1 steam generator and 1 superheater. Depending on the integration strategy the steam generator and superheater use particles or sCO2.

- Receiver integration strategy: uses particles coming from the receiver at 780ºC.
- TES integration strategy: uses particles coming from TES silos at 780ºC and 550ºC.
- sCO2 integration strategy: uses heat recovered from sCO2 in the power block.

Also, while the electrolyzer uses energy coming from PV, CSP or batteries to cover its thermal and electrical need, the grid only receives surplus energy coming from the PV or from the CSP after running the power block. (look at dispatch strategy in section 3.3).

4.2. Elements in the system

This section is going to explain the elements involved in each of the integration strategies as well as their characteristics, design features and range temperatures taking place in each case.

Table 2: Summary of elements taking place in each configuration							
Output	**Thermal**					**H2**	**Electrical**
Element	Heat recovery system	Steam generator	Super heater	Heat booster	Electric heater 2	Soec	Batteries
Receiver based	X	X	X	X		X	X
TES based	X	X	X	X		X	X
sCO2 based	X	X	X	X	X	X	X

4.2.1. Elements thermally involved

Phase 1: Firstly, water exchanges heat with the gases coming out of the electrolyzer at high temperature (750°C) with the aim of minimizing the heat waste. In this way, the heat recovery system warms up water from 26°C to approximately 32°C.

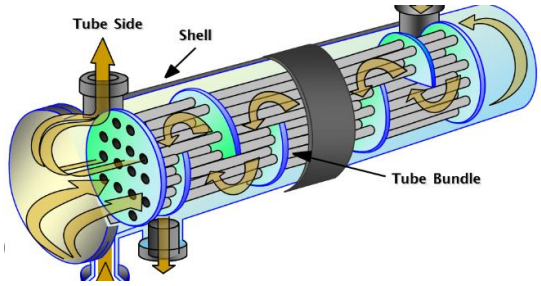

Figure 17. HRS: Shell-tube heat exchanger

The table below explains in detail the data and assumptions that have been made for this device.

Table 3: Heat recovery system data		
Type of heat exchanger	Shell tube	
Shell side (g) | Thot1	H2 and O2	Top = 750°C
Shell side (g) | Thot2	H2 and O2	40°C
Tube side (l) | Tcold1	Water	26°C
Tube side (l) | Tcold2	Water	32°C
Material	Stainless steel	
U (kW/m2 K)	250	

Phase 2 and 3: In a second phase, water coming out from the heat recovery system is warmed up to 100°C in a fluidized bed particle heat exchanger for receiver and TES based configurations and in a shell tube heat exchanger for the sCO2 based configuration. Next, a third phase continues in the super heater heat exchanger to raise the steam temperature up to conditions close to operating temperature. Here, it is used again a fluidized bed particle heat exchanger for receiver and TES based configurations and a shell tube heat exchanger for the sCO2 based configuration. Steam generator next to the super heater transforms water around 32°C into steam up to conditions close to operating temperature (Top≈750°C).

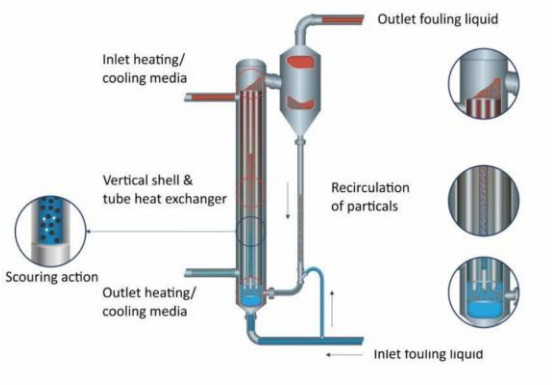

Figure 18. Fluidized bed particle heat exchanger

Table 4: Steam generator and super heater : receiver based configuration		
Type of heat exchanger	Fluidized bed	
Particles (s) | Thot1	Particles receiver	780ºC
Particles (s) | Thot2	Particles receiver	≈550ºC
Fluid (l) | Tcold1	Water	26ºC
Fluid (g) | Tcold2	Steam	<T.operation
Material	Stainless steel	
U (kW/m2 K)	250	

Table 5: Steam generator/Super heater: TES based configuration		
Type of heat exchanger	Fluidized bed / Fluidized bed	
Particles (s) | Thot1	Particles TES cold/ TES hot	550ºC/ 780ºC
Particles (s) | Thot2	Particles TES cold/TES hot	≈300ºC/ ≈550ºC
Fluid (l) | Tcold1	Water /steam	26ºC/100ºC
Fluid (g) | Tcold2	Steam/steam	100ºC/<T.operation
Material	Stainless steel	
U (kW/m2 K)	250	

Table 6: Steam generator and super heater: sCO2 based configuration		
Type of heat exchanger	Shell tube	
Particles (s) | Thot1	sCO2	587ºC
Particles (s) | Thot2	sCO2	≈497ºC
Fluid (l) | Tcold1	Water	26ºC
Fluid (g) | Tcold2	Steam	<T.operation
Material	Stainless steel	
U (kW/m2 K)	250	

For simplicity at receiver and sCO2 based configurations it has been assumed the thermal charge at the steam generator and superheater as a unique thermal charge to cover since the media to use is the same at both devices: particles coming from the receiver and sCO2 respectively. Nevertheless, the thermal charge at TES configuration has been divided for the steam generator and super heater. Now, each one uses its own media: cold and warm particles from the thermal storage (TES) to generate steam and raise steam temperature respectively.

Phase 4: Finally, a heat booster is used to raise steam some final degrees up to operating temperatures before being introduced into the electrolyzer.

4.2.2. Elements electrically involved

When talking about elements electrically involved in the system we can differentiate between elements that are electrically driven like the heat booster or the electric heater and elements that supply electricity like the batteries do.

Electric heater: the electric heater is an element placed between the thermal energy storage (TES) and the photovoltaic field. In this way, particles can be warmed up not only when sent to the receiver but also with surplus of energy coming from the photovoltaic field.

Batteries: batteries store part of the surplus of energy coming from the photovoltaic field. Later, this one is used and injected into the electrolyzer or heat booster when there is no radiation reaching the photovoltaic panels.

4.2.3. Electrolyzer

In the table below it is described the characteristics and design features of the electrolyzer. Here it shown the elements used as well as their properties.

Table 7: SOEC Parameters selection

Element	Parameter	Value	Unit
Electrolyte	Material	Yttria stabilized zirconia (YSZ) [31]	Dimensionless
	Thickness	12,5 [11]	µm
	Conductivity	3.34 x 10^4 exp (1.03 104/T) [32]	Ω-1 *m-1
Cathode	Material	Nickel-YSZ (Ni-YSZ) [31]	Dimensionless
	Thickness	12,5 [11]	µm
	Conductivity	8x10^4 [32]	(Ω^{-1} m^{-1})
	Activation energy	100 [32]	kJ/mol
	Pre- exponential facor (Yc)	1,34x10^{10} [32]	A/m2
Anode	Material	Lanthanum strontium manganite-LSM [31]	Dimensionless
	Thickness (m)	17,5 [11]	µm
	Conductivity	8,4 x10^3 [32]	(Ω^{-1} m^{-1})
	Activation energy	120 [32]	kJ/mol
	Pre-exponential factor (Ya)	2,051 x10^9 [32]	A/m2
Cell	N cells	Asoec/Acell	Dimensionless
	A cell	0,04	m2
	i	4000	A/m2

The materials for the elements chosen were Yttria stabilized zirconia (YSZ) for the electrolyte, lanthanum strontium manganite- (LSM) for the anode and Nickel-YSZ (Ni-YSZ) for the cathode. Having YSZ for the electrolyte will provide good stability in oxidant atmospheres and good ionic conductivity in high temperatures [31] Using Nickel-YSZ (Ni-YSZ) in the cathode is the most widely used option around soec electrolyzer's. The reason why is that these two components result in a great combination when put together. Niquel takes care of the electrons transportation while Yttria stabilized zirconia allows the diffusion of oxygen ions. As a result, a high electric conductivity and

catalytic capacity is achieved. [31]. Finally, lanthanum strontium manganite- (LSM) was used for the anode as it is commonly used for temperatures of around 800 to 900°C because of its good thermal and chemical results [31]. The selection of these materials for the soec design will prevent from future higher voltage losses and it will expand its lifespan.

Chapter 5

Simulation Results and Analysis

In this section the results obtained from the simulations ran in python are going to be shown. As it was detailed in section 3.4.1 a sensitivity analysis was conducted for the three configurations attending to soec installed capacity (MWh), PV size (MWp) and battery size (MWh). Because of the high amount of data resulted from the sensitivity analysis, the results shown are going to be referred to a case. This will be best battery results for simplicity in the postprocessing phase as well as when explaining the results in this report. However, in a future it will be helpful to use a statistical program that could be able to find further and more complex relations between all the parameters in the study (R or SAS are widely used).

In the post processing of the results, data has been analyzed aiming to find the pattern or patterns for minimizing three different functions: first, the levelized cost of the energy, LCOEn or energy indicator (€/MWh), second the electricity indicator (€/MWh) and third, the hydrogen indicator (€/kg h2). These economic parameters follow the definitions described in section 3.6 for key performance indicators. Also, other performance indicators such as the total annual energy produced (GW) as well as the flow distribution of energy in the plant will be analyzed. Now, the results for each of the configurations are going to be shown in detail individually.

5.1. Results for receiver based configuration

5.1.1. Hydrogen Indicator optimization (€/kg h2)

Firstly, the hydrogen indicator value trend is going to be analyzed under the influence of different battery sizes. Secondly, an energy analysis will be conducted to finally conclude with an economical analysis over the optimized scenario found for the configuration.

- **Battery Capacity Influence**

As mentioned at the beginning of this section a first analysis dependent on the battery size was conducted for all the results obtained in the sensitivity analysis. This was done to have a general vision on whether or not the behavior of the plant responded positively to a configuration with a set or batteries resulting this in a huge filter for continuing with next analysis.

Table 8. Receiver based: Best hydrogen indicator scenarios according to battery capacity

	Hydrogen Indicator (€/kg)	Electricity Indicator (€/MWh)	Energy Indicator (€/MWh)	PV size (MW)	Soec installed capacity (MWh)
Batt size = 0.5MWh	10.95	540.63	203.79	100	95
Batt size = 90 Mwh	11.89	523.39	211.61	100	70
Batt size = 180MWh	12.17	534.51	216.43	100	70
Batt size = 270MWh	12.30	824.23	254.26	70	95

The best results in terms of hydrogen indicator are found for a scenario which battery capacity is the lowest under study; 0.5 MWh, PV size of 100MW and a soec installed capacity of 95MWh (Table 8).

The graphs below represent the tendency that the hydrogen indicator follows with respect to the soec installed capacity and the size of the photovoltaic field. Looking at the graphs is very difficult to obtain

a conclusion on what are the parameters or factors that makes this configuration to have lower hydrogen production prices. However, it can be appreciated in both graphs that when increasing the soec capacity installed the results get directly affected. This means that higher hydrogen productions will have a higher influence in the results than small ones where there the trend is linear.

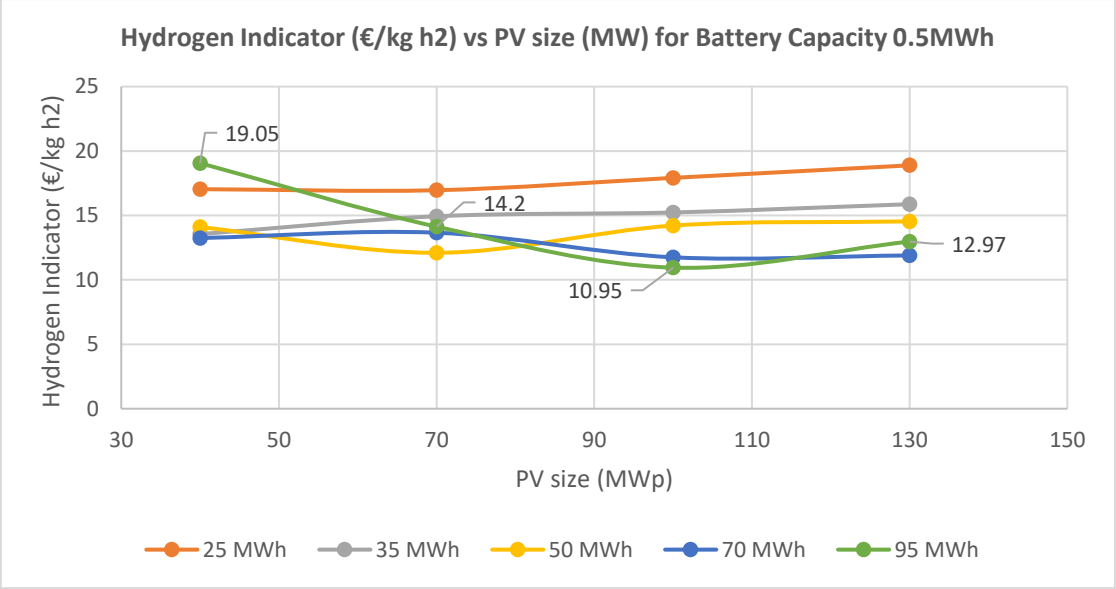

Figure 19. Receiver based: Hydrogen indicator trend for battery capacity of 0.5MWh

Also, these graphs already shows 2 important outcomes. First, in the receiver based configuration is not going to be possible to obtain a hydrogen indicator value below 10€/kg h2. Second, a soec with high capacity needs to be installed as well as batteries with small capacity if the optimized scenario for the hydrogen indicator wants to be implemented.

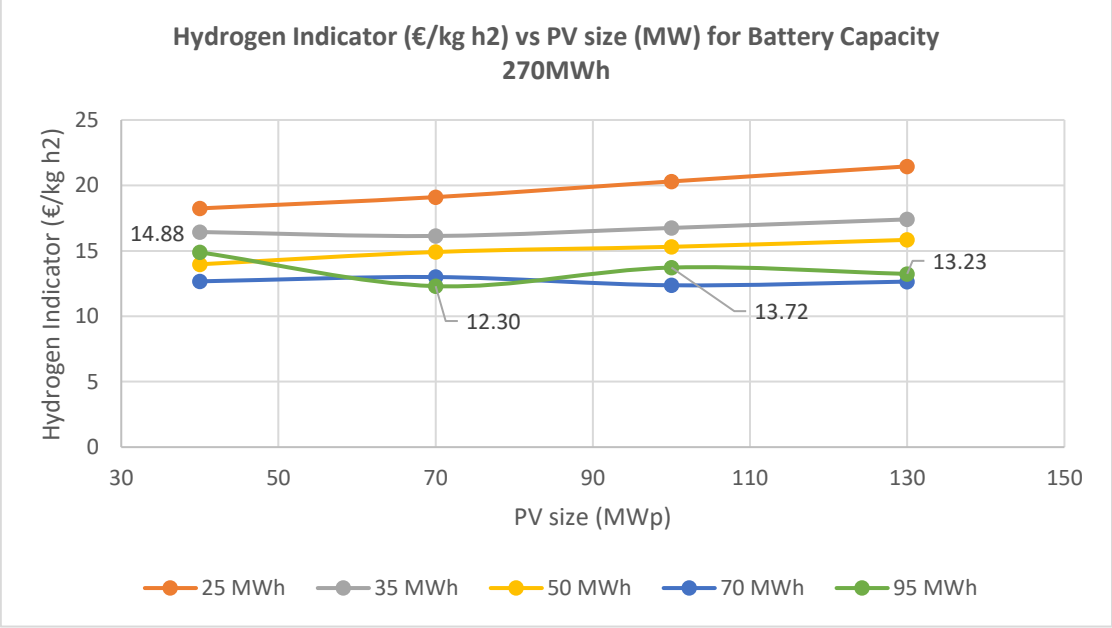

Figure 20. Receiver based: Hydrogen indicator trend for battery capacity of 270MWh

- **Energy Analysis for best hydrogen indicator scenario**

Once the battery size was found to offer better results for a capacity of 0.5MWh a further study was developed to understand how the economic results converge according to technical KPIs: energy injected directly into the grid (from PV or CSP) and energy produced in form of h2. Here, the annual energy generated is going to be represented along with the economic results in a graphical way.

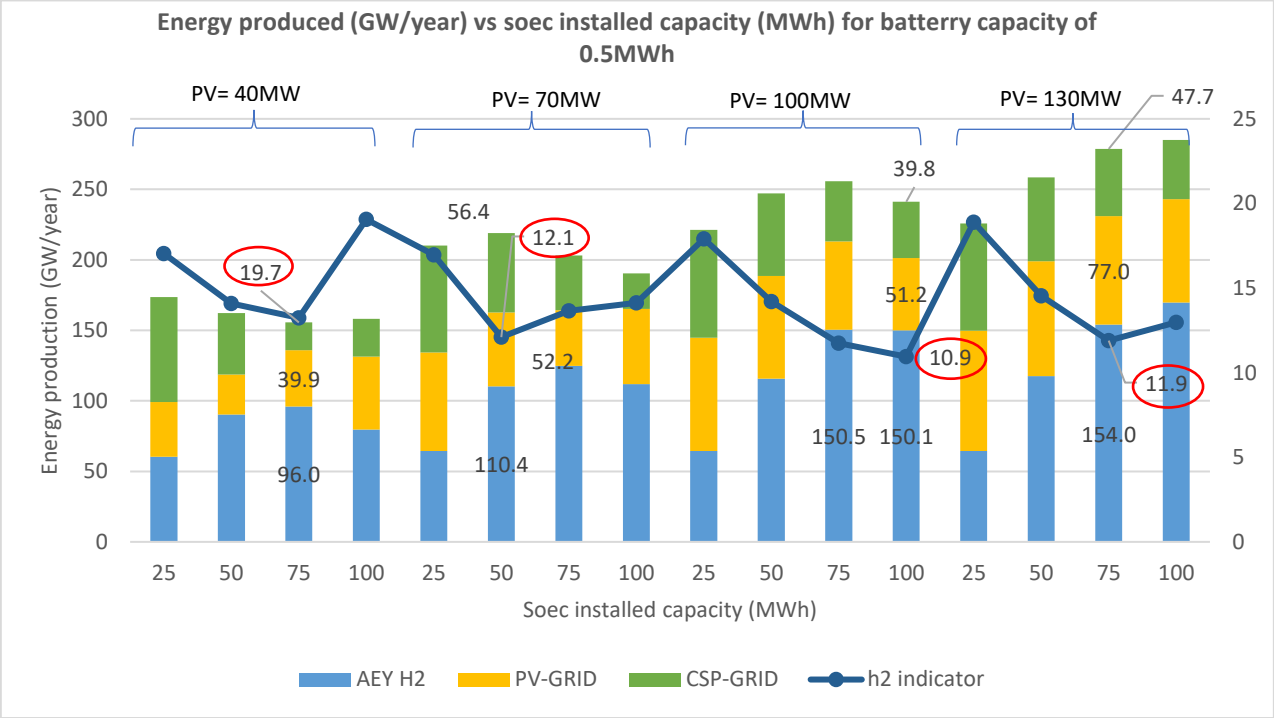

Figure 21. Receiver based: Annual energy produced

Looking at Figure 21 there are 2 main conclusions that can be obtained.: First, when increasing the size of the PV the hydrogen indicator value decreases until it converges at 100MWh for a pv size of 100MWp.

Also, for all PV sizes (except PV=70Mw) it is found that the minimum value for the hydrogen indicator occurs when low energy from the power block gets injected into the grid. This last conclusion fits with the soec thermal requirements of this configuration since the particles coming from the receiver are destinated to cover the thermal need of the electrolyzer and only the surplus goes to the hot silo. Afterwards, the hot particles stored in the hot silo will be used for generating electricity in the power block.

In Figure 22 it is represented the concept that has been just introduced. The thermal need of the electrolyzer is approximately a 40% of its total energy need at an operation temperature of 750ºC. As a result, there is low injection of energy into the grid coming from the CSP specially at high hydrogen productions, provoking as a consequence higher electricity and energy indicators.

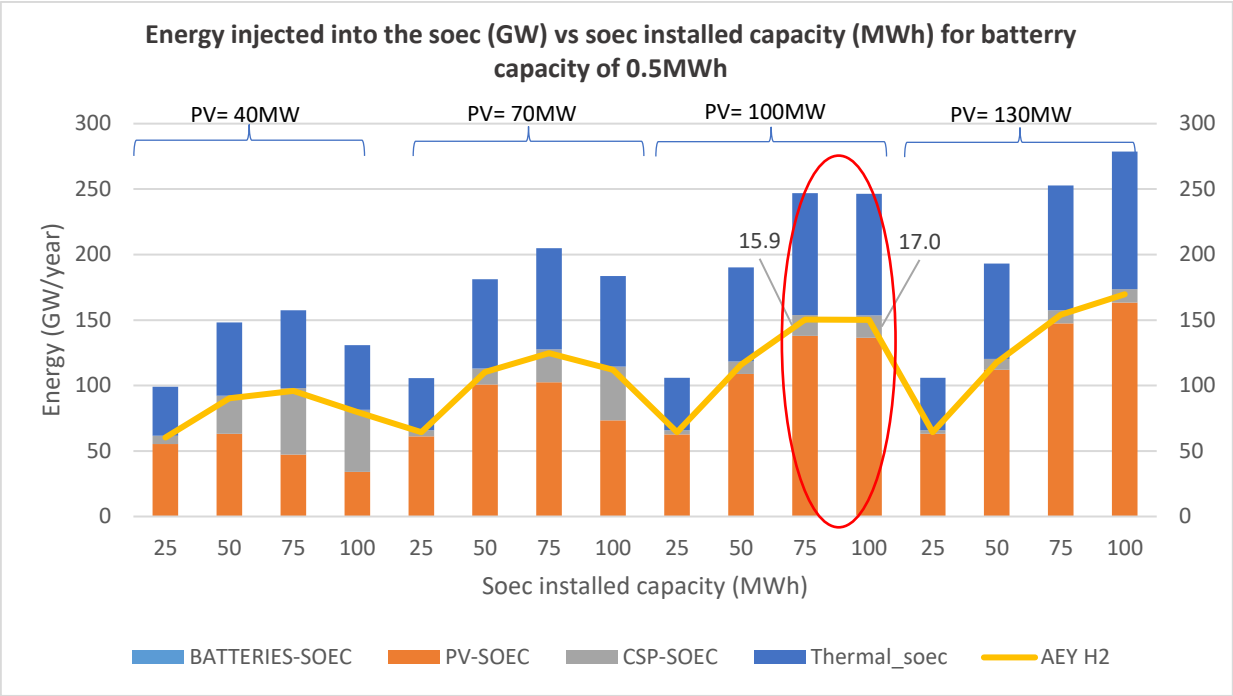

Figure 22. Receiver based: Comparison of hydrogen energy produced and energy injected into the soec

Finally, taking a look to the two configurations bounded under a red circle above, it is found that from a technical point of view their outcome is very similar:

Table 9. Receiver based: Best 2 hydrogen indicator scenarios for battery capacity 0.5MWh

Soec installed capacity (MWh)	Energy in form of h2 (GW/year)	Thermal energy_soec (GW/year)	CSP-Soec (GW/year)	PV-Soec (GW/year)	H2 indicator (€/kg h2)	CAPEX stack replacements (M€)
75	150.5	93	15.9	137.9	11.7	178.6
100	150.1	92.9	17	136.5	10.9	158.8

However, the configuration with lower installed capacity (75MWh) results into a CAPEX slightly higher because its stack needs 2 replacements while the configuration with higher installed capacity just needs 1. Applying the formula for the h2 hydrogen indicator, the best outcome will correspond with the configuration that has lower capex and slightly lower annual hydrogen production.

- **Economic Analysis for best hydrogen indicator scenario**

In the chart below (Figure 23) it is represented the capex distribution for the scenario that represented the lowest hydrogen indicator (10.95 €/kg h2). Here, the cost of integrating hydrogen is put in perspective with the rest of costs in the plant. The fact of needing a high rate production of hydrogen makes the size of the electrolyzer to be really high as well (19143m2). Consequently, its contribution into the total CAPEX becomes as high as the one from the concentrated solar plant (CSP).

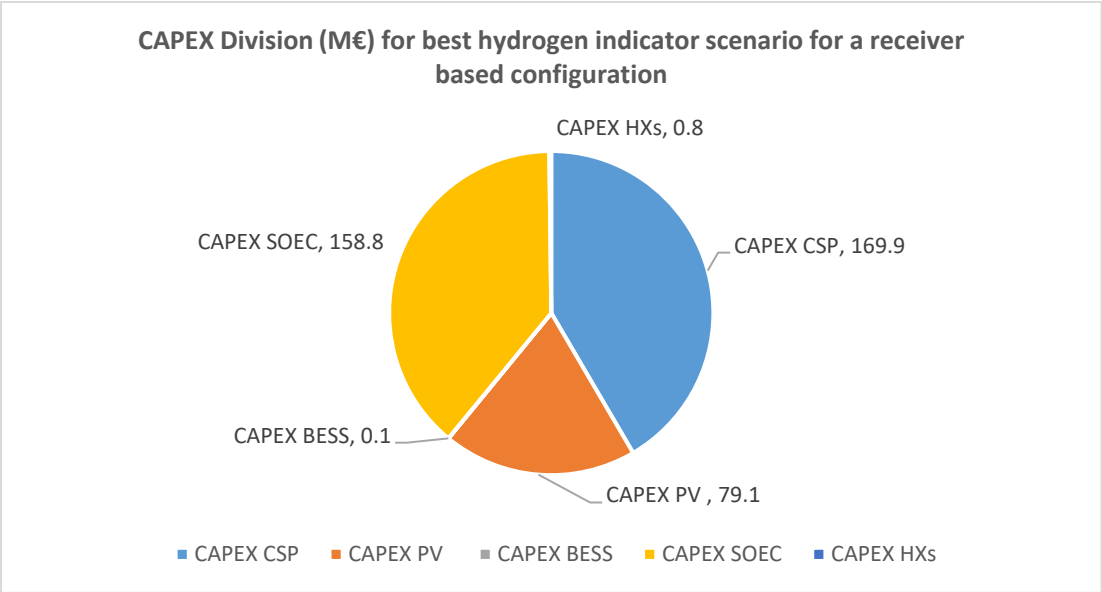

Figure 23. Receiver based: CAPEX distribution for hydrogen indicator optimized scenario

Taking this into account plus a conversion efficiency energy-h2 of approximately a 60% does not make the best hydrogen scenario case like the most feasible from a technical perspective. This is why in the following section, *discussion*, a different approach is going to be used. This approach will seek for not only a configuration that enables implementation from a technical point of view but also offers reasonable values for the production of energy as a global product.

- **Conclusions for hydrogen indicator**

To summarize all mentioned in the economical and technical analysis for the hydrogen indicator we can conclude the following. First, when seeking for lowest hydrogen production prices it should be considered choosing a set of batteries with small capacity or non existing. Also, an equilibrium between the annual production of hydrogen and the electrolyzer costs must be achieved. In other words, it should be optimized the work hours of the electrolyzer during the lifespan of the hybrid plant. Finally, the size of the electrolyzer that would need to be employed as well as its cost and energy conversion efficiency does not make this case as the most feasible.

5.1.2. Electrical and Energy Indicator

Similar to the analysis performed for the hydrogen indicator, the electrical and energy indicator trend will also be studied under the influence of different battery sizes. Secondly, it will take place an analysis to study how electricity and energy production prices varies according to different capacities for the electrolyzer (MWh) and different sizes for the PV field.

In the table below it is presented the scenarios that offered best results for the electrical and energy indicators according to different battery sizes. For all of them the best electrical and energy indicator values correspond to the scenarios where there is no hydrogen production. This, confirms the concept already introduced before: introducing hydrogen production into the system might not lead to direct economic benefits. However, in the energy analysis it is going to be explored the potential and opportunities of introducing hydrogen production while trying to minimize the increasing economic effects on the electrical and energy indicators.

Table 10. Receiver based: Best electricity and energy indicator scenarios according to battery capacity

	Hydrogen Indicator (€/kg h2)	Electricity Indicator (€/MWh)	Energy Indicator (€/MWh)	PV size (MW)	Soec installed capacity (MWh)
Batt size = 0.5MWh	-	99.25	99.25	40	0
Batt size = 90 Mwh	-	110.53	110.53	40	0
Batt size = 180MWh	-	121.83	121.83	40	0
Batt size = 270MWh	-	133.12	133.12	40	0

Furthermore, the best (lowest) results were found for the smallest battery capacity, 0.5MWh. This conclusion was preliminarily expected for the electricity indicator since the battery only transfers energy to the electrolyzer. However, for the case of the energy indicator this was not clear as this parameters studies both, electricity injected into the grid but also energy derived from hydrogen production.

Looking at the graphs below (Figure 24 and Figure 25) it is seen the influence of not only different soec installed capacities but also of different PV sizes for different scenarios that have in common a battery size of 0.5MWh. Here it is represented in a graphical way the effects of imposing bigger hydrogen productions over the electricity and energy production prices. As a result, the lowest numbers are found for a PV size of 40MW and small soec capacities, **below 5MWh** (lowest production prices: 99.25€/MWh and 98.83€/MWh for electricity and energy indicators respectively).

Note that when using big PV sizes the results turn to be rather similar. This happens because the limit of energy injection for the grid is frequently achieved. However, the PV plant results oversized in most of the cases, producing energy that is eventually non used. Waste of energy wants to be avoided specially in presence of a system with hydrogen production.

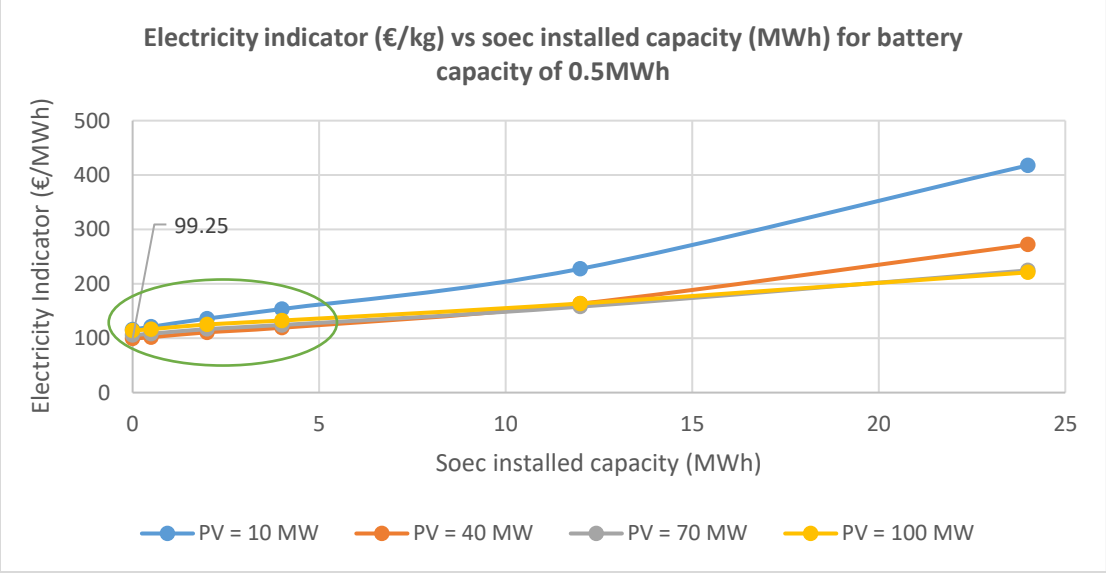

Figure 24. Receiver based: electricity indicator trend

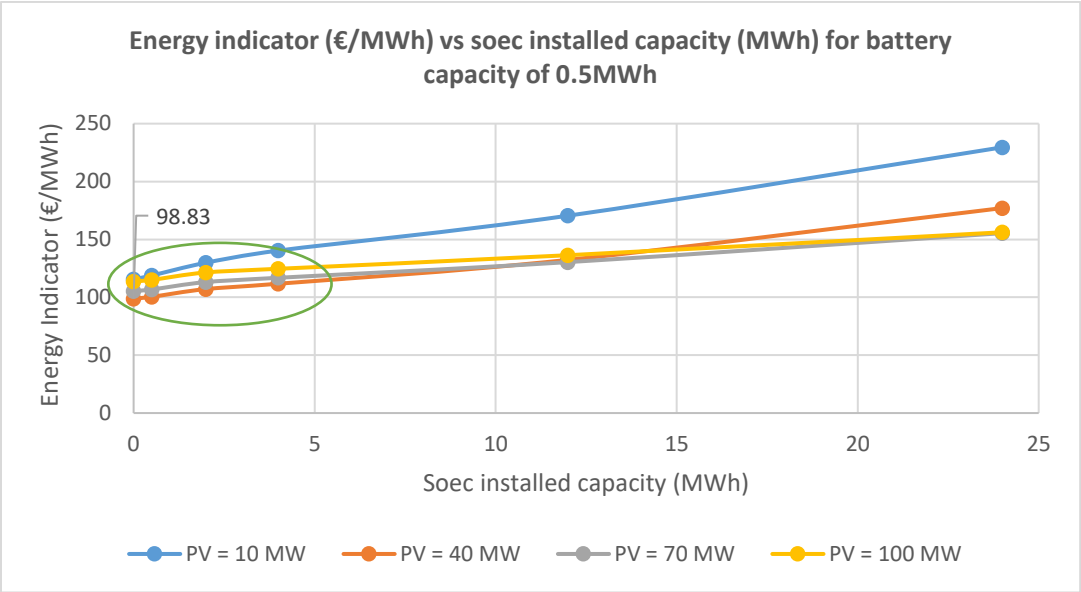

Figure 25. Receiver based: energy indicator trend

In both cases, for the electrical and energy indicators, best results are achieved when no hydrogen production is introduced. However, a certain hydrogen production can be implemented without causing a big alteration in the energy production prices. This concept is going to be study in the next section where a soec capacity of no more than 5MWh will be implemented.

- **Energy Analysis: Electricity Indicator**

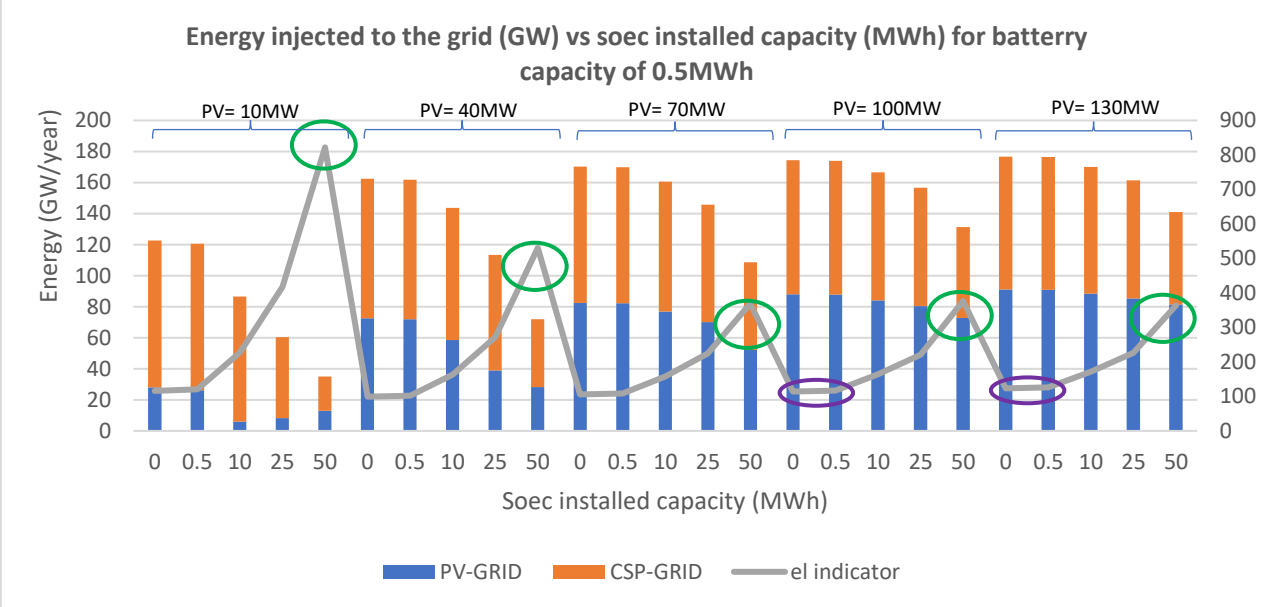

Figure 26. Receiver based: Energy injected into the grid for different soec capacities installed (MWh)

Looking at the plot above (Figure 26) it is clear that when implementing hydrogen production into the plant, the electricity indicator increases. The use of particles coming from the receiver to produce steam and eventually hydrogen stops from producing electricity. As a consequence, less energy is injected into the grid and higher electricity indicator values are obtained. Also, the hydrogen indicator

maximum values follow a descendent trend when increasing the size of the PV plant until it converges for a size of 70MW (look at the points marked with a green circle). As mentioned before, higher sizes of PV allows to cover the electrical demand of the electrolyzer as well as injecting energy into the grid at the same time. However, when selecting sizes above 40MW we are oversizing the system for the majority of the combinations represented in the plot, specially at low mass flow rates (look at points marked with a purple circle).

- **Energy Analysis: Energy Indicator**

Looking at the plot below (Figure 27) it is firstly observed how the total energy produced in the PV and CSP does not correspond with the total annual energy production. This happens because the process of producing hydrogen is not a 100% effective. In particular, this electrolyzer has an efficiency of 60% so hydrogen production will never be as effective as directly injecting energy into the grid. As a consequence and as shown in the plot the energy indicator results are better when the particles are sent to the power block to produce electricity that gets injected into the grid (look at small soec capacities: 0.5-1MWh).

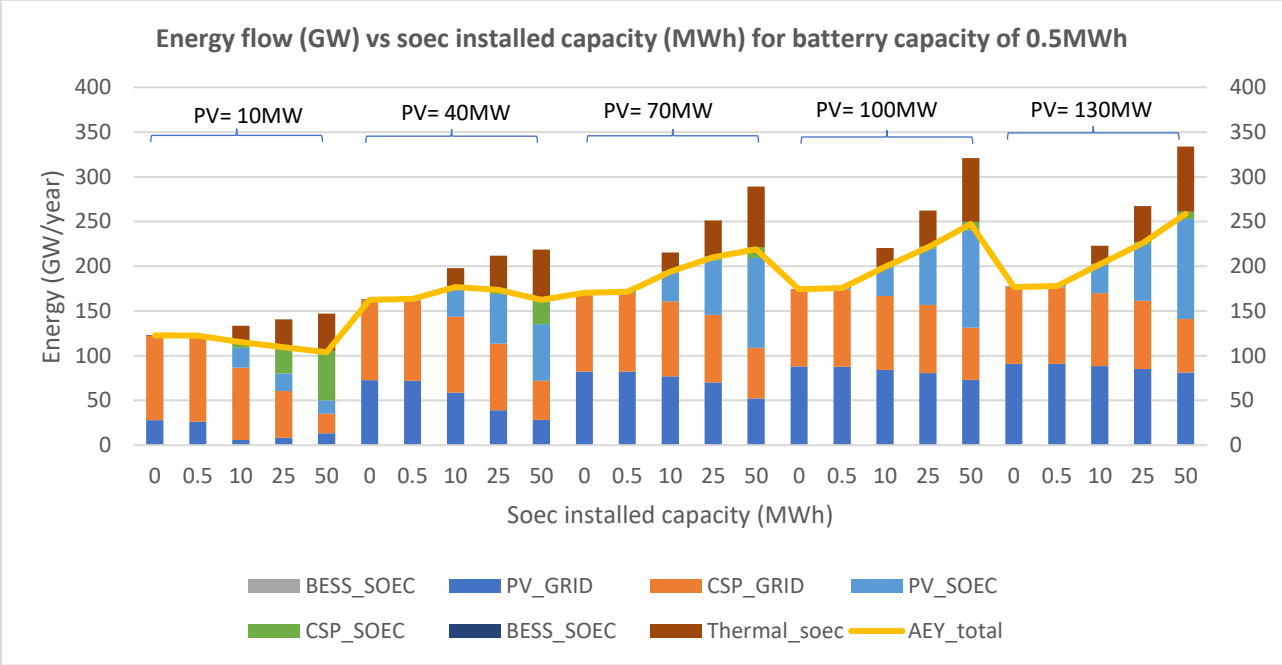

Figure 27. Receiver based: Energy contributions to the soec and grid compared to total energy production

5.2. Results for thermal storage based configuration

The analysis of the results obtained for the thermal energy storage (TES) based configuration will follow the same structure as the results presented for the receiver based configuration.

5.2.1. Hydrogen Indicator

First, the hydrogen indicator value trend is going to be analyzed under the influence of different battery sizes. Secondly, an energy analysis will be conducted to finally conclude with an economical analysis over the optimized scenario found for the configuration.

- **Battery capacity Influence**

Following the same approach as in the previous configuration, firstly an analysis about the results obtained in the sensitivity analysis was conducted according to the different battery capacities.

Table 11. TES based: Best hydrogen indicator scenarios according to battery capacity

	Hydrogen Indicator (€/kg h2)	Electricity Indicator (€/MWh)	Energy Indicator (€/MWh)	PV size (MW)	Soec installed capacity (MWh)
Batt size = 0.5MWh	12.88	269.02	150.10	100	70
Batt size = 90 Mwh	13.03	504.51	219.60	100	50
Batt size = 180MWh	11.65	239.76	141.69	100	25
Batt size = 270MWh	11.42	462.53	209.93	70	25

For this configuration, the best hydrogen indicator result is found for the scenario with highest battery capacity, 270MWh, where the value is 11.42€/kg. However, this is not the configuration that presents the best result in terms of energy indicator. For this reason, the scenario with a battery capacity of 180MWh will be further analyzed instead. This configuration offers the lowest energy indicator 141€/MWh from all the cases described in Table 11 and additionally it has a very similar hydrogen indicator result, 11.65 €/kg. It has to be taken into account that even if it is aimed to seek for the lowest value in terms of €/kg h2, the rest of the results will have to be equally feasible if the configuration wants to be implemented in the future.

The graphs below represent the tendency that the hydrogen indicator follows with respect to the soec installed capacity and the size of the photovoltaic field. Looking at the plots below it seems clear that for a TES based configuration, the results of implementing higher battery capacities are positive as the hydrogen indicator values become smaller. This occurs because there is a higher interaction between the batteries and the electrolyzer as it will be shown in the energy distribution analysis.

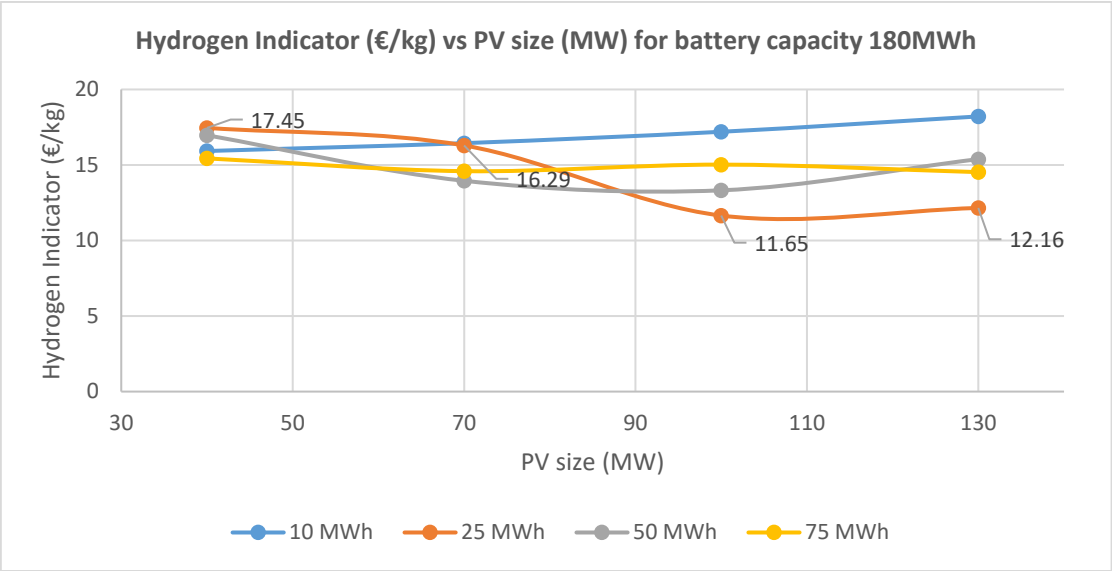

Figure 28. TES based: Hydrogen indicator trend for battery capacity of 180MWh

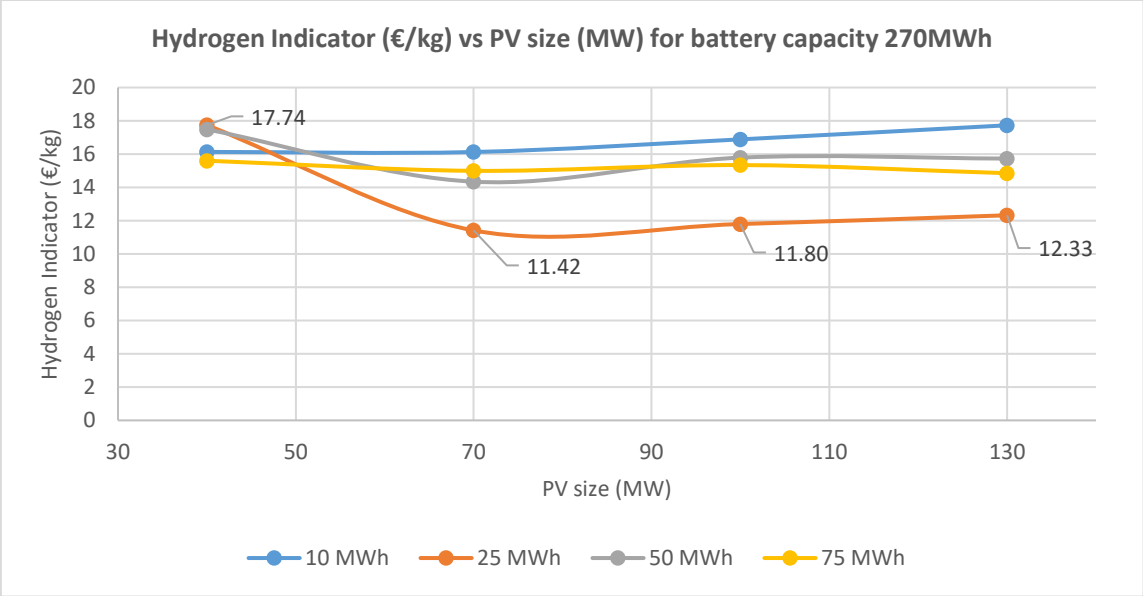

Figure 29. TES based: Hydrogen indicator trend for battery capacity of 270MWh

Also, for both battery capacities represented; 180MWh and 270MWh the hydrogen indicator trend becomes more stable when increasing the PV size. Specially, for the cases represented under a battery capacity of 270MWh. This happens because when implementing big PV sizes, there is a consequent bigger amount of surplus of energy sent directly into the battery. This energy can be sent later into the electrolyzer when there is no radiation together with the particles stored in the silos to cover the electrolyzer's electrical and thermal needs respectively. This makes this configuration very interesting from the energy use point of view (next analysis) since the thermal need of the soec can also be covered even when there is no radiation available.

- **Energy Analysis for best hydrogen indicator scenario**

Once the battery size was found to offer better results for a capacity of 180MWh a further study was developed to understand how the economic results converge according to technical KPIs: energy injected directly into the grid (from PV or CSP) and energy produced in form of h2. Here, the annual energy generated is going to be represented along with the economic results in a graphical way.

Looking at the graph below (Figure 30) there are 2 main conclusions that can be obtained. First, when increasing the size of the PV the local minimum values for the hydrogen indicator decreases until it converges at 25MWh for a pv size of 100MWp (look at the red circles).This happens because when implementing bigger PV sizes, the electrical requirement of the electrolyzer is covered in its majority by the energy coming from the PV (or batteries) so the particles in the silo can be used to cover the thermal need of the electrolyzer.

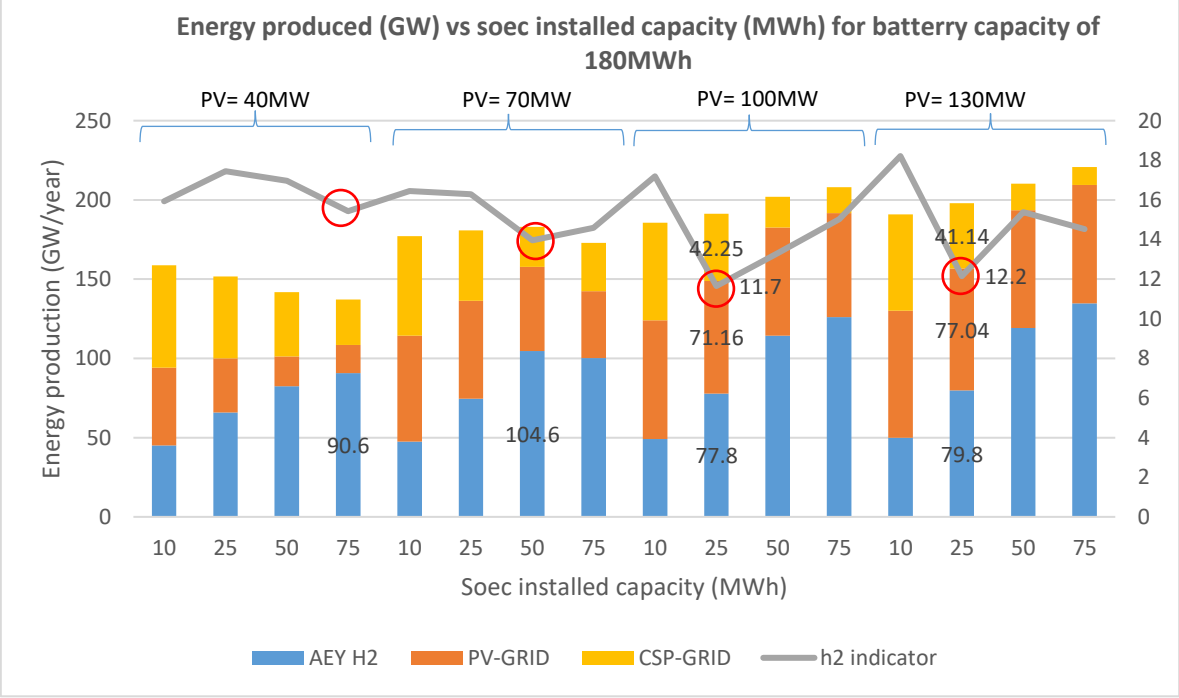

Figure 30. TES based: Annual energy produced

Also, the scenario with best hydrogen indicator does not offer one of the highest hydrogen energy productions (77.78GW/year). However, its stack just needs to be replaced once during the hybrid plant lifespan making this configuration the one that offers the best ratio between the capital costs and the annual hydrogen production.

Furthermore, Figure 31 represents the flow of energy coming from CSP, PV and batteries to the electrolyzer. This plot shows how the contribution of the batteries is noticeable in the TES based configuration contributing with at least 8GW/year for all the scenarios represented in the graph. Also, the electricity sent from the power block to the electrolyzer is minimal when compared to the battery and PV one. This happens as a result of the modeling of this configuration where particles in the TES are used to cover the thermal need of the electrolyzer.

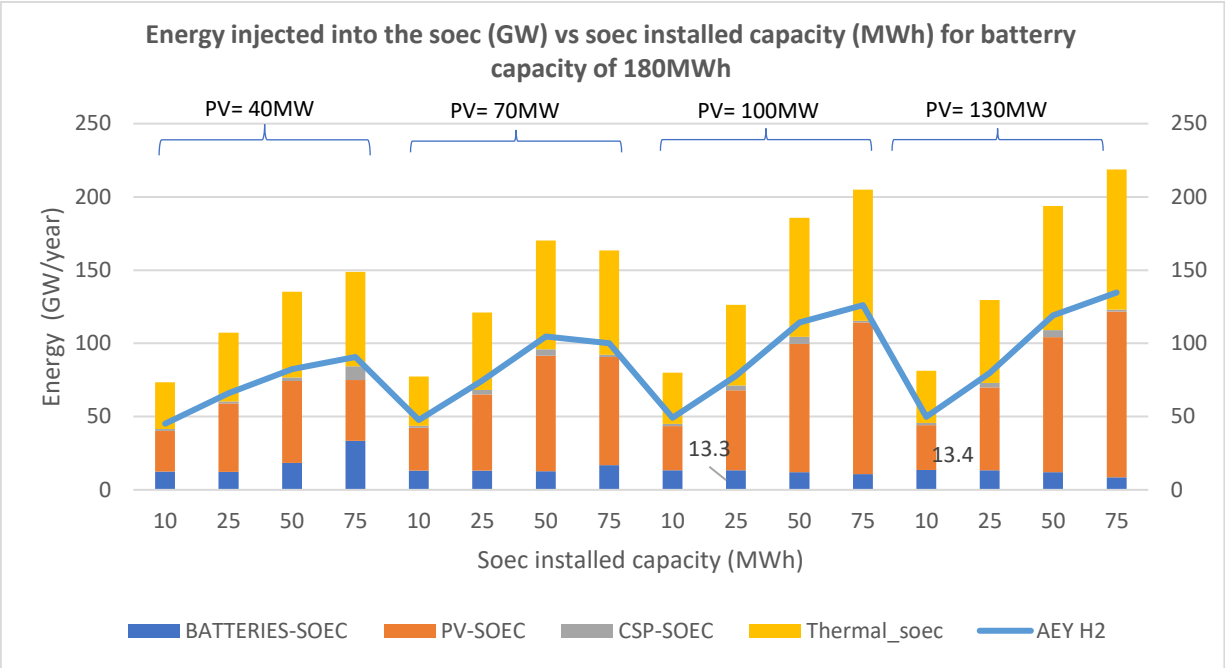

Figure 31. Receiver based: Comparison of hydrogen energy produced and energy injected into the soec

- **Economic Analysis for best hydrogen indicator scenario**

In the chart below it is represented the capex distribution for the scenario that represented the second best hydrogen indicator (11.65 €/kg) and the best LCOEn (141.69€/kg) described in table 11. Here, the cost of implementing hydrogen production following the configuration that offers best hydrogen indicator is put in perspective with the rest of costs in the plant. From a cost point of view, the highest investment costs come from the CSP plant (170M€) followed by the PV plant (79.1M€). In opposite, the lowest costs come from the batteries (49M€), the electrolyzer (19.9M€) and the group of heat exchangers (0.1M€).

However, the size of the electrolyzer results also too high for this configuration (4785m2) as well as its respective electricity indicator (239.76€/MWh). This is why in the following section, *discussion*, a different approach is going to be used. This approach will seek for not only a configuration that enables implementation from a technical point of view but also offers reasonable values for the production of energy as a global product.

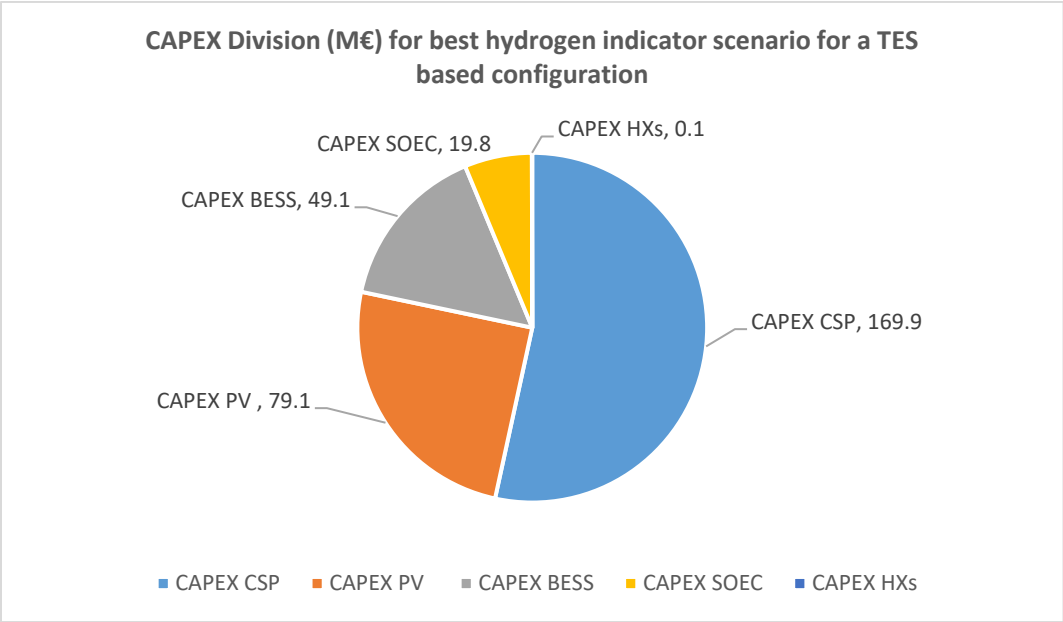

Figure 32. TES based: CAPEX distribution for hydrogen indicator optimized scenario

- **Conclusions for hydrogen indicator**

Summing up the results found in the TES based configuration it can be concluded the following. First, the battery capacity installed makes a positive influence on the hydrogen indicator results when considering big sizes. There is a big electrical input coming from the batteries into the electrolyzer while the contribution of power block is the smallest. Second, an equilibrium between the annual production of hydrogen and the electrolyzer costs must be achieved. In other words, it should be optimized the work hours of the electrolyzer during the lifespan of the hybrid plant finding its optimum value when a PV of 100MW is considered. Finally, this configuration will not result feasible from a soec size perspective since 4785m2 are needed for its installation.

5.2.2. Electrical and Energy Indicator

Similar to the analysis performed for the hydrogen indicator, the electrical and energy indicator trend will also be studied under the influence of different battery sizes. Secondly, it will take place an analysis to study how electricity and energy production prices varies according to different capacities for the electrolyzer (MWh) and different sizes for the PV field.

In Table 12 it is presented the scenarios that offered best results for the electrical and energy indicators according to different battery sizes. For all of them the best electrical and energy indicator values correspond to the scenarios where there is no hydrogen production. This, confirms the concept already introduced before: introducing hydrogen production into the system might not lead to direct economic benefits. However, in the energy analysis it is going to be explored the potential and opportunities of introducing hydrogen production while trying to minimize the increasing economic effects on the electrical and energy indicators.

Table 12. TES based: Best electrical/energy indicator scenarios according to battery capacity

	Hydrogen Indicator (€/kg h2)	Electricity Indicator (€/MWh)	Energy Indicator (€/MWh)	PV size (MW)	Soec installed capacity (MWh)
Batt size = 0.5MWh	-	99.24	99.24	40	0
Batt size = 90 Mwh	-	110.52	110.52	40	0
Batt size = 180MWh	-	121.82	121.82	40	0
Batt size = 270MWh	-	133.14	133.14	40	0

Furthermore, the best (lowest) results were found for the smallest battery capacity, 0.5MWh. This conclusion was preliminarily expected for the electricity indicator since the battery only transfers energy to the electrolyzer. However, for the case of the energy indicator this was not clear as this parameters studies both, electricity injected into the grid but also energy derived from hydrogen production.

Looking at the graphs below (Figure 33 and Figure 34) it is seen the influence of not only different soec installed capacities but also of different PV sizes for different scenarios that have in common a battery size of 0.5MWh. Here it is represented in a graphical way the effects of imposing bigger hydrogen productions over the electricity and energy production prices. As a result, the lowest numbers are found for a PV size of 40MW and small soec capacities, **below 5MWh** (lowest production prices: 99.2€/MWh and 98.8€/MWh for electricity and energy indicators respectively).

Note that when using big PV sizes the results turn to be rather similar. This happens because the limit of energy injection for the grid is frequently achieved. However, the PV plant results oversized in most of the cases, producing energy that is eventually non used. Waste of energy wants to be avoided specially in presence of a system with hydrogen production.

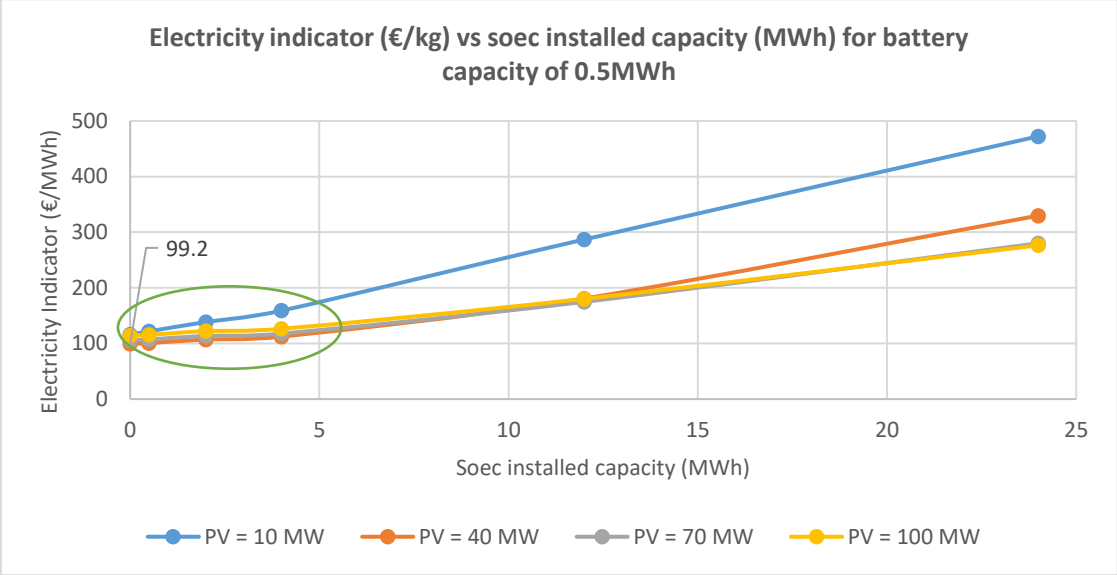

Figure 33. TES based: electricity indicator trend

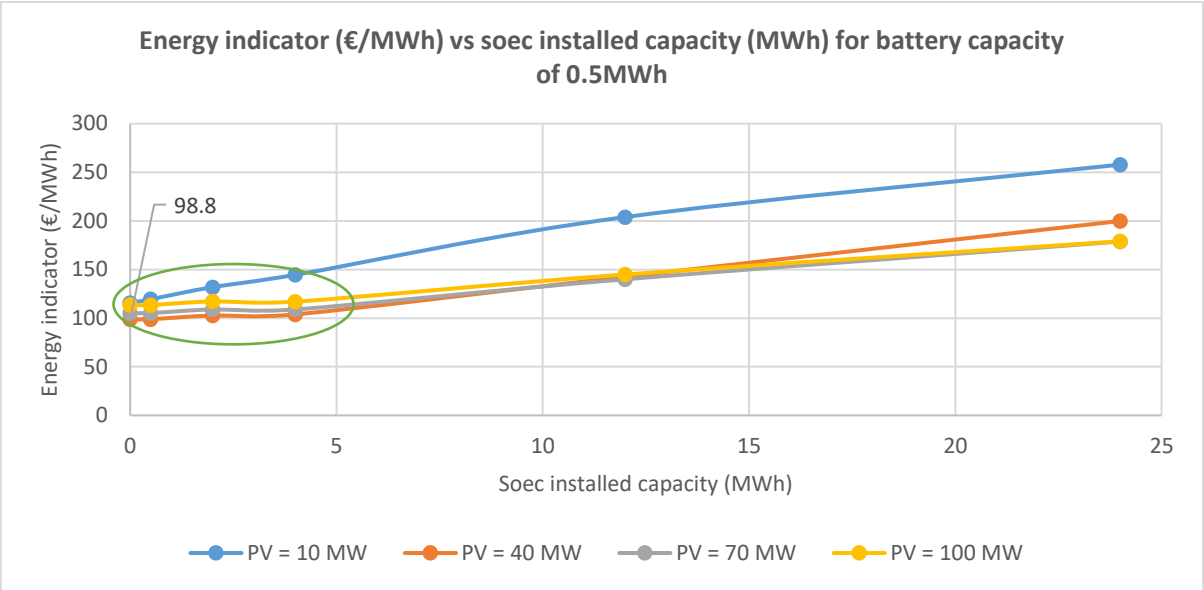

Figure 34. TES based: energy indicator trend

In both cases, for the electrical and energy indicators, best results are achieved when no hydrogen production is introduced. However, a certain hydrogen production can be implemented without causing a big alteration in the energy production prices. This concept is going to be study in the next section where a soec capacity of no more than 5MWh will be implemented

- **Energy Analysis: Electricity Indicator**

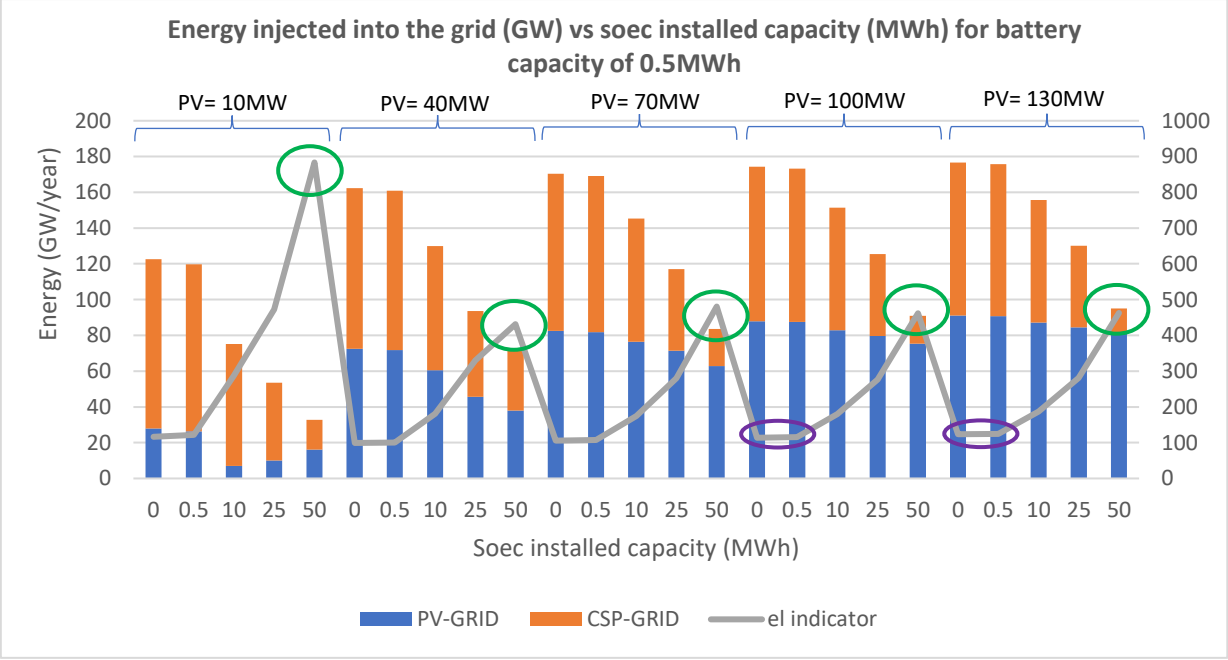

Figure 35. TES based: Energy injected into the grid for different soec capacities installed (MWh)

Looking at the plot above (Figure 35) it is clear that when implementing hydrogen production into the plant, the electricity indicator increases. The use of particles coming from the hot and cold silo to produce steam and eventually hydrogen stops from producing electricity. As a consequence, less energy is injected into the grid and higher electricity indicator values are obtained. Also, the hydrogen indicator maximum values follow a descendent trend when increasing the size of the PV plant until it converges for a size of 40MW (look at the points marked with a green circle). As mentioned before, higher sizes of PV allows to cover the electrical demand of the electrolyzer as well as injecting energy into the grid at the same time. However, when selecting sizes above 40MW we are oversizing the system for the majority of the combinations represented in the plot, specially at low mass flow rates (look at points marked with a purple circle).

- **Energy Analysis: Energy Indicator**

Looking at the plot below (Figure 36) it is firstly observed how the total energy produced in the PV and CSP does not correspond with the total annual energy production. This happens because the process of producing hydrogen is not a 100% effective. In particular, this electrolyzer has an efficiency of 60% so hydrogen production will never be as effective as directly injecting energy into the grid. As a consequence and as shown in the plot, the energy indicator results are better when the particles are sent to the power block to produce electricity that gets injected into the grid (look at small soec capacities: 0.5-1MWh).

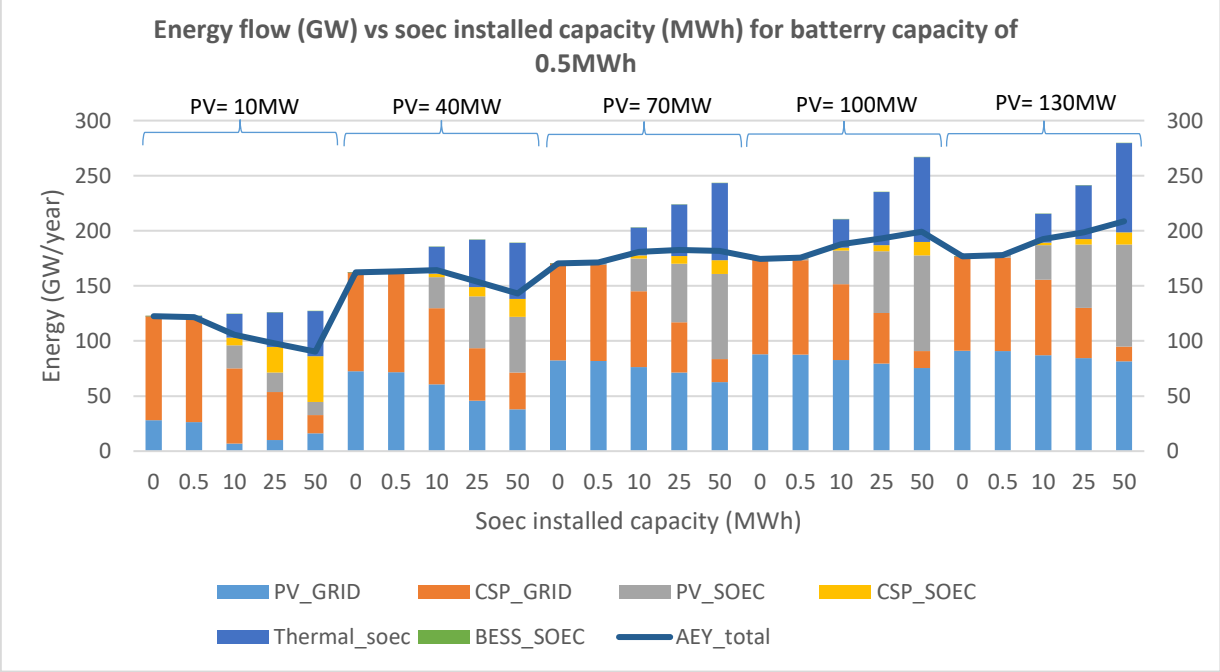

Figure 36. TES based: Energy contributions to the soec and grid compared to total energy production

5.3. Results for sCO2 based configuration

5.3.1. Hydrogen Indicator

First, the hydrogen indicator value trend is going to be analyzed under the influence of different battery sizes. Secondly, an energy analysis will be conducted to finally conclude with an economical analysis over the optimized scenario found for the configuration.

- **Battery capacity Influence**

Following the same approach as in the other 2 previous configuration, firstly an analysis about the results obtained in the sensitivity analysis was conducted according to the different battery capacities.

Table 13. sCO2 based: Best hydrogen indicator scenarios according to battery capacity

	Hydrogen Indicator (€/kg h2)	Electricity Indicator (€/MWh)	Energy Indicator (€/MWh)	PV size (MW)	Soec installed capacity (MWh)
Batt size = 0.5MWh	15.23	695.05	274.97	10	50
Batt size = 90 Mwh	15.35	774.54	288.05	10	50
Batt size = 180MWh	15.94	840	303.87	10	50
Batt size = 270MWh	14.55	636.29	258.15	40	70

In this case, the best hydrogen indicator result is found for a scenario with a battery capacity of 270MWh and a hydrogen production value of 14.55€/kg h2. This scenario not only presents the best hydrogen indicator from the Table 14 but also the lowest electricity and energy indicators. The graphs below represent the tendency that the hydrogen indicator follows with respect to the soec installed capacity and the size of the photovoltaic field.

Looking at Figure 37 and Figure 38 it seems clear that for a TES based configuration, the results of implementing higher battery capacities are positive as the hydrogen indicator values become smaller. This occurs because there is a higher interaction between the batteries and the electrolyzer as it will be shown in the energy distribution analysis.

In opposite to receiver and TES based configurations, sCO2 configuration shows better hydrogen indicator results commonly for the lowest PV size, 10MW. This configuration is designed to cover soec themal needs using sCO2 in the power block so when running the power block to cover soec's electrical need it will be covered its thermal need parallelly.

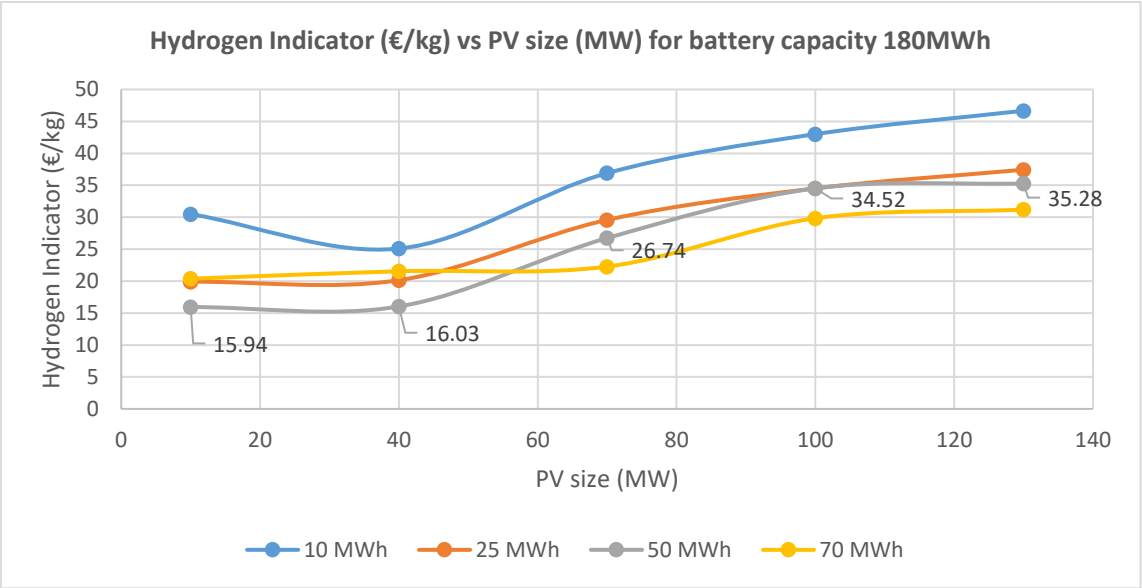

Figure 37. sCO2 based: Hydrogen indicator trend for battery capacity of 180MWh

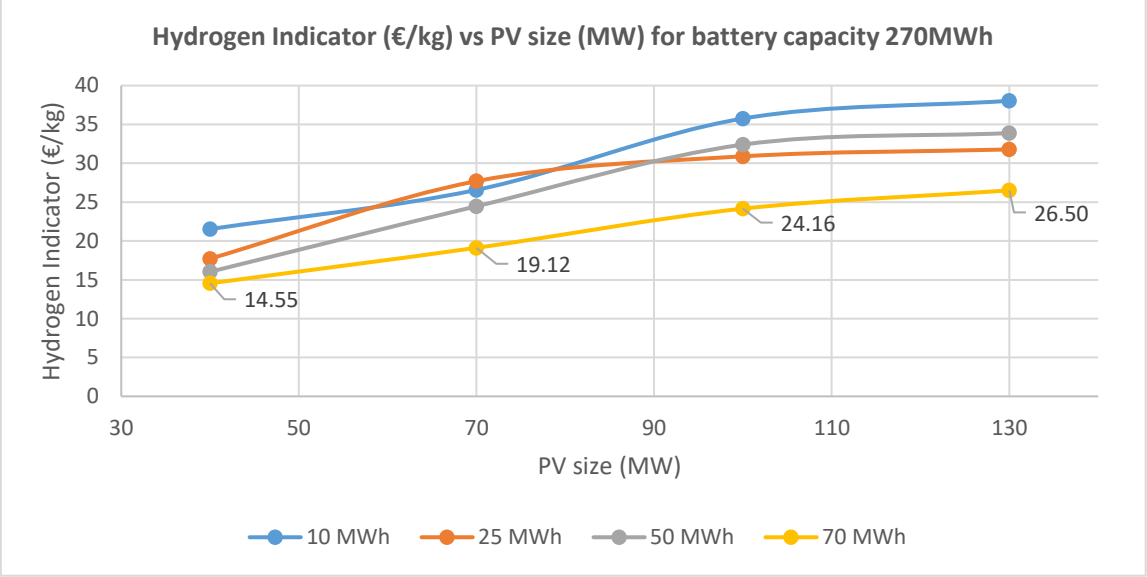

Figure 38. sCO2 based: Hydrogen indicator trend for battery capacity of 270MWh

- **Energy Analysis for best hydrogen indicator scenario**

Once the battery size was found to offer better results for a capacity of 270MWh a further study was developed to understand how the economic results converge according to technical KPIs: energy injected directly into the grid (from PV or CSP) and energy produced in form of h2. Here, the annual energy generated is going to be represented along with the economic results in a graphical way.

Based on the depicted graphs, three key conclusions can be drawn. Firstly, it is evident that the biggest productions yield the most favorable hydrogen indicators values across all PV sizes. (look at the points with the red circles in *Figure 30*Figure 39). This scenarios also correspond with 1 or non

replacements of the soec which means that with less soec working hours and bigger installed soec capacity it is not only obtained less replacements but also higher hydrogen productions.

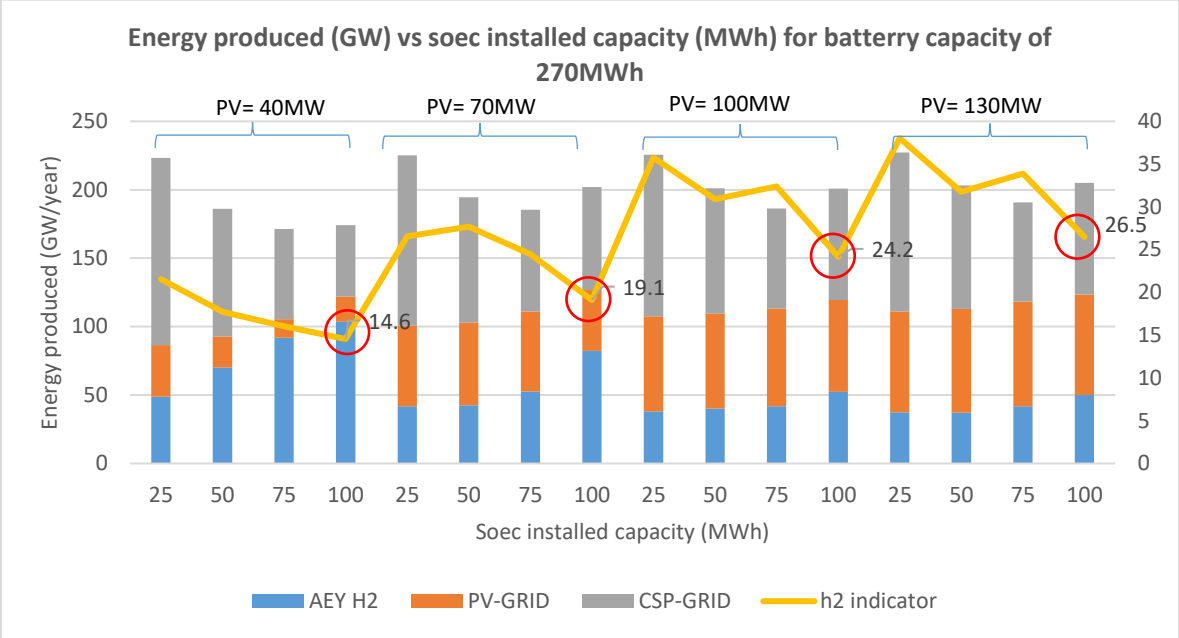

Figure 39. sCO2 based: Annual energy produced

Furthermore, there is a notable trend of the hydrogen indicator increasing as the PV size becomes larger. This stands in high contrast to the behavior observed for the receiver and TES based configurations and it will be further analyzed according to the different energy inputs that the electrolyzer receives.

Another important conclusion is derived from the results of the best-case scenario for the 40 MW PV plant (indicated by the first red circle). It is evident that the hydrogen production surpasses the electricity injected into the grid. This occurs due to the insufficient energy generated by the PV plant to meet the electrical demand of the SOEC. Consequently, a high portion of the power block's electricity production is directed towards the electrolyzer. When this happens the soec's thermal need is also being covered by sCO2 and hydrogen production occurs.

Looking at the plot below and as mentioned in the initial analysis for different battery capacities, it is evident that the batteries significantly influence the prices of the hydrogen production, obtaining the lowest values when implementing the biggest battery capacity under study 270MWh. This makes this configuration the one with a higher contribution of energy coming from the batteries with around 20GW for all the scenarios represented in the plot

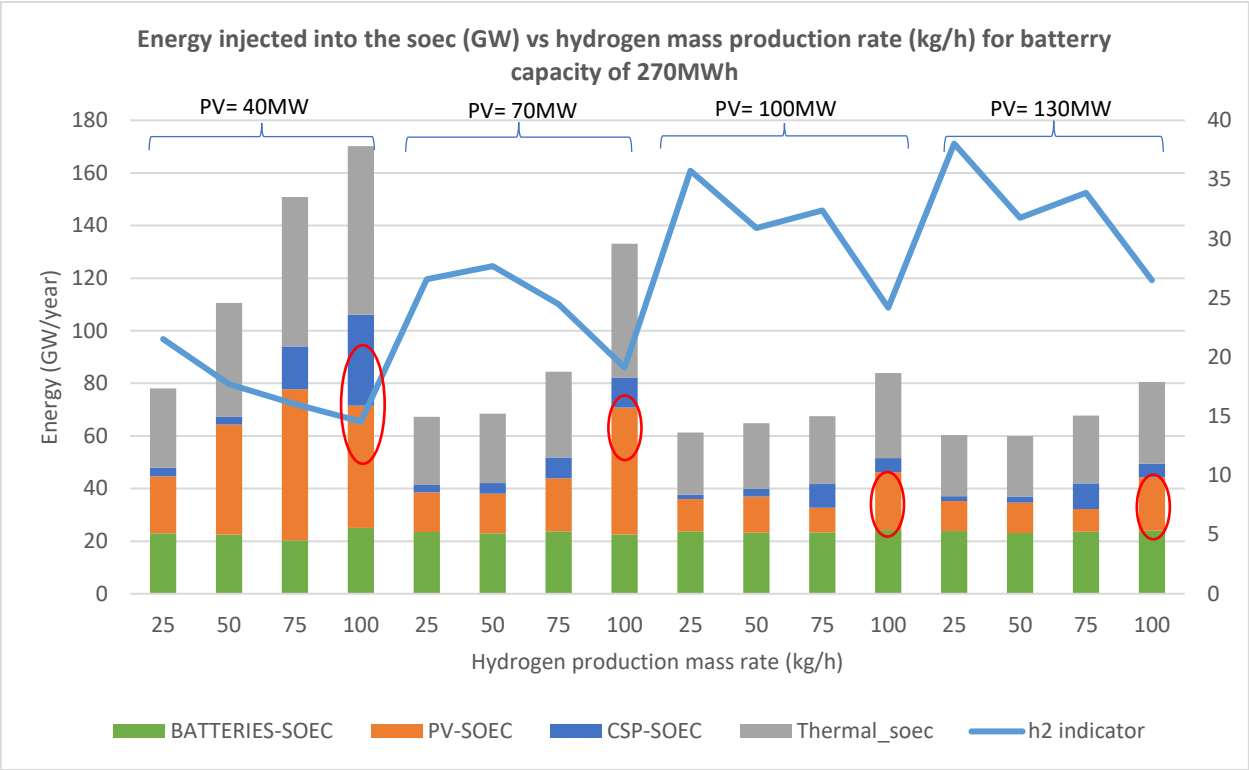

Figure 40. sCO2 based: Comparison of hydrogen energy produced and energy injected into the soec

Finally, when examining the energy transmitted from the Concentrated Solar Power (CSP) system to the SOEC, (indicated by points marked with a red circle in Figure 40), there is a trend towards smaller contributions as the size of the power plant increases. This happens because, as mentioned before higher PV sizes allows to cover the electrical energy of the soec themselves. However, lower hydrogen indicators result when its energy coming from the power block is partially used. This phenomenon can be attributed to the alignment and fulfillment of both electrical and thermal requirements that occur when the power block needs to be ran. Note that, the soec thermal input is derived from the sCO2 circulating in the power block of the CSP system, which can only take place during electricity production.

- **Economic Analysis for best hydrogen indicator scenario**

In the chart below it is represented the capex distribution for the scenario that showed the best hydrogen and energy indicator 14.55 €/kg and 258.15€/kg from Table 14. Here, the cost of integrating hydrogen according to the features of the best scenario is put in perspective with the rest of costs in the plant. The highest investment comes from the CSP plant(169.9 M€), followed by the electrolyzer, (119.1M€), batteries, (73.6 M€). and PV plant (32.2 M€).

Here it is presented in an economic way what it was concluded from a technical point of view before. The batteries represent a 18.5% of the total costs and compared with its energy contribution for hydrogen production represents a 24%. However, to implement such battery capacities might result very inconvenient from a cost and an installation and maintenance point of view. On the other hand the electrolyzer has a size of 14357m2. which from a technical point of view results too high as well as difficult to implement in any real facility.

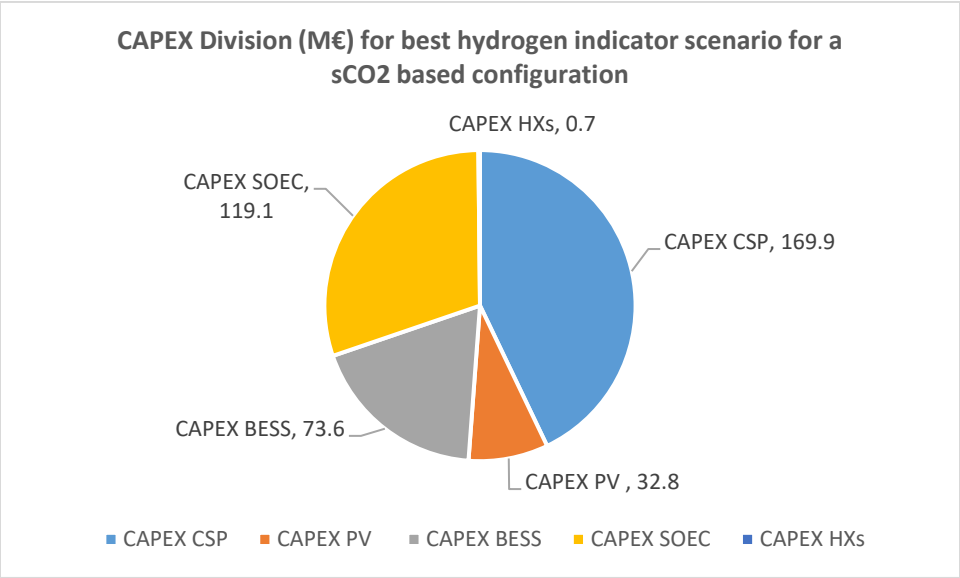

Figure 41. sCO2 based: CAPEX distribution for hydrogen indicator optimized scenario

- **Conclusions for hydrogen indicator**

Summing up the results obtained for the sCO2 based configuration it can be concluded the following: Firstly, high energy contribution coming from the batteries to the soec affects positively into the hydrogen production values. As a result, the soec found at the hydrogen indicator best scenario receives a 24% of its electric energy coming from the batteries. Secondly, the hydrogen indicator values are lower for the scenarios that present low PV sizes. In this case occurs the highest contribution of energy sent from the power block to the soec and eventually results into an alignment and fulfillment of both electrical and thermal requirements that allows the hydrogen production.

Finally, the sizes found for both batteries (270MWh) and electrolyzer (14357m2) are too big making this configuration not technically feasible. This is why in the following section, *discussion*, a different approach is going to be used. This approach will seek for not only a configuration that enables implementation from a technical point of view but also offers reasonable values for the production of energy as a global product.

5.3.2. Electrical and Energy Indicator

Similar to the analysis performed for the hydrogen indicator, the electrical and energy indicator trend will also be studied under the influence of different battery sizes. Secondly, it will take place an analysis to study how electricity and energy production prices vary according to different capacities for the electrolyzer (MWh) and different sizes for the PV field.

In Table 14 it is presented the scenarios that offered best results for the electrical and energy indicators according to different battery sizes. For all of them the best electrical and energy indicator values correspond to the scenarios where there is no hydrogen production. This, confirms the concept already introduced before: introducing hydrogen production into the system might not lead to direct economic benefits. However, in the energy analysis it is going to be explored the potential and opportunities of introducing hydrogen production while trying to minimize the increasing economic effects on the electrical and energy indicators.

Table 14. sCO2 based: Best electrical/energy indicator scenarios according to battery capacity

	Hydrogen Indicator (€/kg)	Electricity Indicator (€/MWh)	Energy Indicator (€/MWh)	PV size (MW)	Soec installed capacity (MWh)
Batt size = 0.5MWh	-	99.62	99.62	40	0
Batt size = 90 Mwh	-	111.07	111.07	40	0
Batt size = 180MWh	-	122.55	122.55	40	0
Batt size = 270MWh	-	133.95	133.95	40	0

Furthermore, the best (lowest) results were found for the smallest battery capacity, 0.5MWh. This conclusion was preliminarily expected for the electricity indicator since the battery only transfers energy to the electrolyzer. However, for the case of the energy indicator this was not clear as this parameters studies both, electricity injected into the grid but also energy derivied from hydrogen production.

Looking at the graphs below (Figure 42 and Figure 43) it is seen the influence of not only different soec installed capacities but also of different PV sizes for different scenarios that have in common a battery size of 0.5MWh. Here it is represented in a graphical way the effects of imposing bigger hydrogen productions over the electricity and energy production prices. As a result, the lowest numbers are found for a PV size of 40MW and small soec capacities, **below 5MWh** (lowest production prices: 99.6€/MWh and 99.2€/MWh for electricity and energy indicators respectively).

Note that when using big PV sizes the results turn to be rather similar. This happens because the limit of energy injection for the grid is frequently achieved. However, the PV plant results oversized in most of the cases, producing energy that is eventually non used. Waste of energy wants to be avoided specially in presence of a system with hydrogen production

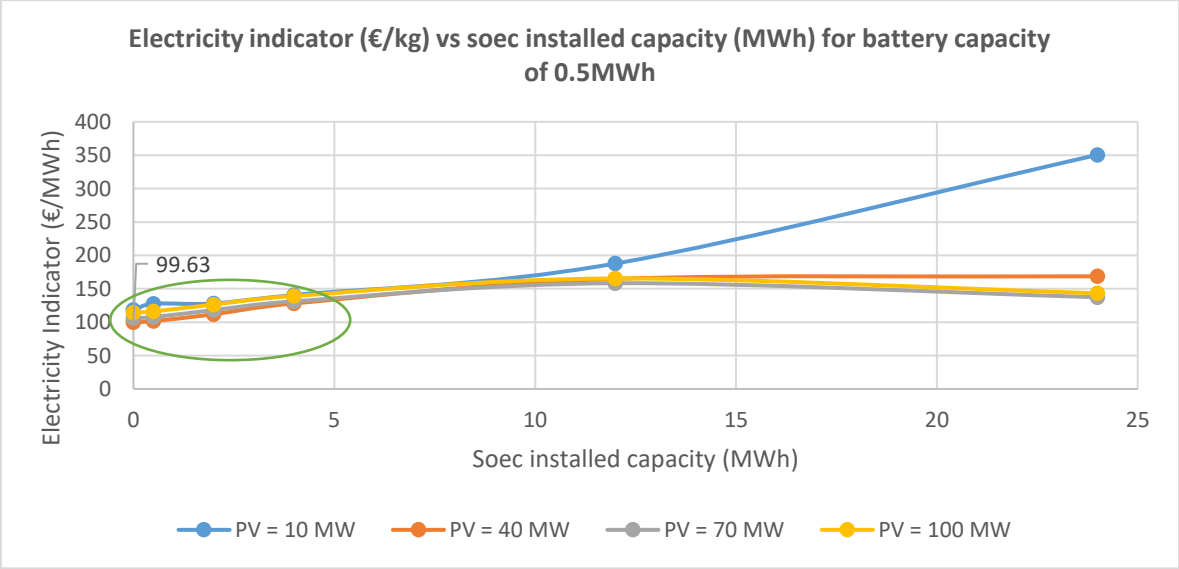

Figure 42. sCO2 based: electricity indicator trend

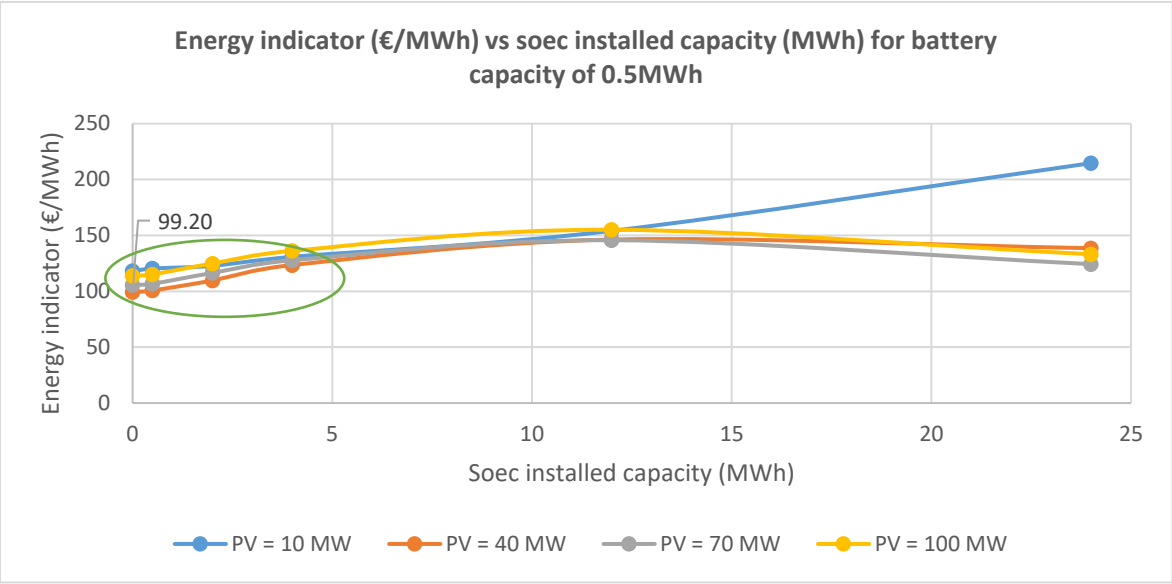

Figure 43. sCO2 based: energy indicator trend

- **Energy Analysis: Energy Indicator**

Looking at the plot below it is firstly observed how the total energy produced in the PV and CSP does not correspond exactly with the total annual energy production. However, the gap between the energy used for the production of hydrogen and the total energy generated is smaller in this case. This happens because the sCO2 configuration is designed to cover the thermal need of the soec with hot sCO2 coming from the outlet of the turbine of the power block. In other words, this configuration re-uses heat still present in the sCO2 increasing the efficiency in the hydrogen production process.

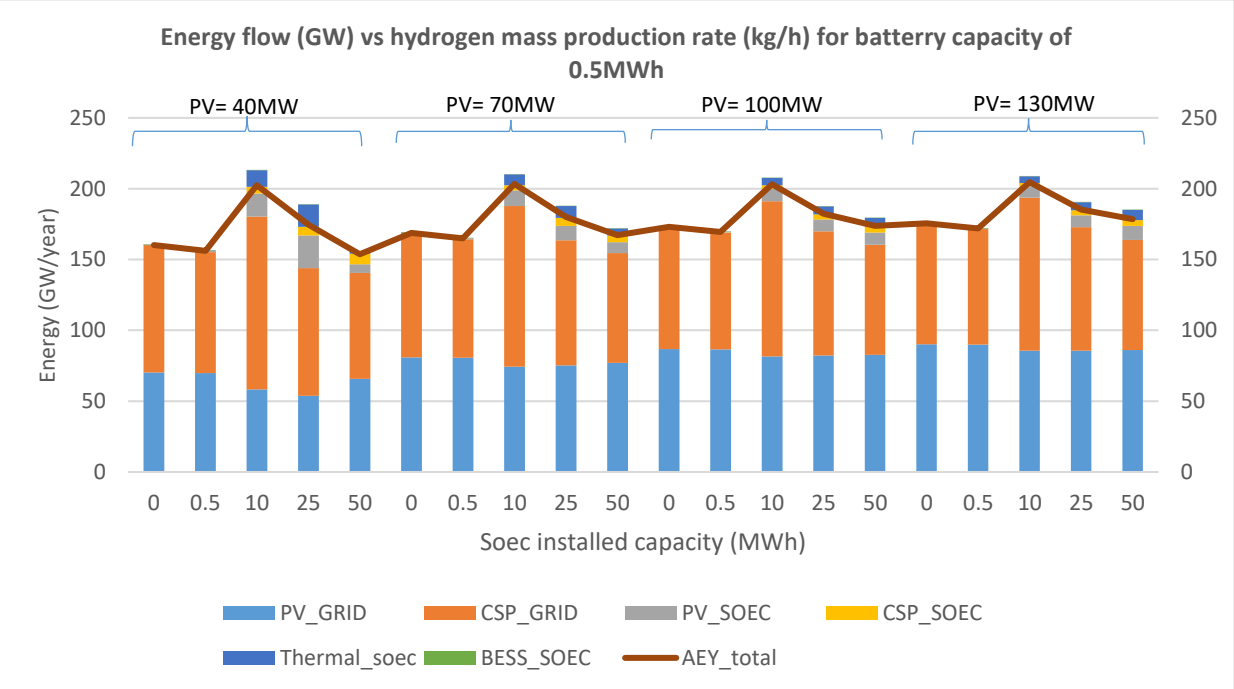

Figure 44. sCO2 based: Energy contributions to the soec and grid compared to total energy production

Chapter 6

Discussion

The previous analysis for the three proposed configurations: receiver, TES and sCO2 does not leave a clear feasible scenario for implementing hydrogen production while maintaining a low economic profile for all indicators under study. Specially, when trying to minimize values for the hydrogen indicator, the scenarios that offer the lowest values are found non-feasible for the following reasons:

Table 15. Global comparison of best hydrogen indicator scenarios

	Hydrogen Indicator (€/kg)	Electricity Indicator (€/MWh)	Energy Indicator (€/MWh)	PV size (MW)	Soec installed capacity (MWh)	Battery size (MWh)	SOEC area (m2)
Receiver based	10.95	540.63	203.79	100	95	0.5	19143
TES based	11.65	239.76	141.69	100	25	180	4785
sCO2 based	14.55	636.29	258.15	40	70	270	14357

- **Energy and electricity indicator values**: When achieving global minimum values for hydrogen indicator there is a need of imposing high soec capacities: 95MWh for receiver configuration, 25 MWh for TES configuration, and 70MWh for SCO2-based configuration. Consequently, the electricity and energy indicators increase, making challenging to establish a reasonable pricing strategy for future electricity or energy production as a marketable product.

- **Size of the electrolyzer**: High soec capacities is directly translated into larger electrolyzers provided with more cells to produce a greater amount of hydrogen per hour. However, this leads to excessively large electrolyzer dimensions that are difficult to construct and implement given the current state of SOEC technology.

- **Capital Expenditure (CAPEX):** The significant size requirements of the electrolyzer requires higher initial investment costs for the stack of the electrolyzer. In the receiver and SCO2-based configurations, the CAPEX of the electrolyzer represents the second-highest investment after the Concentrated Solar Power (CSP) plant one. This represents challenges, considering that process of conversion between energy and hydrogen is not a 100% effective and the current high prices without a significant economy of scale.

- **Battery size:** For TES and SCO2-based configurations, better results are obtained for larger battery sizes, such as 180 MWh and 270 MWh. However, such sizes involve high investment costs, ranking third highest after the electrolyzer costs. From a technical perspective, using batteries only for hydrogen production proves insufficient and future research should explore a set of batteries that can interact with the grid and the electrolyzer simultaneously.

In summary, the individual optimizitation analysis reveals several challenges regarding technical and economic feasibility. These findings need of further research and investigation to identify alternative configurations that address these limitations. In order to determine a feasible set of configurations that allows hydrogen integration, a different approach will be employed in this section.

Various parameters will be analyzed, taking into account a global perspective. The objective is to identify a configuration that is not only economically viable based on multiple indicators but also

capable of being implemented in the future. To achieve this, the results will be evaluated from a global performance perspective, considering factors such as the global energy production price and possible waste of energy.

6.1. Global Analysis

For this analysis is going to be investigated a feasible scenario that includes hydrogen production for each configuration while trying to minimize the values for several economic and technical parameters. This study will be bounded for soec capacities below 5MWh because as shown in the previous analysis, the energy and electricity indicators are less sensitive under small hydrogen productions.

- Economic KPIs: The economic KPIs under study will be the energy indicator and LCOH. For this study, the hydrogen indicator will not be taken into account since we are studying low productions of hydrogen and it is reasonable to divide the CAPEX in this situation.
- Technical KPIs: The main outcome of this discussion is to reveal a scenario that can actually be implemented in a future real situation. To do that, the size of the electrolyzer as well as non-used annual energy (waste) will also be considered.

Also, this study will be conducted not taking into account a set of batteries since from an energy production perspective better prices are obtained in this way.

6.2. Global Analysis for receiver based configuration

First, the energy indicator was studied. The plot below represents the trend that the energy indicator follows for soec capacities below 5MWh under different PV sizes. In this case, the scenarios that obtain the best results for the energy indicator are the ones under a PV size of 40MW.

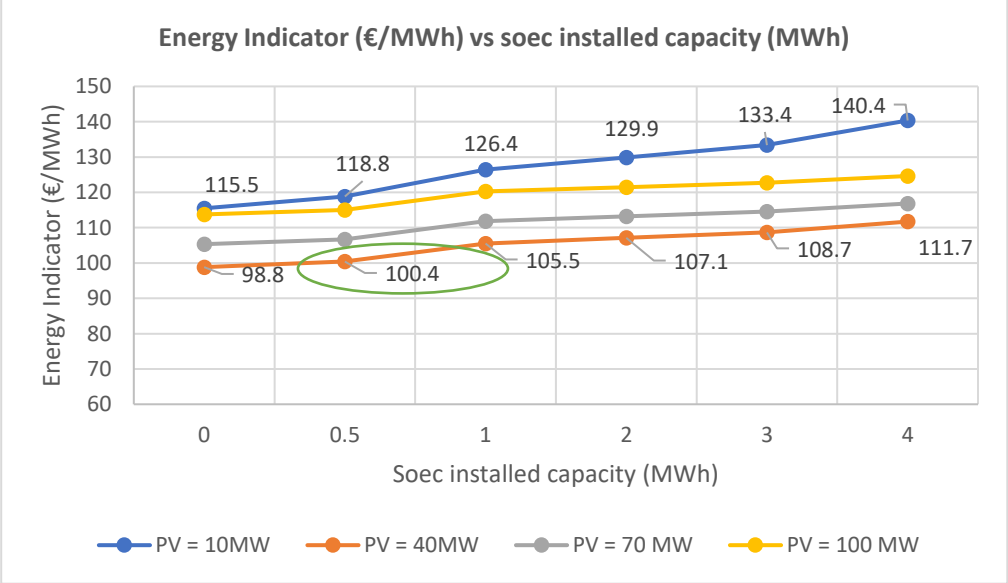

Figure 45. Receiver based: Energy trend for global analysis

As it has been concluded before having no hydrogen production or low is the best in terms of the global energy indicator. However, introducing small production rates of hydrogen into the plant do not affect excessively to the performance of the plant nor the values of the energy indicator. Taking a look at the energy indicator plot for a 40MW PV, the optimum energy indicator (excluding 0MWh) is observed at 100.40€/MWh for a hydrogen production rate of 0.5MWh (20 kg/h). This particular scenario corresponds to a Levelized Cost of Hydrogen (LCOH) of 10.18 €/kg H2, as detailed in Table

16. However, there is a high waste of energy, that it is not used for hydrogen production nor delivering into the grid. This is caused from the grid limit imposed (25MW) so if a similar configuration wants to be implemented in the future, then, a higher limit should be considered or a set of batteries that interact with the grid. This will not only increase the performance of the system but also the annual energy production and therefore the energy indicator.

Table 16. Receiver based: Best energy indicator scenario (below 5MWh)

	Hydrogen Indicator (€/kg)	Electricity Indicator (€/MWh)	Energy Indicator (€/MWh)	CAPEX CSP (M€)	CAPEX PV (M€)	CAPEX SOEC (M€)	SOEC area (m2)	Waste (GW)
PV = 40MW	10.18	101.82	100.40	169.9	32.8	2	119	20.87

Taking a look into the CAPEX distribution, the results seem to be more adequate compared with the configurations in the last section. The stack of the soec needs 3 replacements and has a size of 119m2 (3000cells) so its total capex contribution during the life span of the hybrid plant is below 2M€. After analyzing the potential of implementing hydrogen production into the receiver based configuration it can be concluded that the configuration with soec installed capacity of 0.5MWh (20kg/h) and PV size of 40MW would be the best option when considering energy as a global product. However, a set of batteries might be considered in the future.

6.3. Global analysis for a TES based configuration

Firstly, the energy indicator was studied. The plot below represents the trend that the energy indicator follows for mass flow rates below 0.5MWh under different PV sizes. In this case, the scenarios that obtain the best results for the energy indicator are obtained once again under a PV size of 40MW.

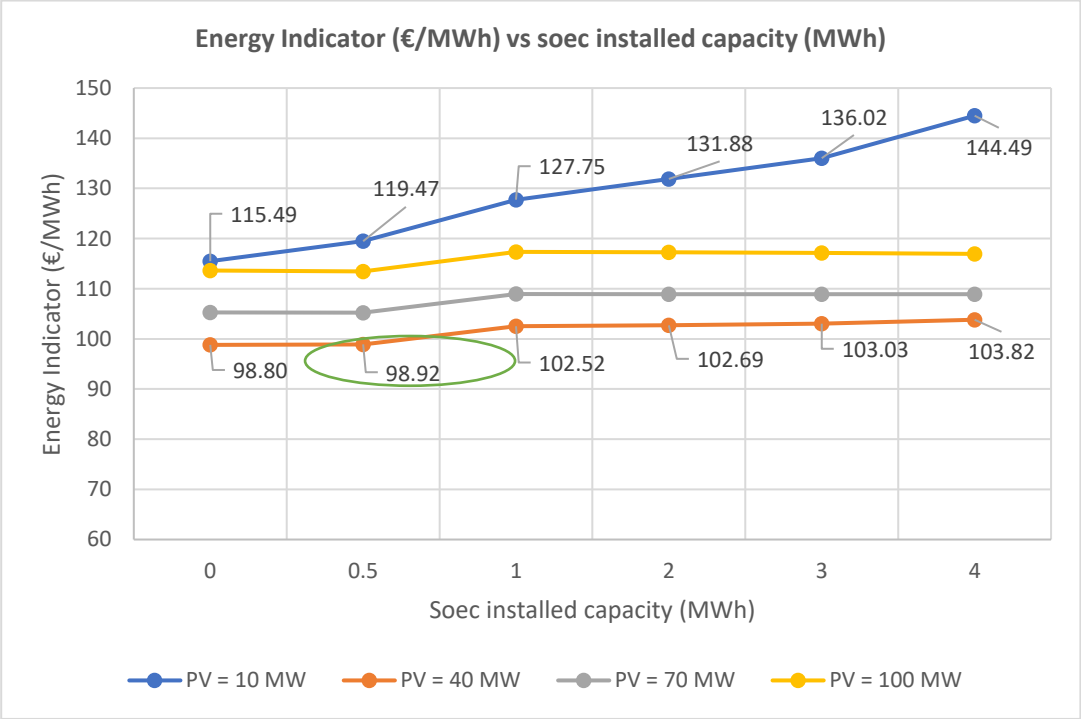

Figure 46. TES based: Energy trend for global analysis

As it has been concluded before having no hydrogen production or low is the best in terms of the global energy indicator. However, introducing small production rates of hydrogen into the plant do not affect excessively to the performance of the plant nor the values of the energy indicator. Taking a look at the energy indicator plot for a 40MW PV, the optimum energy indicator (excluding 0 MWh) is observed at 98.92€/MWh for a soec installed capacity of 0.5MWh (20 kg/h). This particular scenario corresponds to a Levelized Cost of Hydrogen (LCOH) of 7.63 €/kg H2, as detailed in the table below. However, as in the previous configuration there is high amount of energy non used for hydrogen production nor delivering into the grid. This is caused from the grid limit imposed (25MW) so if a similar configuration wants to be implemented in the future, then, a higher limit should be considered or a set of batteries that interact with the grid. This will not only increase the performance of the system but also the annual energy production and therefore the energy indicator.

Table 17. TES based: Best energy indicator scenario (below 5MWh)

	Hydrogen Indicator (€/kg)	Electricity Indicator (€/MWh)	Energy Indicator (€/MWh)	CAPEX CSP (M€)	CAPEX PV (M€)	CAPEX SOEC (M€)	SOEC area (m2)	Waste (GW)
PV = 40MW	7.63	100.66	98.92	169.9	32.8	2.5	119	21.24

Taking a look to the CAPEX distribution, the results seem to be more adequate compared with the configurations in the last section. The stack of the soec needs 4 replacements and has a size of 119m2 (3000cells) so its total capex contribution during the life span of the hybrid plant is 2.5M€. After analyzing the potential of implementing hydrogen production into the TES based configuration it can be concluded that the configuration with soec installed capacity of 0.5 MWh and PV size of 40MW would be the best option when considering energy as a global product. However, a set of batteries might be considered in the future.

6.4. Global analysis for a sCO2 based configuration

First, the energy indicator was studied. The plot below represents the trend that the energy indicator follows for mass flow rates below 0.5MWh under different PV sizes. In this case, the scenarios that obtain the best results for the energy indicator are also the ones under a PV size of 40MW.

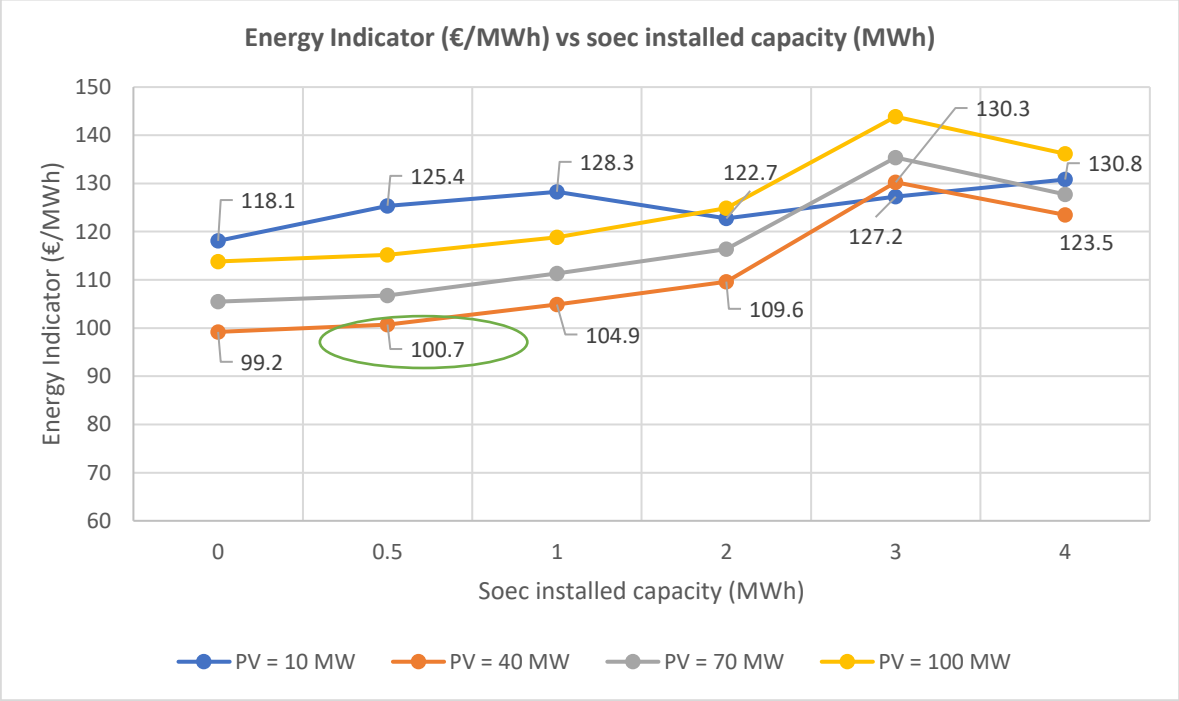

Figure 47. TES based: Energy trend for global analysis

As it has been concluded before having no hydrogen production or low is the best in terms of the global energy indicator. However, introducing small production rates of hydrogen into the plant do not affect excessively to the performance of the plant nor the values of the energy indicator. Taking a look at the energy indicator plot for a 40MW PV, the optimum energy indicator (excluding 0 MWh) is observed at 100.73€/MWh for a soec installed capacity of 0.5MWh (20 kg/h). This particular scenario corresponds to a Levelized Cost of Hydrogen (LCOH) of 9.39 €/kg H2, as detailed in the table below. Also, this scenario presents the lowest amount of energy waste. The reason why is that for sCO2 configurations there is an electric heater in charge of warming up particles at TES cold tank with energy coming from the PV field. The electric heater receives energy after the heat booster and the electrolyzer does, maximizing the use of energy and minimizing losses (look at dispatch strategy in Figure 8)

Table 18. sCO2 based: Best energy indicator scenario (below 5MWh)

	Hydrogen Indicator (€/kg)	Electricity Indicator (€/MWh)	Energy Indicator (€/MWh)	CAPEX CSP (M€)	CAPEX PV (M€)	CAPEX SOEC (M€)	SOEC area (m2)	Waste (GW)
PV = 40MW	9.39	101.7	100.73	169.9	32.8	1	119	0.93

Taking a look to the CAPEX distribution, the results seem to be more adequate compared with the configurations in the last section. For the configuration with a PV size of 40MW it is needed 1 replacement of the stack and a size for the soec of 119m2 (3000cells) so its total capex contribution during the life span of the hybrid plant is 1M€. After analyzing the potential of implementing hydrogen production into the sCO2 based configuration it can be concluded that considering energy as a global product, the best option would be implementing a configuration with soec installed capacity of 0.5 MWh, PV size of 40MW and small battery.

6.5. Conclusion for the global analysis

After analyzing the potential of different configurations bounded for a soec installed capacity below 5MWh it has been found the following scenarios for future possible implementation:

Table 19. Global comparison of best energy indicator scenarios (below 5MWh)

Based	PV	LCOH (€/kg h2)	Electricity Indicator (€/MWh)	Energy indicator (€/MWh)	AEY tot	AEY h2	CAPEX SOEC (M€)	SOEC area (m2)	Waste (GW)
Receiver	40	10.18	101.82	100.40	163.5	1.65	2	119	20.87
TES	40	**7.63**	100.66	**98.92**	163	2.20	2.5	119	21.24
sCO2	40	9.39	101.7	100.73	156	0.9	1	119	0.93

As shown in Table 19, depending on the configuration it can be found suitable scenarios for each case. However, the global best energy indicator as well as LCOH are slightly better for a TES based configuration. This configuration presents an energy indicator of 98.92€/MWh corresponding to a LCOH of 7.63€/kg h2.

As observed in Table 19 the values for energy indicator are very similar since all the configurations presented have a PV size of 40MW and a soec installed capacity of 0.5MWh. However, looking at the results for the LCOH small variations in the production have a big impact on the hydrogen production prices. TES based configuration has the highest hydrogen production. The fact of having TES allows it to operate during the night hence to produce hydrogen during more hours (3630 hours/year). However, this configuration presents a high volume of energy non used during the year. This could be easily fixed by installing a small set of batteries or slightly increasing the injection limit into the grid.

Chapter 7

Conclusions

The study conducted in this master thesis has shown the techno-economic feasibility of high temperature hydrogen production within a hybrid PV-CSP(sCO2) plant. To do so 3 different integration strategies have been conducted and analyzed. Depending on how the thermal need of the soec has been supplied it can be found receiver, TES or sCO2 soec integration. In order to study the feasibility and the set of parameters that lead to the best scenarios several studies have been conducted after a sensitivity analysis, attending to different indicators: electricity, energy and hydrogen indicator as well as others such as LCOH, annual energy delivered into the grid and annual hydrogen production.

The study conducted for the optimization of individual indicators: electricity, energy and hydrogen left several technical and economic challenges because of economic incompatibility reasons. Energy and electricity production prices responded negatively to the integration of hydrogen. As a result of implementing a hydrogen production unit, the system stops injecting all energy produced into the grid. This fact plus an efficiency conversion of 60% energy-hydrogen leads energy production prices to rise. Also, competitive hydrogen production prices (when taking into account all the investment costs of the hybrid plant) are obtained at very high soec capacities. This involves large soec sizes that are not even mentioned in literature. Therefore, if hydrogen production wants to be implemented it will have to be through small soec capacities or in other words through small hydrogen production mass flow rates.

When studying the possibility of small scale hydrogen applications it is found that it is actually possible to install a small soec capacity without negatively influencing the results of the energy and electricity production prices in a big scale. In this way it is actually possible to find a suitable scenario for each of the integration strategies. As a result, the 3 of them present a favorable behavior towards configurations with a PV size of 40MW and soec installed capacity of 0.5MWh (20 kg h2/h). TES based configuration showed specially better results than the other 2 ones with an energy indicator of 98.92€/MWh and a hydrogen production price of 7.63€/kg h2. (LCOH). sCO2 based configuration follows closely the hydrogen production price with 9.39€/kg h2 (LCOH) and an energy indicator of 100.73€/MWh. Finally, receiver based configuration showed the highest hydrogen production price, 10.18€/kg h2 (LCOH) and an energy indicator of 100.40€/MWh.

The fact that TES based configuration offers the lowest results for hydrogen integration is actually very convenient since this integration strategy offers the possibility of hydrogen production when there is no sun radiation. In the future hydrogen production can be dispatchable specially during no radiation hours and it can be also used to contribute during peak hours if storage is implemented. On the other hand, its hydrogen production price is actually along with the prices that can be found in literature for high temperature electrolyzers (7-8.2€/kg h2 [2] [4] [10]) but still far from being competitive with current hydrogen production prices at low temperature electrolyzers (2.75-8.2€/kg h2 [25]).

Limitations and next steps

The main limitations that this master thesis faces can be divided according to design, operation, boundary conditions, energy storage and post-processing tools.

In this study high temperature hydrogen production within a hybrid CSP-PV plant was studied for 3 different integration strategies. As a result, 3 different configurations, 1 for each case have been implemented and analyzed. However, there are several possible ways to build these configurations attending to the researcher purposes, for example maximizing the use of heat waste or implementing energy storage. This fact opens the possibility of keeping building and exploring alternative configurations to the ones already studied. In this way the scope and understanding of the plant behavior under hydrogen production will be bigger as well as possible optimization of the economic and technical indicators.

Also, the operational approach imposed has not taken into account the time at which production of hydrogen takes place nor a capacity factor. Alternative approaches should consider to take into account hydrogen production considering peak hours of the grid, a capacity factor for the electrolyzer to control the number of hours of operation and finally a variable state of charge that allows the electrolyzer to operate with variable energy input.

On the other hand, all studies performed were developed for a CSP size of 50MW and maximum injected power into the grid of 25Mw in order to bound the number of cases ran in the simulation phase. Although the PV size, batteries capacity and soec capacity (MWh) were studied under a high number of possible combinations in the sensitivity analysis, the scalability of the CSP plant and its power block were not and it will require further investigation that allows to expand the scope and draw new conclusions.

In addition, and as mentioned at the beginning of the document, the results drawn do not include technically nor economically storage of hydrogen. This bounds the scope of the results to those areas where energy storage is not contemplated. However, this is a minority of the cases and hydrogen energy storage should be implemented as one of the main outcomes from implementing hydrogen production. Additional energy storage should be also considered, such as a small set of batteries that can help to minimize the waste of energy so energy utilization is maximized.

Finally, the results and trends have been analyzed using several different graphs developed with excel. However, no statistical tool has been used and consequently there might be small conclusions missed such as further complex relationships between parameters that in a first look can not be drawn. For this study is not crucial to implement such a tool but wider sensitivity analysis will probably require it or a similar tool.

Concluding, future research steps and approaches should seek for more competitive hydrogen production prices so its economic feasibility gains territory against other non clean power generation sources. Hydrogen production and storage is necessary for the energy transition and it should be pursued its integration.

BIBLIOGRAPHY

[1] "Fuel Cells and Hydrogen 2 Joint Undertaking, Hydrogen roadmap Europe : a sustainable pathway for the European energy transition," Publications Office, 2019. [Online]. Available: https://data.europa.eu/doi.

[2] J. K. D. K. W.-B. H. S. K. Dohyung Jang, "Techno-economic analysis and Monte Carlo simulation of green hydrogen production technology through various water electrolysis technologies," *Energy Conversion and Management,* vol. 258, p. 115499, 2022.

[3] M. M. Amin Mohammadi, "Thermodynamic and economic analyses of hydrogen production system using high temperature solid oxide electrolyzer integrated with parabolic trough collector 2019," *Journal of Cleaner Production,* vol. 212, pp. 713-726.

[4] Y. A. a. K. O. Abdulrahman Joubi, "Techno-Economic Analysis of Solar Thermal Hydrogen Production in the United Arab Emirates," *MDPI Journal,* p. 389–401, 2022.

[5] "Hydrogen Production Costs from PEM Electrolysis," [Online]. Available: https://www.hydrogen.energy.gov.

[6] O. o. E. E. &. R. Energy, "Renewable Energy," [Online]. Available: https://www.energy.gov/eere/renewable-energy.

[7] "European Comission - Energy - Hydrogen," European Union, [Online]. Available: https://energy.ec.europa.eu/topics/energy-systems-integration/hydrogen_en.

[8] "Fuell Cell and Hydrogen Energy Association (FCHEA)," [Online]. Available: https://www.fchea.org/hydrogen-as-storage.

[9] D. F. E. S. Aruna Chandrasekar, "Operational challenges for low and high temperature electrolyzers exploiting curtailed wind," vol. 46, pp. 28900-28911, 2021.

[10] M. M. Amin Mohammadi, "Techno-economic analysis of hydrogen production by solid oxide electrolyzer coupled with dish collector," *Elsevier,* vol. 173, pp. 167-178, 2018.

[11] M. K. Mehdi Mehrpooya, "Hydrogen production using solid oxide electrolyzer integrated with linear Fresnel collector, Rankine cycle and thermochemical energy storage tank," *Energy Conversion and Management,* vol. 224, 2020.

[12] I. D. Abdullah A. AlZahrani, "Design and analysis of a solar tower based integrated system using high temperature electrolyzer for hydrogen production," *Elsevier,* vol. 41, pp. 8042-8056.

[13] M. G. M. J. E. O. J. S. H. Edwin A. Harvego, "Parametric evaluation of large-scale high-temperature electrolysis hydrogen production using different advanced nuclear reactor heat sources," *Elsevier,* vol. 239, pp. 1571-1580, 2009.

[14] I. D. Abdullah A. AlZahrani, "Thermodynamic and electrochemical analyses of a solid oxide electrolyzer for hydrogen production," vol. 42, pp. 21404-21413, 2017.

[15] J. Y. Z. Y. Y. D. Tianye Liu, "Techno-economic feasibility of solar power plants considering PV/CSP with electrical/thermal energy storage system," *Elsevier,* vol. 255, 2022.

[16] Irena, "Renewable Power Generation Costs in 2021," 2021.

[17] Solar Paces, [Online]. Available: https://www.solarpaces.org/worldwide-csp/.

[18] S. T. R. G. B. L. S. M. A. T. Salvatore Guccione, "TECHNO-ECONOMIC OPTIMIZATION OF A HYBRID PV-CSP PLANT WITH MOLTEN SALT THERMAL ENERGY STORAGE AND SUPERCRITICAL CO2 BRAYTON POWER CYCLE," 2022.

[19] N. A. M. S. S. Anam Kalair, "Role of energy storage systems in energy transition from fossil fuels to renewables," *Energy Storage,* vol. 3, 2020.

[20] M. R. A.-G. O. K. P. S. N. Montaser Mahmoud, "A review of mechanical energy storage systems combined with wind and solar applications," vol. 210, 2020.

[21] C. O. T. W. M. R. M. A. A. A. H. A. –. A. A.G. Olabi, "Critical review of energy storage systems," *Elsevier,* vol. 214, 2021.

[22] Europe, Hydrogen, "Myths and The colors of hydrogen," Hydrogen Europe, [Online]. Available: https://hydrogeneurope.eu/in-a-nutshell/.

[23] Acciona, "What Are The Colours Of Hydrogen And What Do They Mean?," Acciona, [Online]. Available: https://www.acciona.com.au/updates/stories/what-are-the-colours-of-hydrogen-and-what-do-they-mean/?_adin=02021864894.

[24] G. Mirabella, "The many colors and applications of hydrogen," *Elsevier,* 2022.

[25] iea, "The future of Hydrogen," 2019.

[26] "The National Hydrogen Strategy," 2020. [Online]. Available: https://www.bmwk.de.

[27] "Renewable energy statistics," [Online]. Available: https://ec.europa.eu/eurostat/statistics.

[28] "IRENA (International Renewable Energy Agency)," [Online]. Available: https://www.irena.org/Energy-Transition/Technology/Hydrogen.

[29] M. K. L. D. Y. L. Meng Ni, "Parametric study of solid oxide steam electrolyzer for hydrogen production," *International Journal of Hydrogen Energy,* vol. 32 , no. 13, pp. 2305-2313, 2007.

[30] T. B.-H. O. E. H. W. M. Thomas Holm, "Hydrogen costs from water electrolysis at high temperature and pressure," *Energy Conversion and Management,* vol. 237, p. 114106, 2021.

[31] E. F. Guerrero, *Estado del arte de electrolizadores de óxido sólido.,* Sevilla: Universidad de Sevilla (Departamento de Ingeniería Energética), 2020.

[32] S. S. X. C. G. L. J. C. Houcheng Zhang, "Configuration design and performance optimum analysis of a solar driven high temperature steam electrolysis system for hydrogen production," *International Journal of Hydrogen Energy,* vol. 38, no. 11, pp. 4298-4307, 2013.

[33] P. H. Fateme Ahmadi Boyaghchi, "Thermoeconomic assessment and multi objective optimization of a solar micro CCHP based on Organic Rankine Cycle for domestic application," *Energy Conversion and Management,* vol. 97, pp. 224-234,, 2015.

Appendix A

Equations used in the code

Operational equations for Soec

$$j_o = j_{o,a} + j_{o,c} = \Upsilon_a * \exp\left(\frac{-E_{act,a}}{RT}\right) + \Upsilon_c * \exp\left(\frac{-E_{act,c}}{RT}\right) \quad [32]$$

$$V_{operation.SOEC} = E_{Nerst} + V_{ohm} + V_{ohm} + V_{conc} \quad [30]$$

$$E_{Nerst} = E^0 + \frac{RT}{2F}\ln\left(\frac{P^0_{H2}\, P^0_{O2}{}^{\frac{1}{2}}}{P^0_{H2O}}\right) \quad [30]$$

$$E^0 = \frac{1}{4}\, 1.29 + 0.000292\,(T + 273) \quad [32]$$

$$V_{ohm} = jR_{ohm} = j\left(\frac{L_a}{\sigma_a} + \frac{L_c}{\sigma_c} + \frac{L_e}{\sigma_e}\right) \quad [32]$$

$$V_{conc} = \frac{RT}{2F}\ln\left(\frac{P^*_{H2O} * P^0_{H2O}}{P^*_{H2} * P^0_{H2}}\right) + \frac{RT}{4F}\ln\left(\frac{P^*_{O2}}{P^0_{O2}}\right) \quad [11]$$

$$V_{act} = \frac{2RT}{nF} sinh^{-1}\left(\frac{i}{2i_{o,a}}\right) + \frac{2RT}{nF} sinh^{-1}\left(\frac{i}{2i_{o,c}}\right) \quad [11]$$

$$\sigma_e = 3.34 * 10^4 * \exp\left(\frac{-1.03 * 10^4}{T}\right) \quad [32]$$

$$P_{Soec} = I_{Soec} * A_{cell} * N_{cell} * V_{operation.SOEC} \quad [11]$$

Production equations for Soec

$$m_{H2} = \frac{i_{soec} * A_{cell} * N_{cell} * M_{H2}}{2F} \quad [11]$$

$$m_{O2} = \frac{i_{soec} * A_{cell} * N_{cell} * M_{O2}}{4F} \quad [11]$$

$$m_{H2O,in} = m_{H2} + m_{O2} \quad [11]$$

Thermal efficiency equations for Soec

$$S_{gen} = 2F(V_{act} + V_{ohm} + V_{conc}) \quad [11]$$

$$Q_{heat,soec} = m_{H2O}[T\Delta S - S_{gen}] \quad [11]$$

$$\eta_{th} = \frac{m_{H2} * LHV_{H2}}{P_{Soec} + Q_{heat,soec}} \quad [11]$$

Heat exchangers

$$\Delta TLM = \frac{(Tout,hot - Tin,cold) - (Tin,cold - Tout.cold)}{\ln\left(\frac{Tout,hot - Tin,cold}{Tin,cold - Tout,cold}\right)}$$

$$Q = mhot\ (hin, hot - hout, hot)$$

$$Q = mhot\ (hin, cold - hout, cold)$$

$$Q = U \cdot AHX \cdot F \cdot LMTD$$

Appendix B

Preliminary Analysis Results

Summary Prelimanary Analysis	973-0	973-2000	973-4000	973-6000	973-8000	1023-0	1023-2000	1023-4000	1023-6000	1023-8000
Changing cells										
Operating Temperature (K)	973	973	973	973	973	1023	1023	1023	1023	1023
Current Density (A/m2)	0	2000	4000	6000	8000	0	2000	4000	6000	8000
Result cells:										
Operation Voltage (V)	1,09	1,21	1,29	1,36	1,41	1,07	1,14	1,20	1,25	1,29
Ohm Losses (V)	0,00	0,03	0,06	0,09	0,12	0,00	0,02	0,04	0,05	0,07
Activation Losses (V)	0,00	0,09	0,15	0,18	0,21	0,00	0,06	0,10	0,13	0,15
Concentration Losses (V)	0,02	0,02	0,02	0,02	0,02	0,02	0,02	0,02	0,02	0,02
Electrical need (W)	**0,00**	**1157848,19**	**1236590,98**	**1297455,01**	**1349772,80**	**0,00**	**1094704,28**	**1151955,92**	**1198616,32**	**1238507,76**
Total Losses (V)	0,02	0,14	0,22	0,29	0,34	0,02	0,09	0,15	0,20	0,24
h2 mass (kg/s)	0,01	0,01	0,01	0,01	0,01	0,01	0,01	0,01	0,01	0,01
h2o mass (kg/s)	0,00	0,09	0,09	0,09	0,09	0,00	0,09	0,09	0,09	0,09
Sgen	3280,02	27213,98	43088,53	55358,72	65905,98	3448,57	17470,08	29012,01	38418,75	46460,86
s (J/kg K)	9342,06	9342,06	9342,06	9342,06	9342,06	9456,84	9456,84	9456,84	9456,84	9456,84
ΔS (J/Kg K)	8962,96	8962,96	8962,96	8962,96	8962,96	9077,74	9077,74	9077,74	9077,74	9077,74
Thermal need (W)	**0,00**	**776701,69**	**775283,46**	**774187,23**	**773244,94**	**0,00**	**828100,21**	**827069,05**	**826228,65**	**825510,17**

Summary Prelimanary Analysis	1073-0	1073-2000	1073-4000	1073-6000	1073-8000	1123-0	1123-2000	1123-4000	1123-6000	1123-8000
Changing cells										
Operating Temperature (K)	1073	1073	1073	1073	1073	1123	1123	1123	1123	1123
Current Density (A/m2)	0	2000	4000	6000	8000	0	2000	4000	6000	8000
Result cells:										
Operation Voltage (V)	1,06	1,10	1,14	1,17	1,21	1,04	1,07	1,09	1,12	1,14
Ohm Losses (V)	0,00	0,01	0,02	0,03	0,04	0,00	0,01	0,01	0,02	0,03
Activation Losses (V)	0,00	0,03	0,06	0,08	0,10	0,00	0,02	0,04	0,05	0,07
Concentration Losses (V)	0,02	0,02	0,02	0,02	0,02	0,02	0,02	0,02	0,02	0,02
Electrical need (W)	**0,00**	**1051678,35**	**1089430,85**	**1123387,80**	**1153807,82**	**0,00**	**1021554,24**	**1045350,83**	**1068181,55**	**1089833,61**
Total Losses (V)	0,02	0,06	0,10	0,14	0,17	0,02	0,05	0,07	0,09	0,12
h2 mass (kg/s)	0,01	0,01	0,01	0,01	0,01	0,01	0,01	0,01	0,01	0,01
h2o mass (kg/s)	0,00	0,09	0,09	0,09	0,09	0,00	0,09	0,09	0,09	0,09
Sgen	3617,12	11781,97	19392,87	26238,60	32371,27	3785,67	8694,86	13492,25	18094,93	22459,98
s (J/kg K)	9567,82	9567,82	9567,82	9567,82	9567,82	9675,33	9675,33	9675,33	9675,33	9675,33
ΔS (J/Kg K)	9188,72	9188,72	9188,72	9188,72	9188,72	9296,23	9296,23	9296,23	9296,23	9296,23
Thermal need (W)	**0,00**	**879797,56**	**879117,60**	**878506,00**	**877958,10**	**0,00**	**931905,88**	**931477,28**	**931066,08**	**930676,11**

Summary Prelimanary Analysis	1173-0	1173-2000	1173-4000	1173-6000	1173-8000	1223-0	1223-2000	1223-4000	1223-6000	1223-8000
Changing cells										
Operating Temperature (K)	1173	1173	1173	1173	1173	1223	1223	1223	1223	1223
Current Density (A/m2)	0	2000	4000	6000	8000	0	2000	4000	6000	8000
Result cells:										
Operation Voltage (V)	1,03	1,04	1,06	1,07	1,09	1,01	1,02	1,03	1,04	1,05
Ohm Losses (V)	0,00	0,00	0,01	0,01	0,02	0,00	0,00	0,01	0,01	0,01
Activation Losses (V)	0,00	0,01	0,02	0,03	0,04	0,00	0,01	0,01	0,02	0,03
Concentration Losses (V)	0,02	0,02	0,02	0,02	0,02	0,02	0,02	0,02	0,02	0,02
Electrical need (W)	**0,00**	**998492,97**	**1013640,28**	**1028563,90**	**1043177,74**	**0,00**	**979214,49**	**989148,36**	**999028,16**	**1008829,32**
Total Losses (V)	0,02	0,04	0,05	0,07	0,08	0,02	0,03	0,04	0,05	0,06
h2 mass (kg/s)	0,01	0,01	0,01	0,01	0,01	0,01	0,01	0,01	0,01	0,01
h2o mass (kg/s)	0,00	0,09	0,09	0,09	0,09	0,00	0,09	0,09	0,09	0,09
Sgen	3954,23	7031,62	10085,32	13093,93	16040,07	4122,78	6131,00	8133,66	10125,43	12101,35
s (J/kg K)	9779,66	9779,66	9779,66	9779,66	9779,66	9881,04	9881,04	9881,04	9881,04	9881,04
ΔS (J/Kg K)	9400,56	9400,56	9400,56	9400,56	9400,56	9501,94	9501,94	9501,94	9501,94	9501,94
Thermal need (W)	**0,00**	**984514,25**	**984241,43**	**983972,64**	**983709,43**	**0,00**	**1037664,24**	**1037485,32**	**1037307,38**	**1037130,85**

Summary Prelimanary Analysis	973-0	973-2000	973-4000	973-6000	973-8000	1023-0	1023-2000	1023-4000	1023-6000	1023-8000	1073-0	1073-2000	1073-4000	1073-6000	1073-8000
Changing cells															
Operating Temperature (K)	973	973	973	973	973	1023	1023	1023	1023	1023	1073	1073	1073	1073	1073
Current Density (A/m2)	0	2000	4000	6000	8000	0	2000	4000	6000	8000	0	2000	4000	6000	8000
Result cells:															
Operation Voltage (V)	1,09	1,21	1,29	1,36	1,41	1,07	1,14	1,20	1,25	1,29	1,06	1,10	1,14	1,17	1,21
Ohm Losses (V)	0,00	0,03	0,06	0,09	0,12	0,00	0,02	0,04	0,05	0,07	0,00	0,01	0,02	0,03	0,04
Activation Losses (V)	0,00	0,09	0,15	0,18	0,21	0,00	0,06	0,10	0,13	0,15	0,00	0,03	0,06	0,08	0,10
Concentration Losses (V)	0,02	0,02	0,02	0,02	0,02	0,02	0,02	0,02	0,02	0,02	0,02	0,02	0,02	0,02	0,02
Electrical need (W)	**0,00**	**1157848,19**	**1236590,98**	**1297455,01**	**1349772,80**	**0,00**	**1094704,28**	**1151955,92**	**1198616,32**	**1238507,76**	**0,00**	**1051678,35**	**1089430,85**	**1123387,80**	**1153807,82**
Total Losses (V)	0,02	0,14	0,22	0,29	0,34	0,02	0,09	0,15	0,20	0,24	0,02	0,06	0,10	0,14	0,17
h2 mass (kg/s)	0,01	0,01	0,01	0,01	0,01	0,01	0,01	0,01	0,01	0,01	0,01	0,01	0,01	0,01	0,01
h2o mass (kg/s)	0,00	0,09	0,09	0,09	0,09	0,00	0,09	0,09	0,09	0,09	0,00	0,09	0,09	0,09	0,09
Sgen	3280,02	27213,98	43088,53	55358,72	65905,98	3448,57	17470,08	29012,01	38418,75	46460,86	3617,12	11781,97	19392,87	26238,60	32371,27
s (J/kg K)	9342,06	9342,06	9342,06	9342,06	9342,06	9456,84	9456,84	9456,84	9456,84	9456,84	9567,82	9567,82	9567,82	9567,82	9567,82
ΔS (J/Kg K)	8962,96	8962,96	8962,96	8962,96	8962,96	9077,74	9077,74	9077,74	9077,74	9077,74	9188,72	9188,72	9188,72	9188,72	9188,72
Thermal need (W)	**0,00**	**776701,69**	**775283,46**	**774187,23**	**773244,94**	**0,00**	**828100,21**	**827069,05**	**826228,65**	**825510,17**	**0,00**	**879797,56**	**879117,60**	**878506,00**	**877958,10**